ULTRA-WIDEBAND POWER AMPLIFIER DESIGN FOR LARGE SIGNAL APPLICATION

RAGAVAN A/L KRISHNAMOORTHY

FACULTY OF ENGINEERING
UNIVERSITY OF MALAYA
KUALA LUMPUR

2020

ULTRA-WIDEBAND POWER AMPLIFIER DESIGN FOR LARGE SIGNAL APPLICATION

RAGAVAN A/L KRISHNAMOORTHY

THESIS SUBMITTED IN FULFILMENT OF THE REQUIREMENTS FOR THE DEGREE OF DOCTOR OF PHILOSOPHY

FACULTY OF ENGINEERING
UNIVERSITY OF MALAYA
KUALA LUMPUR

2020

UNIVERSITI MALAYA

ORIGINAL LITERARY WORK DECLARATION

Name of Candidate: **RAGAVAN A/L KRISHNAMOORTHY**

Matric No: **KHA 150117**

Name of Degree: **DOCTOR OF PHILOSOPHY**

Title of Project Paper/Research Report/Dissertation/Thesis ("this Work"):

ULTRA-WIDEBAND POWER AMPLIFIER DESIGN FOR LARGE SIGNAL APPLICATION

Field of Study: **ELECTROMAGNETIC**

I do solemnly and sincerely declare that:

(1)I am the sole author/writer of this Work;
(2)This Work is original;
(3)Any use of any work in which copyright exists was done by way of fair dealing and for permitted purposes and any excerpt or extract from, or reference to or reproduction of any copyright work has been disclosed expressly and sufficiently and the title of the Work and its authorship have been acknowledged in this Work;
(4)I do not have any actual knowledge nor do I ought reasonably to know that the making of this work constitutes an infringement of any copyright work;
(5)I hereby assign all and every rights in the copyright to this Work to the University of Malaya ("UM"), who henceforth shall be owner of the copyright in this Work and that any reproduction or use in any form or by any means whatsoever is prohibited without the written consent of UM having been first had and obtained;
(6)I am fully aware that if in the course of making this Work I have infringed any copyright whether intentionally or otherwise, I may be subject to legal action or any other action as may be determined by UM.

Candidate's Signature Date:

Subscribed and solemnly declared before,

Witness's Signature Date:

Name:

Designation:

ABSTRACT

Broadband power amplifier design has become one of the most critical enabling block in today's wireless communication technology. Numerous research efforts have been carried out throughout the years to establish high efficiency over wideband RF transmitter. This research work presents two approaches in achieving ultra-broadband power amplifier for RF transmitter. Firstly, a new technique for the design of ultra-broadband RF power amplifier is introduced, in which a combination of the reactance compensation and third-harmonic tuning are adopted. The design goal is to achieve 40 dBm (10W) output power across a wide frequency bandwidth operation. Theoretical design equations were developed to enable a designer to replicate the amplifier in the need of a highlighted specifications. The experimental result shows high efficiency achievement, more than 60%, throughout a wide bandwidth between 0.4 - 2.0 GHz. Another new design technique for broadband RF power amplifier is introduced for second approach, with combination of large signal X-parameter and Real-Frequency Technique (RFT). A theoretical analysis of large signal X-parameter is revisited, and a simplification method is introduced to determine the optimum large signal impedances of GaN HEMT device in use. With the optimum impedance extraction over the wide frequency range (0.3 - 2.0 GHz), a wideband matching network is constructed employing RFT and the final design is implemented with practical mixed-lumped elements. The prototype broadband RF PA demonstrates an output power of 40 dBm (10 W). The average drain efficiency of the PA is found to be more than 60% over the frequency band of (0.3- 2.0 GHz). These techniques demonstrated small size area and lower cost implementation which are suitable for RF communications applications.

Keywords: RFPA, reactance compensation, X-parameter, GaN HEMT, broadband

ABSTRAK

Rekabentuk penguat elektronik jalurlebar merupakan salah satu blok pemangkin yang kritikal dalam teknologi komunikasi tanpa wayar. Sejak beberapa tahun kebelakangan ini, banyak usaha penyelidikan telah dilaksanakan bagi mengecapi pemancar radio jalur lebar dengan kecekapan yang tinggi. Kertas penyelidikan ini membentangkan dua pendekatan yang diambil bagi mencapai peguat elektronik ultra-jalurlebar untuk pemancar radio. Pertamanya, satu teknik yang baru dalam penguat elektronik ultra-jalurlebar diperkenalkan, iaitu gabungan diantara pampasan reaktan dan penalaan harmonika-ketiga di adaptasikan. Objektif utama rekabentuk ini adalah untuk mencapai julat dinamik pengeluaran sebanyak 40 dBm (10W) merentas kelebaran jalur radio yang besar. Persamaan teori rekabentuk telah dihasilkan bagi membolehkan seorang pereka dapat mereplikasikan penguat elektroik tersebut dalam keperluan spesifikasi yang diketengahkan. Keputusan eksperimen menunjukkan pencapaian kecekapan yang tinggi, lebih daripada 60% sepanjang kelebaran jalur radio yang besar diantara 0.4 – 2.0 GHz. Manakala bagi pendekatan yang kedua, suatu teknik rekabentuk yang baru untuk penguat elektronik jalurlebar diperkenalkan, iaitu kombinasi isyarat besar parameter-X dan teknik Frekuensi-Nyata (RFT). Analisis teori isyarat besar parameter-X dilihat semula dan suatu cara yang mudah diperkenalkan bagi menentukan galangan elektrik yang optimum bagi peranti Gan HEMT. Dengan pengekstrakan galang elektrik yang optimum dalam julat frekuensi yang lebar (0.3 hingga 2.0 GHz), suatu rangkaian yang padan bagi jalur yang lebar dapat dihasilkan dengan menggunakan teknik RFT dan rekabentuk akhir dilaksanakan dengan elemen campuran yang praktikal. Prototaip penguat RF jalurlebar ini menunjukkan ia dapat menghasilkan julat dinamik sebanyak 40 dBm (10W). Kecekapan penguat ini juga didapati adalah lebih dari 60% bagi jalur frekuensi dari 0.3 hingga 2.0 GHz. Teknik-teknik ini juga menunjukkan saiz

kawasan yang kecil dan kos pelaksanaan yang rendah dimana ianya sangat sesuai untuk aplikasi komunikasi radio.

Kata kunci: penguat elektronik, pampasan reaktan, parameter-X, GaN HEMT, jalur lebar

ACKNOWLEDGEMENT

The road leading to doctoral degree was told to be a long journey of perseverance and indeed it was. I was fortunate in obtaining divine grace in enduring the path full of trial and tribulations in the labour of studies while working for the past 4 years. Many individuals deserve warm gratitude for making this research work a reality.

First and foremost, I would like to thank my supervisor, Associate Professor Dr. Narendra Kumar for his invaluable guidance throughout this project. His wealth of knowledge has assisted me in identifying the problem of the project. I look up to him as an excellent research advisor and would like to express my utmost gratitude. I am also indebted to my second supervisor, Associate Professor Dr. Harikrishnan. His professionalism and great technical advice as well as enthusiastic technical inputs have inspired me to continuously challenge myself to reach new levels.

My acknowledgements would not be complete without expressing my gratitude to my parents Mr & Mrs Krishnamoorthy and my family members for their unconditional love, support and care throughout my studies. Their love and overwhelming support in the face of any obstacles or adversity I faced was not only instrumental but essential in the completion of this thesis. I would not be where I am today without their contributions and foundations that they have provided throughout the years.

Following in my appreciation is dedicated to my ever supporting fellow friends and to all individuals who have directly and indirectly offered help, support and suggestions in completing this project.

Last but not least, I would like to express my special gratitude toward GOD. I feel very fortunate to be blessed by HIS endless love ever. HE is the true shepherd of my life.

TABLE OF CONTENTS

LIST OF FIGURES

LIST OF TABLES

LIST OF SYMBOLS AND ABBREVIATIONS

CPWG	:	Coplanar Wave Guide
HEMT	:	High-electron-mobility Transistor
PA	:	Power Amplifier
PAE	:	Power Added Efficiency
PCB	:	Printed Circuit Board
PHD	:	Poly Harmonic Distortion
RF	:	Radio Frequency
RFPA	:	Radio Frequency Power Amplifier
RFT	:	Real Frequency Technique
SDR	:	Software Defined Radio
Z	:	Impedance
Y	:	Admittance
X	:	Reactance
B	:	Susceptance
Q	:	Quality factor
θ	:	Electrical length
ω	:	Angular frequency
Γ	:	Reflection coefficient

CHAPTER 1 : INTRODUCTION

1.1 Background

In 19th century, the term wireless communication was introduced. This technology allows information to be transmitted from one medium to another. Today, the world has witnessed the rapid development of wireless communication technology. Mobile communication is one of the wireless technology that has evolved rapidly over the time, allowing users to communicate from all over the world.

One of the prominent enabling blocks in mobile wireless communication device is the transmitter. Transmitter block consist of power amplifier (PA), that amplifies radio frequency (RF) signal which is modulated with data to be delivered to desired receiver. Without transmitter PA, one cannot establish the communication link with another user or receiver. Therefore, designing a robust radio frequency power amplifier (RFPA) line-up has become very critical. Even though there are many types of PAs, which being used for different types of applications, they are still bounded to certain common key criteria of design such as output power, drain efficiency, gain and linearity. In mobile communication, PA design for a transmitter system needs to be efficient while delivering desired output power for specified bandwidth of application.

Wireless communication is established at various frequency bands or channels, depending on user's communication medium or standard. For a single device to operate at various frequency bands, it requires wideband transceiver. In today's world this has become one of the requirements for mobile communication device. Therefore, it has become essential to design a PA line-up that encapsulates broader bandwidth to meet current demand without trading off any of the key performance criteria, which can be challenging.

1.2 Motivation

Two-way radio/ wireless communication device is being used widely especially for mission critical application. High power (more than 40 dBm or 10 W) RF transmitter is normally used for mobile communication. The reason is that the user will be mobile and consistent power is required to maintain the communication throughout the journey. The total bandwidth of the mobile communication technology covers a wide operational bandwidth of more than one octave, ranging from 0.4 – 2.0 GHz. In today's software-oriented world, a Software Defined Radio (SDR) that allows users to choose their bandwidth of operation is highly in demand. To achieve this, the mobile transmitter should consist of broadband power amplifier. The broadband power amplifier must be able to deliver flat desired output power across wide bandwidth with high efficiency, ensuring optimum transmit current is being drawn during operation.

1.3 Problem Statement

Designing a broadband PA that covers more than one octave is rather challenging. This is due to:

- Harmonics of the lower frequency is within the bandwidth of operation. Effort to minimize harmonics of lower frequency may affect the performance of higher frequencies. Therefore, optimum impedance matching network is required to ensure maximum power transfer from PA to the output. The PA need to be well matched to the output network to exhibit desired output power across wide bandwidth while maintaining high drain efficiency. It is important for the design to maintain flat gain across the bandwidth too.

- For optimum RFPA design, the designer needs to know PA input and output impedances across desired frequencies. These can be obtained by characterizing the PA device under two-port condition. These device impedances need to be matched to 50 Ω input and output port via matching network. S-parameters are basically characterization model for two-port network under linear condition. Measurement setup using Vector Network Analyser is used to measure S-parameters for two-port network, in terms of incident waves and scattered waves. However, the characterization performed using S-parameters is under small signal condition. Matching will not be accurate because the RFPA works under large signal condition. The signal behaves nonlinearly under large signal conditions, at which, harmonics will be generated. Therefore, to ensure optimum design performance, the nonlinear behavior of the device need to be taken into consideration and large signal impedances of the device need to be matched to 50 Ohm. This can be more complicated for broadband matching.
- Characterizing nonlinear behavior of PA can be tedious and time consuming. It also requires complex and expensive setup. A methodology that can eliminate longer design time by simplifying large signal RFPA design process, without compromising any of the key specification, would be essential in today's competitive environment.

Objectives mentioned in next section are established in order to address the above-mentioned problem statements.

1.4 Thesis Objective

The aim of this research work is to design a wideband power amplifier for large signal application especially for operation bandwidth that covers more than one octave. In aforementioned section, this is quite challenging due to the harmonics of lower frequencies are within the bandwidth of operation and may compromise the efficiency of the PA design. Besides, matching impedance of the device to 50 Ohm for wider bandwidth, especially under large signal condition could be tough.

In this regard, the following objectives are established:

1) To design an ultra-broadband 10-W GaN HEMT power amplifier based on a combination of the reactance compensation technique. Output matching network is combined with third-harmonic tuning to cover more than one octave frequency bandwidth of 0.4 - 2.0 GHz with more than 60% drain efficiency.
2) To introduce a new simplified method to determine the optimum large signal impedances of a GaN HEMT device using X-parameter. A wideband matching network (0.3 - 2.0 GHz) is constructed employing RFT using these large signal impedances.

With the above research aims, the proposed design techniques are applied to design high efficiency wideband PA.

1.5 Organization of the Thesis

Throughout this thesis, the author has explained in detail on how this research has been carried out. In Chapter 2, literature review is presented. It begins with general background

studies on PA design. Classes of operation of PA is revisited as well, and in-depth review has been performed on Class-E and F operation. Basic operation and theoretical background for Real Frequency Technique (RFT) and large signal X-parameter is presented. Detailed research has been carried out to review the state-of-art work carried out in wideband PA design.

Chapter 3 discusses methodologies in designing wideband PA. Two approaches have been taken to perform the designs. Firstly, a simple lumped load network based on a combination of the reactance compensation technique and third-harmonic tuning to cover a half-decade frequency bandwidth of 0.4 - 2.0 GHz with high operating efficiency is discussed. Secondly, a new design approach of broadband RF power amplifier (PA) is introduced in this work with combination of large signal X-parameter and Real-Frequency Technique (RFT).

In chapter 4, simulation and measurement results of high efficiency ultra-broadband RF power amplifier is discussed. Both the designs are able to deliver 40 dBm output power covering a half-decade frequency bandwidth of 0.4 - 2.0 GHz and 0.3 – 2.0 GHz respectively, with high operating efficiency.

Finally, in chapter 5, conclusion of the overall work is presented. In addition, suggestion for future enhancement is discussed as well.

CHAPTER 2 : LITERATURE REVIEW

2.1 Introduction

In a transmitter system, designing Power amplifier (PA) line-up is very important. Function of PA is to amplify a small signal to a desirable output power so that the signal can be delivered to or detected by receiver system. The amplification level of the signal depends on the application of the system.

In this section, background studies on PA, its class of operations and key criteria will be shared. Detailed studies on PA characterization using X-parameter modelling techniques will be discussed. Different attempts in the last decades in utilizing Real frequency technique (RFT) for broadband matching network will be discussed as well. Finally, in depth studies of different topologies for wideband PA design and current state-of-art work will be presented.

2.2 Radio Frequency Power Amplifier (RFPA)

In general, radio frequency power amplifier (RFPA) is used to amplify Radio Frequency (RF) signal to establish communication with receiver system or station. It is being widely used in applications such as Wireless Communication, TV transmissions, Radar, and RF heating (Raab et al., 2002).

In mobile communication solution, it requires a transmitter system that consists of RFPA to amplify power to a certain amount of output power and transmit the RF signal to communicate with RF receiver. Figure 2.1 shows basic RF transmitter block diagram of a mobile device. Based on given block diagram, RF signal from mixer will be amplified by

RFPA system, transmitted out through antenna. The amplification of the power depends on the architecture design and capability of the PA.

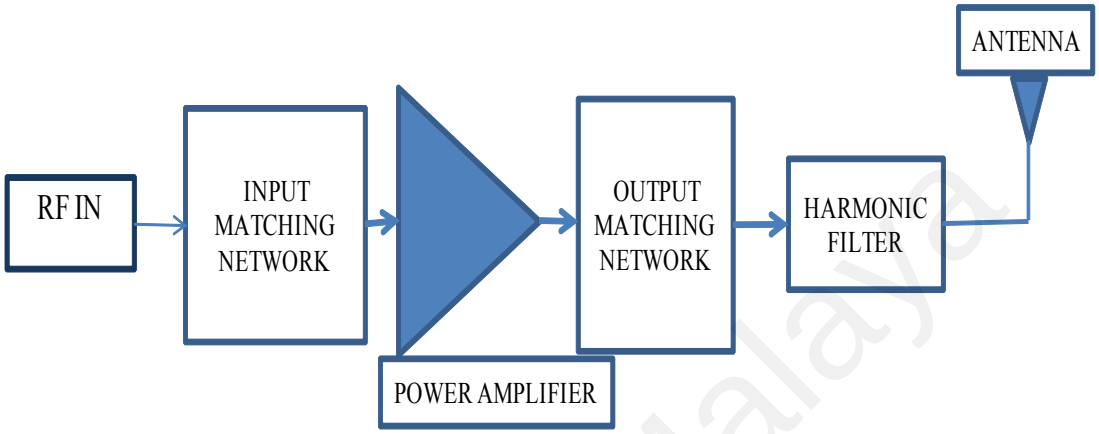

Figure 2.1: RF Transmitter block diagram

When designing a RFPA, key parameters given below should be taken into consideration:

- Output Power
- Gain
- Efficiency

RFPA design is divided into number of classes of operations depending on its application and requirement for the system. The classes that will be discussed further in this chapter will be:

- Class-A
- Class-B
- Class-AB
- Class-E
- Class-F

2.2.1 Output Power

RFPA line-up needs to be designed in such way that it can deliver the power from source to the load, provided the source is perfectly matched to the load. Having said that, this is not always the scenario, at which not all power can be delivered to the load. There will be some power that will be reflected, depending on the perfection of the matching network between source and load. Amount of power that being delivered to the load can be defined as available or transferable power and power that has been reflected is defined as dissipated power (Mass, 2003). Given below is the equation for output power:

$$P_{out} = \frac{1}{2} V_{dc} I_{dc} \ , \tag{2.1}$$

where $I_{dc} = I_{max}/2$ and $V_{dc} = V_{max}/2$; I_{max} and V_{max} maximum drain current and voltage. Therefore, maximum transferable power as function of frequency can be expressed as:

$$P_{ave}(\omega) = \frac{1}{8} \frac{|V_s(\omega)|^2}{\mathrm{Re}\{Z_s(\omega)\}}, \tag{2.2}$$

where $V_s(\omega)$ is a max value of a sinusoidal voltage applied at the input. $\mathrm{Re}\{Z_s(\omega)\}$ is the real part of the source impedance.

And the power dissipated in the load defined as:

$$P_d(\omega) = \frac{1}{2} \frac{|V_L(\omega)|^2}{\mathrm{Re}\{Z_L(\omega)\}} \ , \tag{2.3}$$

where $V_L(\omega)$ is a peak value of a sinusoidal output voltage and $\mathrm{Re}\{Z_L(\omega)\}$ is the real part of the load impedance.

2.2.2 Gain

When choosing or designing a RFPA, one should also consider the gain of the line-up. Gain of RFPA is the ratio of output power to the input power as expressed in equation below:

$$G = \frac{P_L}{P_S}, \text{ or} \tag{2.4}$$

$$G(dB) = P_L(dB) - P_S(dB), \tag{2.5}$$

where P_L is power delivered to the load and P_S is source power.

This is also known as transducer gain (Doudorov, 2003). The transducer power will be at its maximum when both the input and output ports of the PA are matched conjugately.

2.2.3 Efficiency

It is essential to design an efficient RFPA. The drain efficiency of a PA design can be expressed as (Doudorov, 2003):

$$\eta = \frac{P_{out}}{P_{dc}}, \tag{2.6}$$

where P_{out} is the fundamental output power and P_{dc} is the DC power consumption.

Based on this drain efficiency equation, one can also know the amount of power being dissipated as heat (Doudorov, 2003; Gonzalez, 1996). In the event a design has 60% drain efficiency, it reinstates that 40% of the power is dissipated as heat. Inefficient design will dissipate more power as heat and deliver less output power.

Efficiency of a PA can also be defined by taking input power, P_{in} into account. This often known as the Power Added Efficiency (PAE) and can be expressed by:

$$PAE = \frac{P_{out} - P_{in}}{P_{dc}} \tag{2.7}$$

In general, when a design is inefficient, not only the P_{out} is less than dissipated power, but it also means PA draws more current. This is essential in determining battery life of mobile device, which can lessen the sustainability of the battery when often used.

2.3 Classes of Operation

2.3.1 Class-A, B and AB

Class-A amplifier is the most linear compared to all amplifier types. Operating region of Class-A amplifier is in active region at all times as shown in Figure 2.2, hence resulting linear amplification of input signal or amplifies the entire cycle of input signal (Raab et al., 2002). Having said that, the transistor conducts for full cycle of input signal or in other word, the conduction angle of the transistor is 360˚. However, Class-A amplifier has a very big drawback; it is well known for inefficiency. Since it is being biased at all time, it causes high power dissipation, also leading to an event where the device becomes very hot. Theoretically, Class-A amplifier has an efficiency of 50%, but this is not always the case in real world, hence making it not favourable for battery-operated devices.

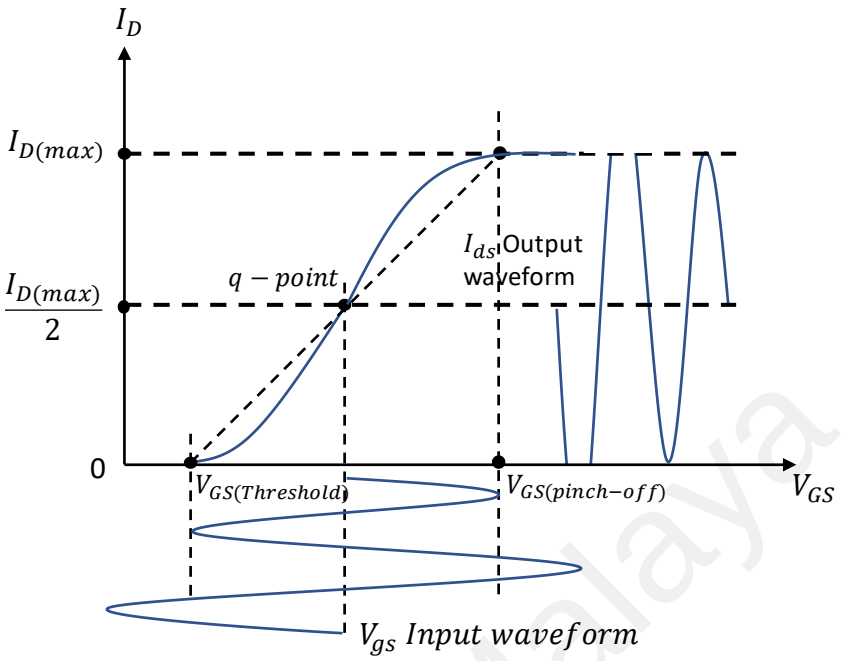

Figure 2.2: Operating region of Class-A.

Class-B amplifier has better efficiency compared to Class-A. The reason is it only amplifies half of the input wave cycle. Therefore, in Class-B operation, the amplifier continually switches on and off, yielding less heat dissipation and provide better efficiency. According to the Figure 2.3, the transistor is only biased at threshold voltage. So, output current exists only when there is an input signal, unlike Class-A, theoretically Class-B operation needs input drive of 6 dB or more to achieve its 180˚ conduction angle. Even though, Class-B operation able to achieve efficiency as high as 78%, it is less linear compared to Class-A, and more prone in creating distortion due to its half cycle operation (Pedro, Nunes, & Cabral, 2015).

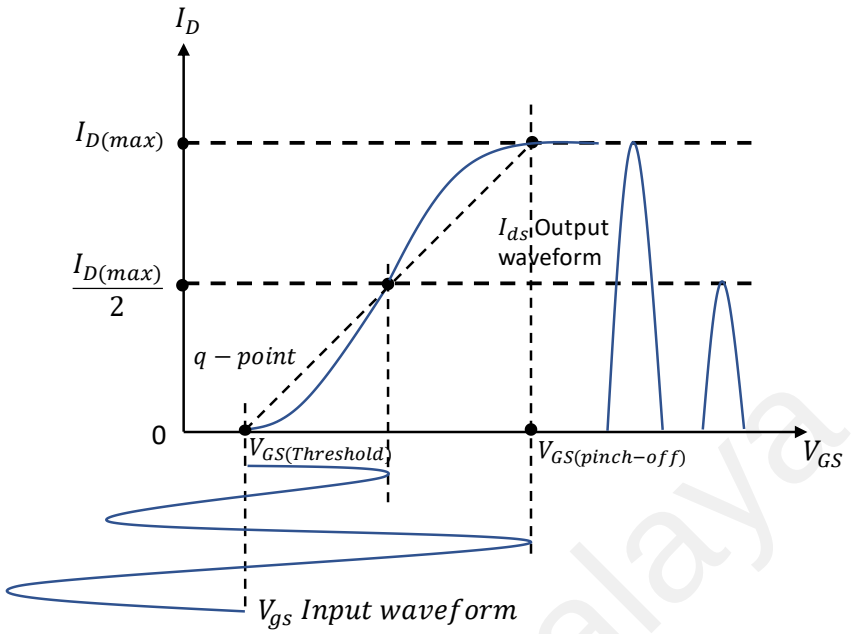

Figure 2.3: Operating Region of Class-B.

Class-AB is combination of both Class-A and Class-B operation. It compromises between the advantage of both the classes, in terms of efficiency and linearity (Weiguo, Chengguo, Shuai, Zhipeng, & Jingwei, 2016). The conduction angle for this class is between 180˚ and 360˚. Class-AB has better efficiency compared to Class-A, ranging from 50% to 78%, and better linearity compared to Class-B. Since the operation region of this class is between A and B, approximately 3dB higher gain can be achieved compared to Class-B. Transfer characteristics of Class-AB is illustrated in Figure 2.4.

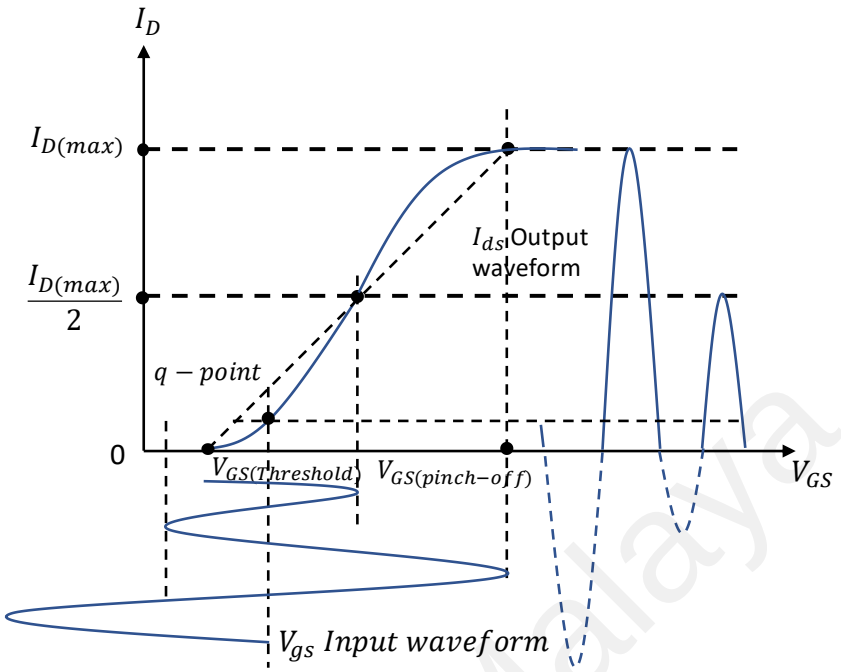

Figure 2.4: Operating region of Class-AB.

2.3.2 Class-E

In Class-E operation, as opposed to linear classes of operations, the transistor is used as switch, either ON (close) or OFF (open) (Mindan & Hong, 2010). When the switch is closed, the AC current flows into the switch and when the switch is open, current flows into the load which causes a voltage.

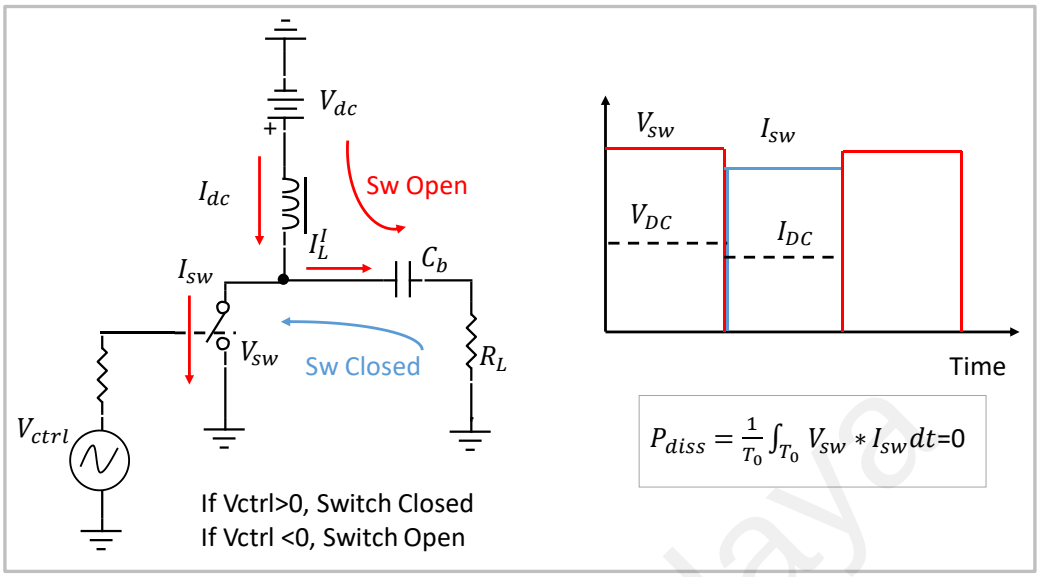

Figure 2.5: Switchmode amplifier.

According to Figure 2.5, there is no overlap in time between voltage and current, thus, theoretically there is no power dissipation and it should be extremely efficient (A. Grebennikov, 2016). However, this is not the case as the power still will be dissipated or lost at the harmonic frequencies. Therefore, to further enhance the topology, in Class-E operation, resonator is placed at the output. This resonator helps to short at the fundamental and becomes open at harmonics. So, when the switch is closed, AC current will flow into the switch and when the switch is open, to allow the resonator to pull back the current from the switch, a capacitor is placed in parallel to the switch, creating sinusoidal current waveform which alternately flows between the switch and capacitor. To minimize dissipation power, a series inductor is placed to perform phase shifting to ensure there is no overlap between current and voltage especially when the switch is closed. Class-E topology is given below in Figure 2.6.

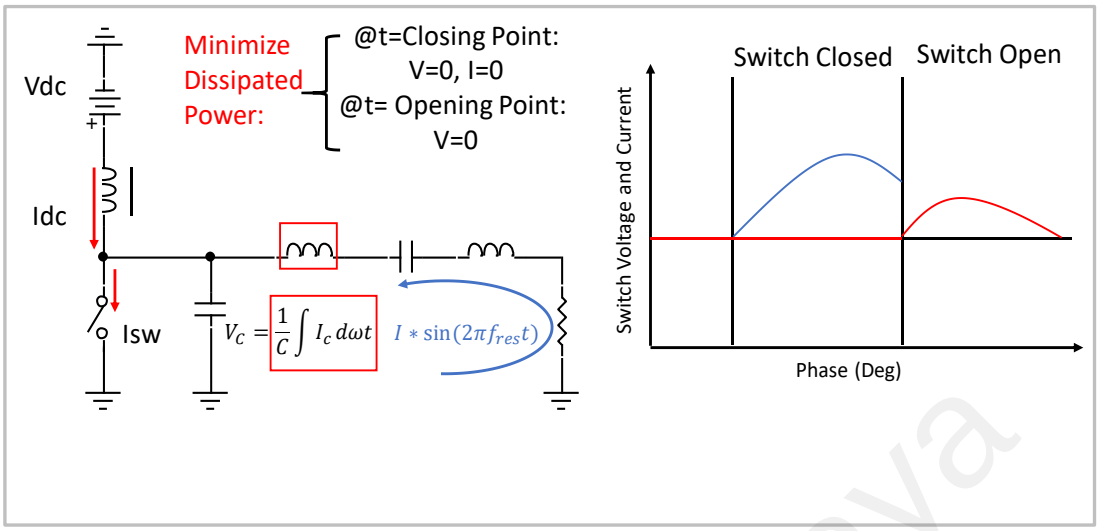

Figure 2.6: Class-E topology.

In recent years, many research works have been carried out by using Class-E amplifier. Modified topology has been proposed by (Hayati, Roshani, Roshani, Kazimierczuk, & Sekiya, 2018) which is different from conventional Class-E PA. The work has suggested by adding a shunt capacitor between phase shifting inductor and the resonant capacitor as shown in Figure 2.7, it helps to reduce 22% of peak switch voltage. This method presents different impedances for different frequencies (harmonics) unlike conventional Class-E circuit, hence, guarantees high efficiency and zero-switching loss at high frequencies.

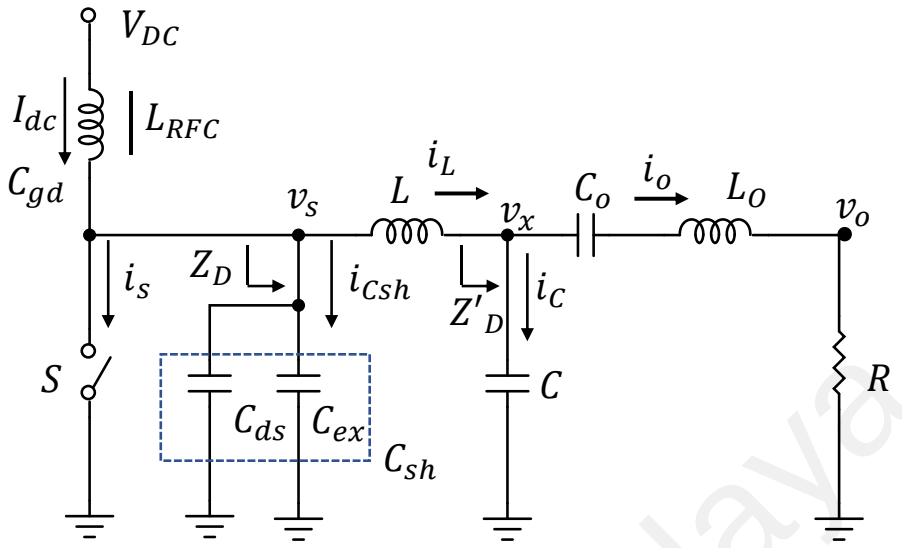

Figure 2.7: Class-E topology with shunt capacitor between phase shift inductor and resonant circuit.

It is claimed that more accurate Class-E PA design can be achieved by considering non-linear drain-to-source, linear gate-to-drain and gate-to-source MOSFET capacitance (Hayati, Roshani, Kazimierczuk, & Sekiya, 2016). The work suggested, non-linear parasitic output capacitance, C_{ds}, linear input capacitance, C_{gs} and C_{gd}, and in addition, input series resistance, R_S, will affect Class-E PA phase shift, switch voltage and output power. For example, lower output power will be delivered when maximum switch current is lower, while maximum switch voltage is higher. This could occur when suggested parameters are not considered. Figure 2.8 shows the circuit used for analysis by author.

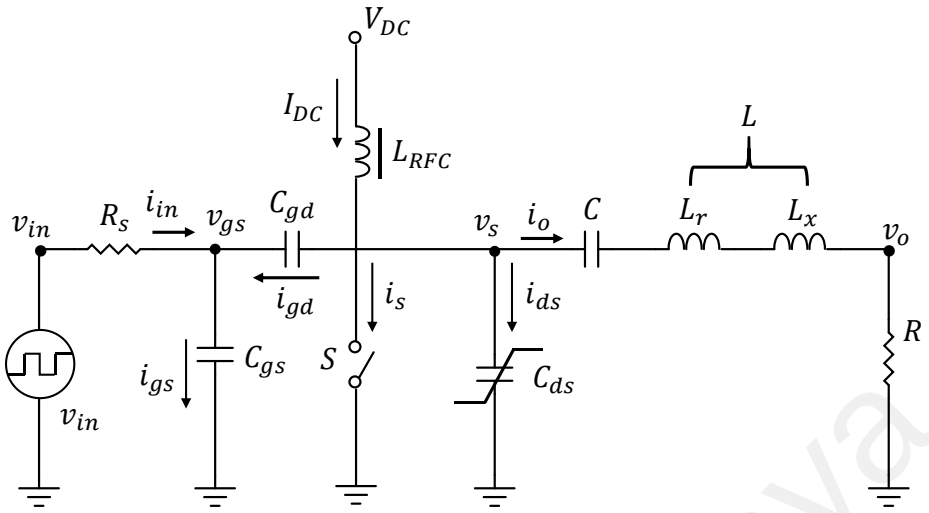

Figure 2.8: Class-E power amplifier circuit considering parasitic input and output capacitances.

By varying three different parameters, (Du, Nan, Chen, & Shao, 2014) has proposed a solution for Class-E PA. Analytical design equations have been developed with finite DC inductor as function of ratio of the resonant frequency of shunt inductor and shunt capacitor to operating frequency, the normalised slope of the switch voltage when switch turns on and the switch duty ratio. To achieve the design equations, a new parameter is introduced to solve the initial phase of load network. The method helps to design Class-E PA faster and convenient to extend the operating frequency. Even though the proposed new solution has higher switch voltage and current, due to higher breakdown voltage in GaN, this may not cause an issue.

Due to high efficiency and simple topology of Class-E PA, it is also a well-known option to be used as power source in high frequency wireless power transfer system. But it is sensitive to load variation. Therefore, (Liu, Liu, Yang, Ma, & Zhu, 2017) has proposed a design methodology to develop current-mode and voltage-mode Class-E PA, for wireless power transfer system, which increases/ decreases (respectively) when the load increases

while maintaining high efficiency. This new approach proved to be more reliable compared to conventional Class-E PA as wireless power transfer system.

2.3.3 Class-F

Similar to Class-E PA, Class-F is also a switchmode PA. It is learned that power is dissipated whenever the sinusoidal voltage and current waveform overlap in time. To reduce the dissipation power or in other word to improve efficiency of the PA, the transistor bias can be adjusted to rectify the current waveform. This shift the operation of the PA from Class-A, AB and to B. These changes however reduce the gain. When the current waveform is half rectified, this is called Class-B PA. Further rectification from here, may cause severe degradation in gain. From this stage, if the voltage can be made as square wave as shown in Figure 2.9, the efficiency can be improved rapidly, ideally, 100% (Ozalas, 2005).

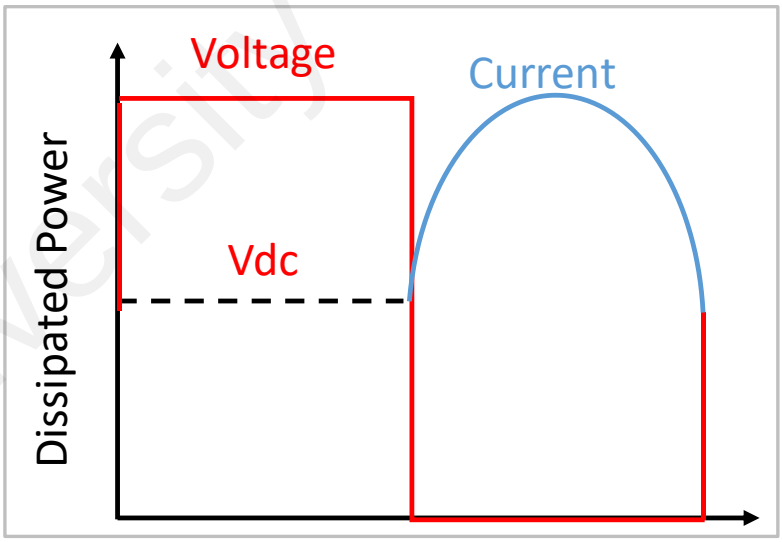

Figure 2.9: Ideal square voltage wave with half rectified current wave.

In Class-F operation, harmonic termination is used to shape the voltage to square wave. Literally, a square waveform can be achieved by combining two different frequencies' sinusoidal waveforms. For Class-F operation, for example, fundamental waveform and third

harmonic waveform is combined to make the wave squarish. So, adding on more odd harmonics with correct phase, will help sinusoidal wave to become square wave. However, at higher frequencies, this scenario is tough to be achieved. To overcome, one can use the device's parasitics as part of their harmonic termination network (Ozalas, 2005). So, at the fundamental, a simple low pass match is used to cancel out the reactive part of the load. To short second harmonic, a series parasitic inductance is included while parallel parasitic capacitance resonates with that external short to present a high impedance (open) termination to the third harmonic. This topology is presented in Figure 2.10.

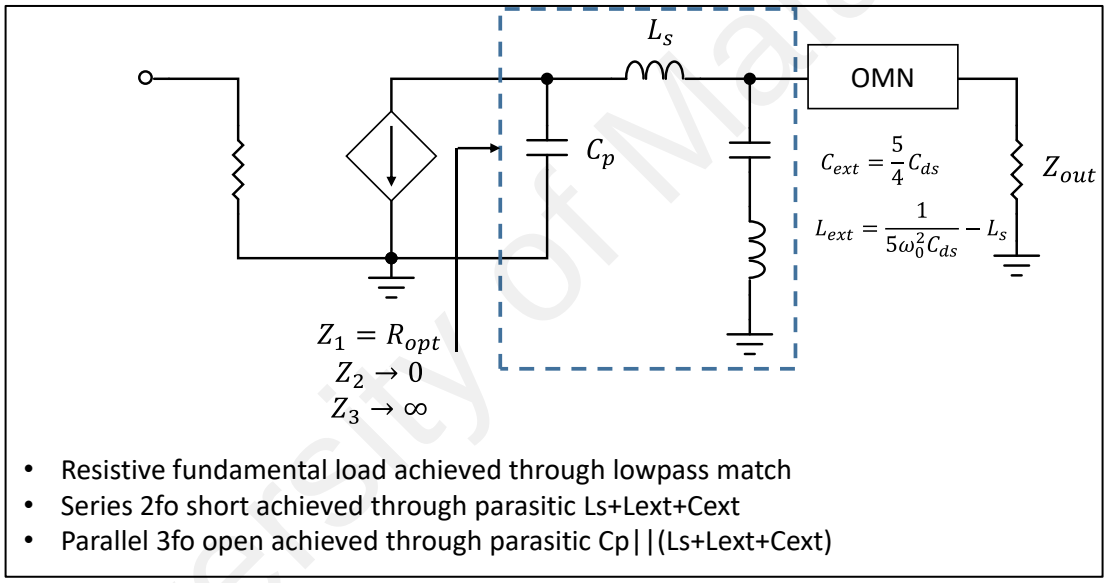

Figure 2.10: Class-F PA topology.

High efficiency PA is essential in achieving longer battery life in mobile communication system. Number of research work has been carried out in designing high efficiency PA by adopting Class-F topology. (Hayati, Sheikhi, & Grebennikov, 2015) reported by using bowtie-shaped harmonic control circuit, higher PAE can be achieved for Class-F PA. The method also provides advantage in terms size and simplicity. Figure 2.11 shows the schematic for the work.

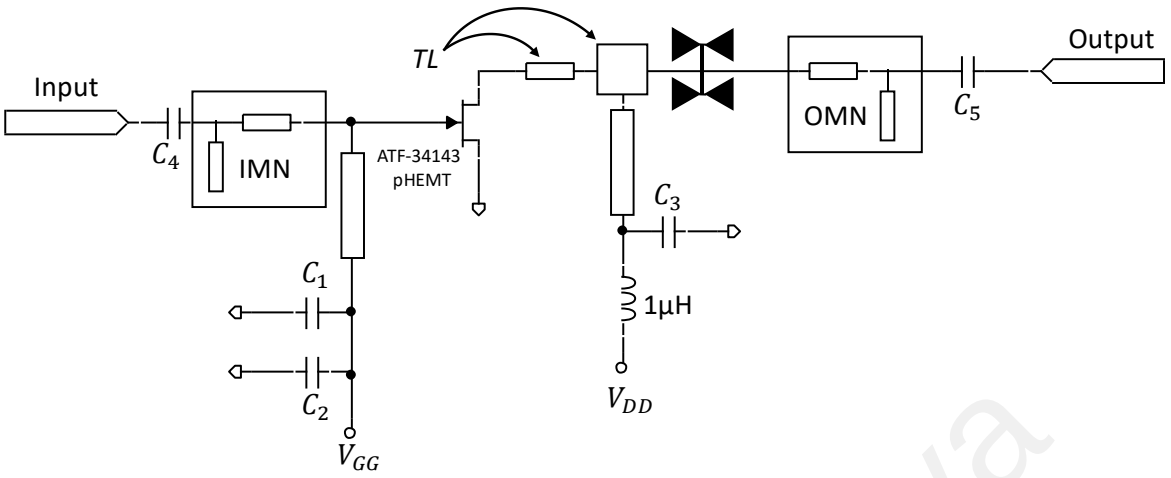

Figure 2.11: Class-F PA with bowtie-shaped harmonic control circuit.

Broadband and high efficiency continuous inverse Class-F PA design is proposed by (Yang et al., 2016). The work alleviates the common issue faced in wideband design, which is, highest frequency of the desired bandwidth will be close to second harmonic of lowest frequency. This may not be able to resolve with traditional Chebyshev low-pass filter. Therefore, it is suggested by adopting proposed modified elliptic low pass filter, a quick transition or sharp roll-off between fundamental highest frequency and second harmonic of lowest frequency can be achieved. Hence, high efficiency wideband PA design is presented.

Further investigation has been carried out on continuous Class-F PA using nonlinear embedding model (Aggrawal, Rawat, & Roblin, 2017). Nonlinear embedding transfer function is used to analyse design space for possible load impedances of broadband Class-F PA. The approach helps to alleviate the constraint of anticlockwise trajectory of second harmonic impedance on Smith chart, thus, a broadband PA design with fractional bandwidth of 50% is achieved.

High efficiency Class-F PA is deployed using hybrid cavity microstrip filtering circuit (Guo, Zhang, Xu, Li, & Xue, 2017). Low loss passband is achieved due to high Q value of the metal cavity resonator. It also provides high selectivity bandpass responses.

Besides, the approach is not complex to be integrated with transistor for matching purpose. The cavity can act as heatsink for the transistor and this is an added advantage in this design.

2.4 Reactance Compensation Technique

Reactance compensation techniques can be simply explained using circuit shown in Figure 2.12 below. The shunt and series resonant circuit, both tuned to same fundamental frequency, provide opposite reactance behaviour with respect to frequencies (Kumar, Prakash, Grebennikov, & Mediano, 2008).

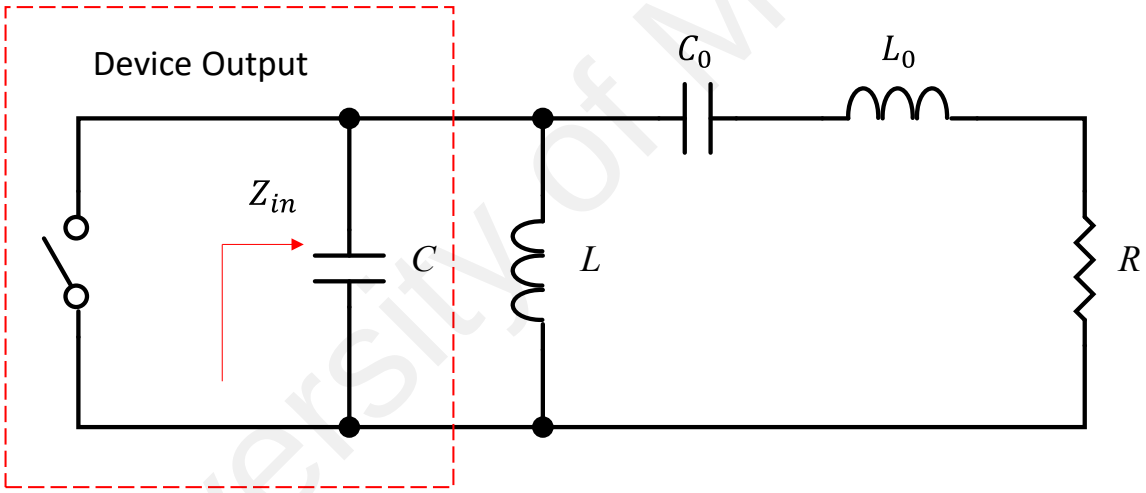

Figure 2.12: Reactance compensation circuit.

The series circuit provides positive reactance slope and shunt circuit provides negative reactance slope, hence reduces the overall reactance slope as shown in Figure 2.13 below. By making a wise choice on the circuit components, this technique can be used to develop wideband power amplifier matching network.

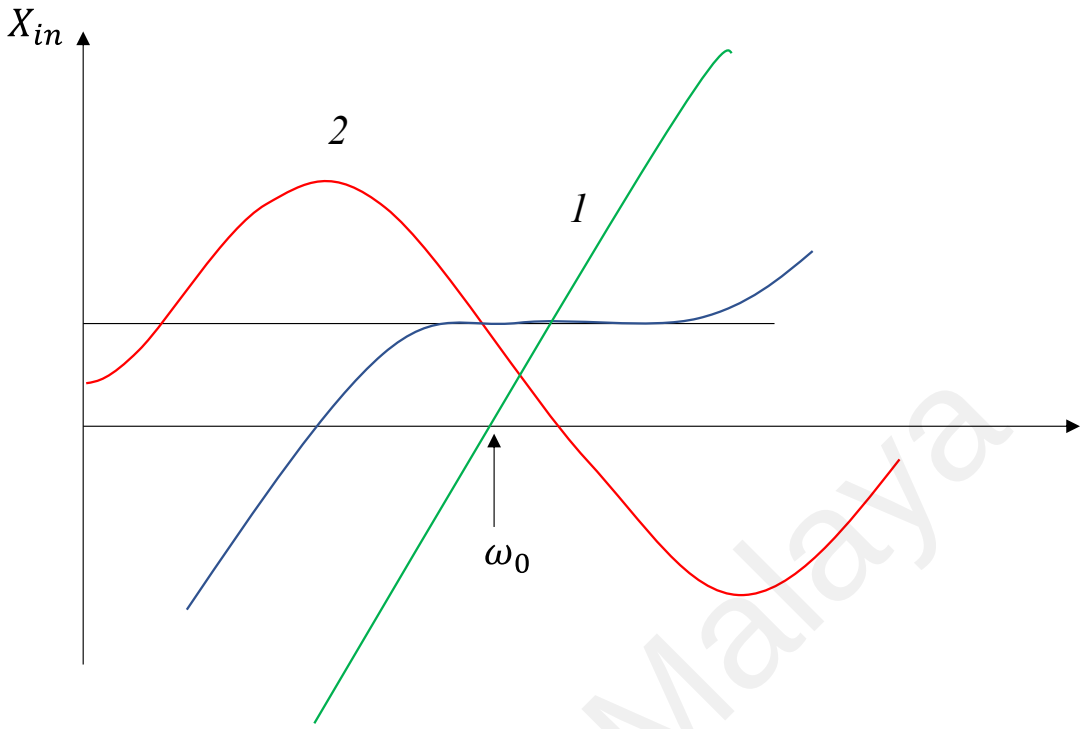

Figure 2.13: Reactance compensation principle.

2.4.1 Research work using Reactance Compensation Technique

Numerous research work employing reactance compensation technique have been performed in the past. (Lin & Chang, 2010) suggested class-E power amplifier (PA) using a 0.5 um enhancement/ depletion-pseudomorphic high-electron mobility transistor (E/D-PHEMT) process. Even though Class E PA is one of the most popular for its high efficiency, the conventional method has limitation in terms of bandwidth. Therefore, in this work, high efficiency and broadband Class-E PA design is realized by employing reactance compensation technique. The proposed research work exhibits 27 dBm of output power with PAE more than 62% and fractional bandwidth of 87%.

A research work in developing dual-band transmission-line parallel Doherty amplifier has been proposed by (Grebennikov & Wong, 2012). In this work, for the device output to be able to see optimum Class-E impedances across the wide frequency range, the

carrier and peaking amplifiers are designed based on reactance compensation technique. The proposed method able to achieve 73% of drain efficiencies across the frequency range from 1.7 – 2.7 GHz with an output power of 39 dBm.

Numerous Class-E PA design has been proposed to offer better drain efficiency compared to Class-D PA. However, mostly the design is limited by the parasitic drain capacitance of the transistor, and requires complex output circuit. In one of the recent work, (Afanasyev, Grebennikov, Farrell, & Dooley, 2020) proposed a new approach using double reactance compensation technique. A L-shaped impedance transformer is used as output matching circuit as shown in Figure 2.14, yielding double reactance compensation hence provides efficiency of 60% across 1.4 – 2.8 GHz for an output power of 40 dBm.

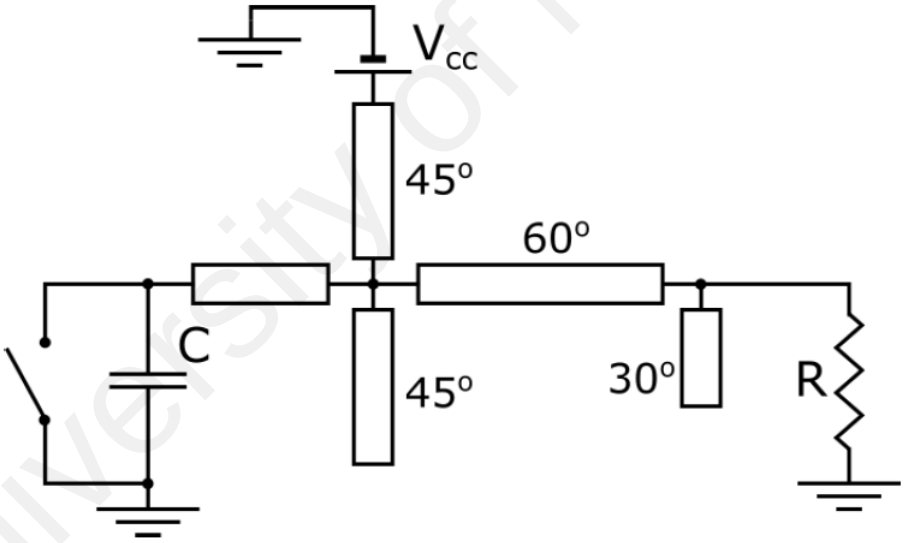

Figure 2.14: L-shaped output matching circuit.

2.5 S-parameters

S-parameter is basically a characterization model for two-port network (Gonzalez, 2008). It is being used extensively in characterizing and designing any microwave circuitry due to its simplicity and correlation under linear condition. Measurement setup using Vector Network Analyser is used to measure S-parameter for two-port network. This linear characterization is based on analysis performed in terms of incident waves, *a*, and scattered waves, *b*. Simple explanation is given below referring to Figure 2.12.

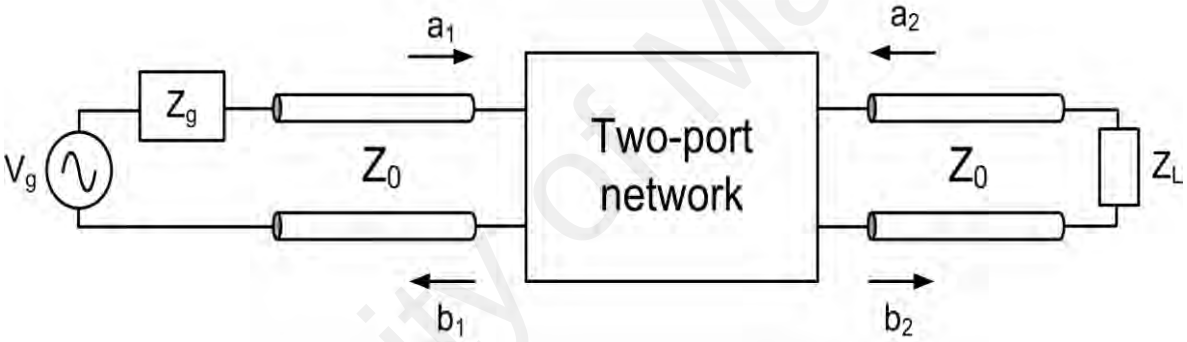

Figure 2.15: Two-port network and traveling waves.

The two-port network can be represented as:

$$S = \begin{bmatrix} S_{11} & S_{12} \\ S_{21} & S_{22} \end{bmatrix} \tag{2.8}$$

and,

$$b_1 = S_{11}a_1 + S_{12}a_2 \tag{2.9}$$

$$b_2 = S_{21}a_1 + S_{22}a_2 \tag{2.10}$$

where,

$$\text{Input return loss, } S_{11} = \frac{b_1}{a_1}\Big|_{a_2=0} \tag{2.11}$$

Output return loss, $S_{22} = \frac{b_2}{a_2}\Big|_{a_1=0}$ (2.12)

Forward transmission gain, $S_{21} = \frac{b_2}{a_1}\Big|_{a_2=0}$ (2.13)

Reverse transmission gain, $S_{12} = \frac{b_1}{a_2}\Big|_{a_2=0}$ (2.14)

a_1 and a_2 will be zero when the two-port network or transmission line is perfectly matched to the source and load respectively.

Based on above equation and characterization model, one can analyse and design microwave circuitry. However, it is limited to only small signal analysis. S-parameter won't be able to characterize any two-port network under large signal condition or in other word, for high driven power.

2.6 Large signal X-parameter

The concept of X-parameter is based on Poly Harmonic Distortion (PHD) modelling technique. It is simply an extension of S-parameters under large signal conditions, where S-parameters merely describes a linear relationship, while X-parameter represents two-port characteristics under non-linear circumstances.

2.6.1 Phase Normalization

PHD model is very different from S-parameters because, it describes not only linear relationship, but also nonlinear behaviour. Discrete tone signals are assumed to be present with both incident and scattered waves. These discrete tones appear at arbitrary frequencies (J. Verspecht, Williams, Schreurs, Remley, & McKinley, 2005). To have better

understanding of PHD model concept, throughout this section, signals are represented as periodic or narrowband modulated signals consist of fundamental and harmonics. With this understanding, harmonic indexes are used, DC signal is denoted as zero, fundamental as one, two for second harmonic and so forth.

To begin with, output spectral components B_{pm} for a DUT is a multivariate complex function, $F_{pm}(.)$ of all input spectral component A_{qn} that are relevant, and this spectral mapping is mathematically expressed as (Demenitroux et al., 2010):

$$B_{pm} = F_{pm}(A_{11}, A_{12} \ldots, A_{21}, A_{22}, \ldots) \tag{2.15}$$

whereby q and p range from one to the number of signal ports, and whereby m and n range from zero to the highest harmonic index. The concept is illustrated in Figure 2.13, with an assumption that fundamental frequency is a known constant and $F_{pm}(.)$ as describing functions.

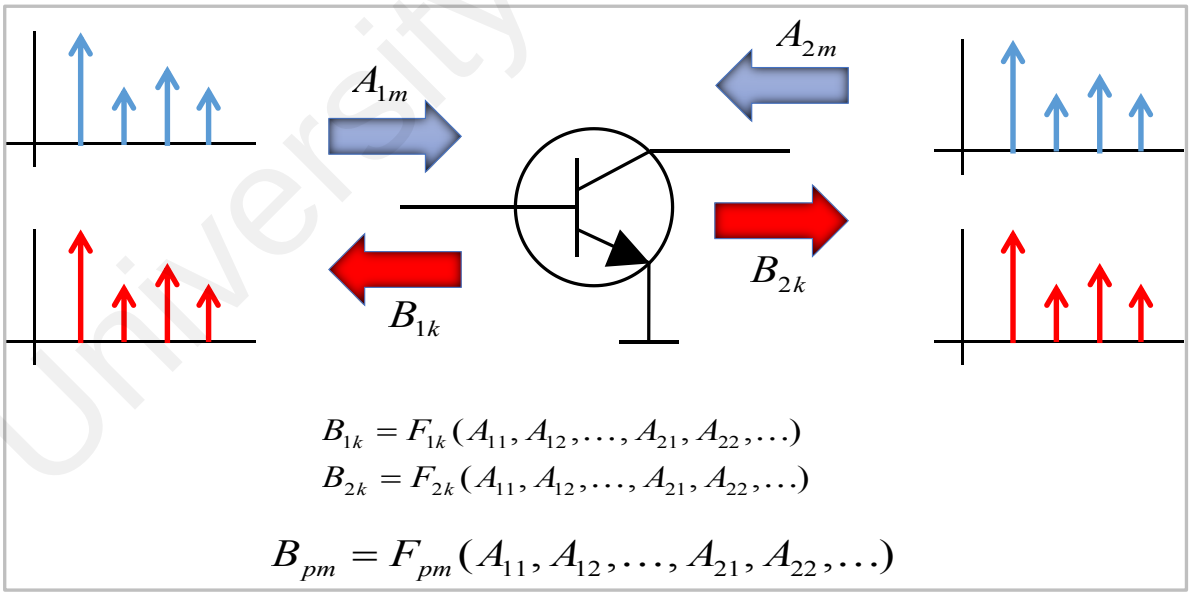

Figure 2.16: The concept of describing functions.

Equation (2.15) is a general mathematical framework which is used to develop practical model in the frequency domain. By linearizing around the signal, PHD model will be approximated using this equation.

Certain mathematical properties have been explored for further analysis. First and foremost, $F_{pm}(.)$ describes a time-invariant system, meaning, the same delay will be resulted for output signals, the scattered B-waves, when applying an arbitrary delay to the input signals, incident A-waves (Woodington, 2011). Applying a time delay in frequency domain is equivalent to phase shift that is proportional to frequency, and this is mathematically expressed as:

$$\forall\theta : B_{pm}e^{jm\theta} = F_{pm}(A_{11}e^{j\theta}, A_{12}e^{j2\theta}, \dots\dots A_{21}e^{j\theta}, A_{22}e^{j2\theta}, \dots.) \tag{2.16}$$

Phase normalization need to be performed (Verspecht & Root, 2006) in order to set the phase of the injected fundamental signal at the input port to zero. If θ applied to the system describing function, as expressed in (2.16) is equal to the inverted phase of $A_{11,}$ the large signal fundamental stimulus wave, the describing function can be formulated as:

$$B_{pm} = F_{pm}(|A_{11}|, A_{12}P^{-2}, A_{13}P^{-3} \dots\dots A_{21}P^{-1}, A_{22}P^{-2}, \dots.)vP^{m} \tag{2.17}$$

where

$$P = e^{j\varphi(A_{11})} \tag{2.18}$$

The first input argument, A_{11} which is the amplitude of the fundamental stimulus wave at the input port is a positive real number instead of a complex number, hence helps in simplifying further formulation.

2.6.2 Polyharmonic distortion model and X-parameters

Unlike S-parameters, it is learnt that, with non-linear design framework based on PHD model, X-parameter able to characterize, model and design non-linear systems. Under large signal condition, superposition principle will not work. However, in the event where only one large input signal with relatively small harmonics, this is feasible for the harmonics, and called harmonic superposition principle (Verspecht & Root, 2006) as shown in Figure 2.14. The input component A_{11} (black arrow) generates output spectral components B_{21}, $B_{22}, \ldots B_{2n}$ (black arrows at output port). By adding relatively small harmonic component at the input, namely A_{12} (red arrow at the input), one can observe that it has generated superposition component for all output spectral components (in red arrows at the output port). Similar effect observed as more harmonics added at the input port (green and blue arrows). This harmonic superposition principle is true for all practical power amplifier design cases, and this is the key for PHD model.

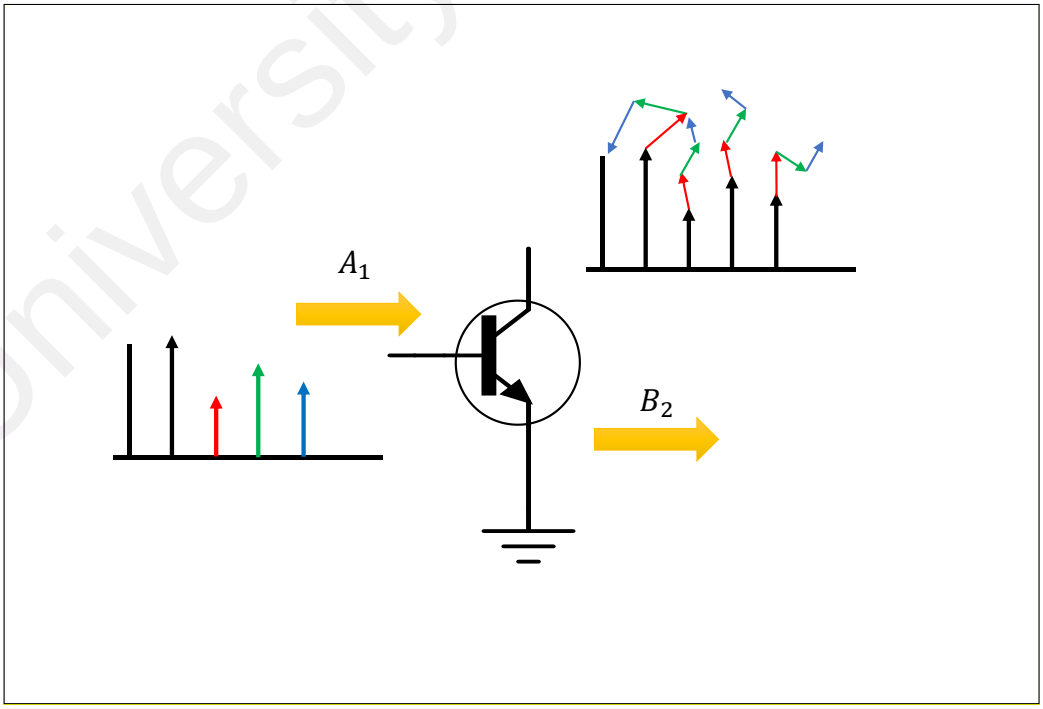

Figure 2.17: Harmonic Superposition Principle

Linearization of (2.17) yields:

$$B_{pm} = K_{pm}(|A_{11}|)P^{+m} + \sum_{qn} G_{pq,mn}(|A_{11}|)P^{+m}\, Re\left(A_{qn}P^{-n}\right) +$$

$$\sum_{qn} H_{pq,mn}(|A_{11}|)P^{+m}\, Im\left(A_{qn}P^{-n}\right), \tag{2.19}$$

whereby

$$K_{pm}(|A_{11}|) = F_{pm}(|A_{11}|, 0, \dots 0), \tag{2.20}$$

$$G_{pq,mn}(|A_{11}|) = \left.\frac{\partial F_{pm}}{\partial Re\left(A_{qn}P^{-n}\right)}\right|_{|A_{11}|,0,\dots 0} \tag{2.21}$$

$$H_{pq,mn}(|A_{11}|) = \left.\frac{\partial F_{pm}}{\partial Im\left(A_{qn}P^{-n}\right)}\right|_{|A_{11}|,0,\dots 0} \tag{2.22}$$

The nonanalyticity of spectral mapping is the second property that is being exploited in PHD model. Under small signal, it is noted the spectral mapping is analytic (Lee, Lin, Lin, & Lee, 2016; Verspecht & Root, 2006). However, as the input signal A_{11} gets larger, the spectral mapping becomes nonanalytic. This nonanalytic behavior is represented by $G_{pq,mn}$ and $H_{pq,mn}$ in (2.21) and (2.22) respectively. By replacing real and imaginary parts in (2.19) with a linear combination of the input arguments and its corresponding conjugates, yields expression below:

$$Re\left(A_{qn}P^{-n}\right) = \frac{A_{qn}P^{-n} + conj\left(A_{qn}P^{-n}\right)}{2} \tag{2.23}$$

$$Im\left(A_{qn}P^{-n}\right) = \frac{A_{qn}P^{-n} - conj\left(A_{qn}P^{-n}\right)}{2j} \tag{2.24}$$

$$B_{pm} = K_{pm}(|A_{11}|)P^{+m} + \sum_{qn} G_{pq,mn}(|A_{11}|)P^{+m}\left(\frac{A_{qn}P^{-n} + conj\left(A_{qn}P^{-n}\right)}{2}\right) +$$

$$\sum_{qn} H_{pq,mn}(|A_{11}|)P^{+m}\left(\frac{A_{qn}P^{-n} - conj\left(A_{qn}P^{-n}\right)}{2j}\right) \tag{2.25}$$

This can be further expressed as below and yield X-parameter model (Horn et al., 2008; Simpson, Horn, Gunyan, & Root, 2008):

$$B_{pm} = X^F_{pm}(DC, |A_{11}|)P^m + \Sigma_{qn} X^S_{pm,qn}(DC, |A_{11}|)P^{m-n}A_{qn} + \Sigma_{qn} X^T_{pm,qn}(DC, |A_{11}|)P^{m+n}A^*_{qn} \quad (2.26)$$

whereby

$$X^F_{pm}(|A_{11}|) = K_{pm}(|A_{11}|), \quad (2.27)$$

$$X^S_{pm,qn}(|A_{11}|) = \frac{G_{pm,qn}(|A_{11}|) - jH_{pm,qn}(|A_{11}|)}{2}, \ \forall\, p, q \neq 1 \quad (2.28)$$

$$X^T_{pm,qn}(|A_{11}|) = \frac{G_{pm,qn}(|A_{11}|) + jH_{pm,qn}(|A_{11}|)}{2}, \ \forall\, p, q \neq 1 \quad (2.29)$$

where the model coefficients X^F_{pm}, $X^S_{pm,qn}$ and $X^T_{pm,qn}$ are identified as X-parameters, p and q are the port indexes (1,2), m (1, 2,..) and n (1, 2,..) are the corresponding harmonic indexes. Due to linear nature of equation (2.19), it is simply straightforward to obtain the PHD model coefficients. Only three measurements are theoretically enough to determine and compute each set of X^F_{pm}, $X^S_{pm,qn}$ and $X^T_{pm,qn}$ coefficients (Gou, Lin, Wu, & Fu, 2015).

2.6.3 X-parameters State-of-art Research works

X-parameter is simply an extension of S-parameter, where, it describes nonlinear components under large signal conditions. It can be accurately measured by automated set of experiments on Agilent Nonlinear Vector Network Analyzer (NVNA) instrument. The measured X-parameters data can be used in CAD tool to design nonlinear circuits. Numerous research work has been performed in this context. (Pelaez-Perez, Woodington, Fernandez-Barciela, Tasker, & Alonso, 2012) developed an analytical design procedure using PHD model and X-parameter formulation to design RF oscillator. The author has suggested new approach to accurately predict oscillator performance under nonlinear condition instead of

usual negative-resistance method which is limited by linear components. New closed-form expressions based on load-independent parameters has been presented in order to enable microwave oscillator analytical design procedure that incorporates nonlinear effects. A 5 GHz microwave oscillator has been designed and manufactured to validate the new analytical approach. Results justifies the analytical expression helps to accurately predict the fundamental power and oscillation frequency. This PHD based X-parameter analytical modeling, not only able to design RF oscillator accurately but also help to speed up the design process.

(Nielsen, Dieudonne, Gillease, & Root, 2012) presents on how X-parameters of GaN power transistor is extracted and modelled to simulate complete Doherty Power amplifier design. The device is used in measurement setup with active load-pull and its fundamental and harmonics impedances are tuned and measured. The corresponding X-parameter model has been extracted and used in simulation for development of complete Doherty power amplifier design. Based on simulation design, a prototype has been fabricated and the measurement results of the board correlated well with simulation. It is proven that an active device can be accurately modeled with X-parameter due to its capability of characterizing nonlinear components. Such capability is vital for any circuit design using active device under large signal condition.

For polar power amplifier design, phase and envelope of the input modulated signal are required. Since envelope port is neither RF or DC, X-parameter modeling may not work to characterize the effect of this port. Nevertheless, (Wang, Nielsen, Sira, Jensen, & Larsen, 2013) suggested a technique whereby a combination of X-parameter and low pass filter simulation is used in modeling polar PA. X-parameter based modeling for RF path and, a low pass filter simulation for envelope path helps to create a robust polar PA model. This

model is applicable to polar PAs design that have similar topology. To validate the model, comparison between simulated and measurement results were carried out. It is learnt that both the results are comparable and almost correlated.

(Barmuta, Ferranti, Lewandowski, Knockaert, & Schreurs, 2014) proposed an efficient multidimensional X-parameter model for microwave transistor. Sequential technique is utilized to generate this model with small number of samples while guaranteeing X-parameters' validity. Two common empirical GaAs HEMT models have been investigated with respect to their validity region using sequential sampling. Then X-parameter radial basis function model is developed for the empirical models. Further comparison with standard tabular model interpolated with cubic spline functions, helps to overcome simulator convergence issues. This is an efficient and accurate modeling technique for X-parameters using sequential sampling. The model guarantees fast convergence and minimum error even for a small number of samples.

A research work is carried out in simulation to minimize the complexity of harmonics load-pull measurement setup for X-parameter based modeling technique (Wang, Nielsen, Jensen, & Larsen, 2015). The work suggested to eliminate impedance tuning for 3^{rd} harmonic in device characterization. A 6W GaN RF power transistor is modeled using load-dependent X-parameters by simulations and tuned only up to 2^{nd} harmonic. The model created has been validated and compared with preliminarily created device model which its impedance tuned up to 3^{rd} harmonic. It is proven the newly developed concept still able to predict the transistor behavior for 3^{rd} harmonic. A high efficiency 2 GHz power amplifier is designed using this concept and validated.

(Lee, Lin, & Lin, 2016) presents an investigation based on X-parameter performed on output power of pHEMT under different load conditions and output impedances for large signal. The author suggests characterization of fundamental output power at different load using conventional hot S-parameters (without X^T terms) is less accurate compared to characterization performed using X^T terms. On the other hand, large signal output impedance incorporating both X^S and X^T terms also yields high accuracy. Based on the comparison made between with and without X^T terms, the work proves that under load mismatch conditions as well as for robust output matching design, X^T terms plays a vital role in achieving high accuracy design.

Characterizing an active device and extracting X-parameter model helps in further development of RF design using the same device. However, this is bounded to the conditions set for the modeling. Scalable X-parameter for device modeling has been proposed by (Root et al., 2012). This technique allows to characterize devices that are geometrically scaled or simulated at different frequencies. (Biernacki, Marcu, & Root, 2017) optimizes geometrical X-parameter scaling for further improvement.

An approach based on X-parameter is proposed (Joujili, Mivehchy, & Habibi, 2016) to minimize specific harmonic output power by calculating load reflection coefficient at the fundamental frequency. X-parameter is considered load independent when the analysis is limited within a small area around the Z_{ref}, load impedance used to extract X-parameter. In this context, X-parameter can be considered independent of reflected signal from the load and optimum load impedance, Z_{opt} can be calculated. Given the analysis area is much wider, using same X-parameter to find Z_{opt} is not valid. This is because the more the distance between Z_{ref} and load reflection coefficient, the more error it will be. This work suggests

Minimization Blind Iterative Analytical Process (MBIAP) to calculate optimum load reflection coefficient to minimize the output power at a specific harmonic.

2.7 Real frequency technique (RFT)

There are many designing methods for power amplifier matching network or line-up. An essential method for broadband matching is real frequency techniques (RFT), which is primarily introduced by (Carlin, 1977) and further developed by (B. S. Yarman, 2010). RFT is wideband semi-analytic design methods to synthesis and realize lossless matching networks with optimum circuit topologies (B. S. Yarman & Ejaz, 2015). According to RFT (Yarman, 2010), the impedances below used to describe the lossless matching networks:

$$Z_B(p) = \frac{N(p)}{D(p)} \tag{2.30}$$

where $p = \sigma + j\omega$ is a complex variable.

Any positive real impedance, in any general case, is able to describe as:

$$Z_B(p) = Z_M(p) + Z_F(p). \tag{2.31}$$

In this equation, $Z_M(p)$ is a minimum reactance function which is free of Right Half Plane (RHP) and $j\omega$ poles; and on $j\omega$ axis it is expressed as:

$$Z_M(j\omega) = R_M(\omega^2) + JX_M(\omega). \tag{2.32}$$

On the other hand, $Z_F\ (p)$ is a Foster function and expressed as

$$Z_F(j\omega) = jX_F\,, \tag{2.33}$$

$$X_F(\omega) = -1/\ (C_{n+1}.\omega), \tag{2.34}$$

C_{n+1} is the term that represents a DC block capacitor.

For a lumped element circuit, the real part $R_M(\omega)$ is a non-negative even function in angular frequency ω.

In Figure 2.15, instead of choosing the circuit topologies, they are fully described by means of their Darlington driving point network functions (Ceylan, Yagci, & Yarman, 2010). The matching network will be evaluated in terms of transducer power gain, *T(ω)* (Aridas, Yarman, & Chacko, 2014):

$$T(\omega) = \frac{4R_M R_L}{(R_M+R_L)^2+(X_M+X_F+X_L)^2} \tag{2.35}$$

whereby in an ideal case, $T(\omega) = 1$ over an entire frequency band $B(\omega) = \omega_2 - \omega_1$, otherwise zero.

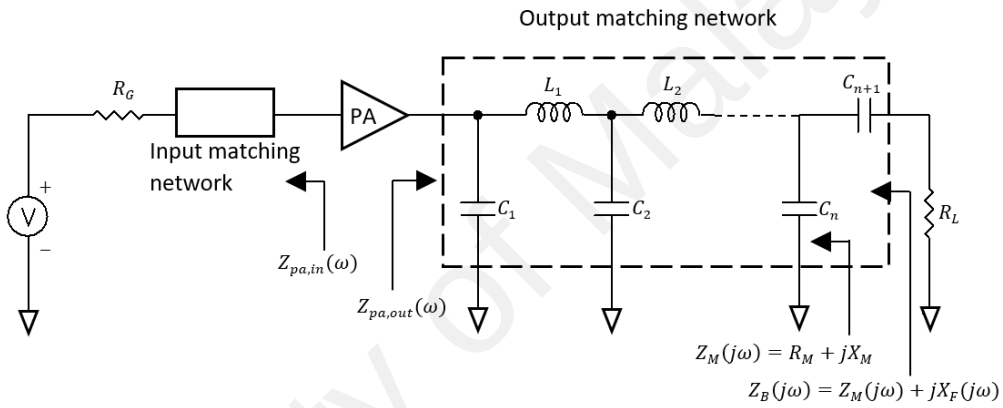

Figure 2.18: Representation of the broadband matching network.

Within the band of operation, error function is defined as:

$$\varepsilon(\omega) = (R_M - R_L)^2 + (X_M - X_F)^2 \tag{2.36}$$

Eventually, the error function is minimized by means of a non-linear optimization algorithm which yields the desired impedances $Z_M(p)$ and $Z_F(p)$ to approximate the ideal gain characteristic.

2.7.1 Recent research work employing RFT

When it comes to broadband RF power amplifier matching network, RFT is widely being used in many research works and applications. Recent state of art works employing RFT have been analyzed and presented in this section. A broadband Doherty power amplifier

is designed using RFT (G. Sun & Jansen, 2012). The work pointed out the limitation in designing wideband Doherty PA. Simplified RFT (SRFT) is used with desired frequency-dependent optimum impedances to realize broadband matching using GaN transistor.

A highly efficient dual-band power amplifier is proposed in (Ma, Zhou, & Yu, 2015). The author proposed short-circuited and open-circuited transmission lines to control harmonics. But to establish wideband matching network at fundamental, 2.1-2.6 GHz, Simplified RFT (SRFT) is used. The method is verified using 10W GaN transistor. It is proven the combination of two approaches yield highly efficient PA design at desired dual band frequencies.

A dual-transformation simplified real frequency technique (DT-SRFT) is developed in (Meng, Zhu, Xia, & Yu, 2018). The suggested method helps to improve the bandwidth of Doherty power amplifier as it proposes co-design of both carrier and peaking amplifier output matching networks using RFT. With the combination of the output matching network optimization process, the matching network can be optimized at back-off and saturation power levels simultaneously. The method able to achieve more than 50% fractional bandwidth.

A novel cost function of the RFT is proposed (Dai et al., 2015). This method simplifies optimization expression as it could straightforwardly describe PA optimal impedance along with frequency change. A commensurate transmission line based on Richard transformation is deployed so that the PA matching could be convenient expressed by a real positive function and it could be directly implemented with a distributed matching network through synthesis theory. It proposed new calculation applicable by computer aided design.

2.8 State-of-art work in designing wideband PA application

In this section, recent state-of-art research work in designing wideband PA will be discussed. A research has been done to design a high efficiency broadband PA with second harmonic manipulation (Sharma et al., 2016). Since, practical broadband matching network design space will always have limitations in terms of impedance mismatch, this work investigates on a wider design space for a more flexible high efficiency broadband PA design. Initiated from ideal Class-F^{-1} condition, a series of voltage and current waveforms that is better than Class-B RF performance, including Class-F^{-1}, is identified in proposed methodology. A contiguous design space is created by extending these waveforms via continuous-mode concept. Within this expanded design space, fundamental and second harmonic matching trajectory for wider bandwidth for highly efficient PA can be extracted. Actual measurement results show that more than 75% of drain efficiency can be achieve for fractional bandwidth of 57%.

Another research work has been performed based on Class-F^{-1} for broadband PA. Theoretically, Continuous Class-F^{-1} (CCF^{-1}) PA, extended version of Class-J PA, provides high efficiency design. However, this concept requires a proper matching at both fundamental and harmonics. In broadband design, especially for an octave bandwidth, the highest frequency of the band will be very close to second harmonic of lowest frequency. Traditional matching techniques may cause degradation in efficiency especially at lowest frequency due to high second harmonic. (Yang et al., 2016) suggested a technique to ensure the harmonic of lowest frequency is truncated, hence, providing high efficiency broadband solution. The work suggests implementing a modified elliptical low pass filter as shown in Figure 2.16 at the output matching network, which provides sharp roll off between highest fundamental frequency and second harmonic of the lowest frequency. PA design with drain

efficiency of more than 68% is achieved for fractional bandwidth of 60% with proposed technique.

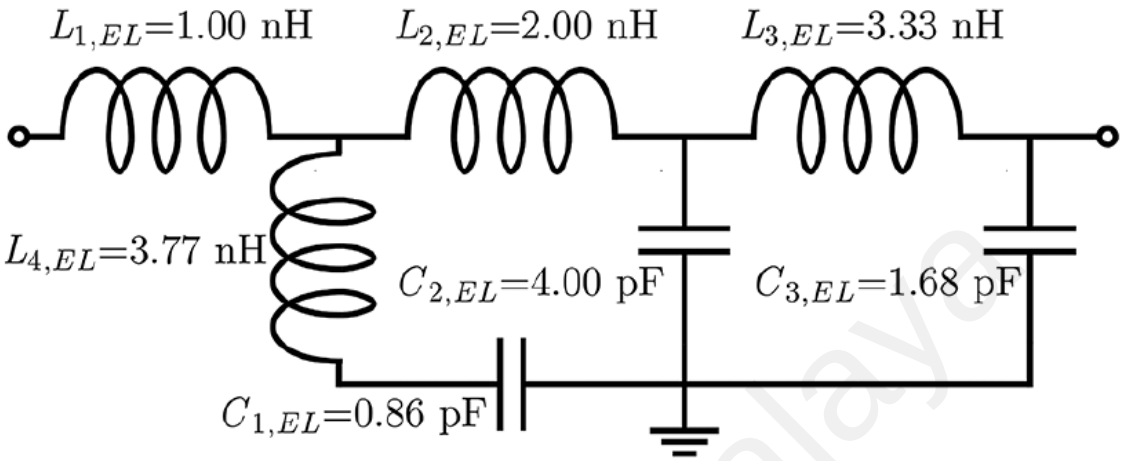

Figure 2.19: Modified elliptical low pass filter.

Class-E PA design act as on-off switch which yield in non-overlapping voltage and current waveform, hence minimizing power dissipation and maximize power efficiency. This can be realized with shunt capacitor and series filter which is tuned to suppress harmonics. (A. Grebennikov, 2016) proposes a technique which uses shunt filter instead of series filter as shown in Figure 2.17, achieving new load network which provides broadband capabilities on top of high efficiency. Two methods have been employed to realize broadband Class-E mode PA, one with shunt filter with lumped elements and the other with transmission line elements. A test board with transmission line elements using GaN HEMT is able to achieve 41 dBm across the frequency band from 1.4 – 2.7 GHz with average drain efficiency of 68%.

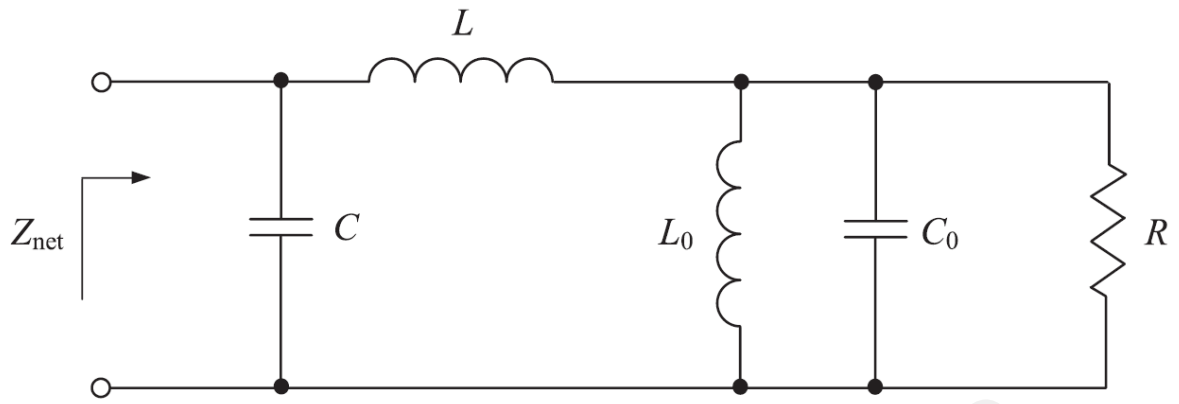

Figure 2.20: Equivalent circuit of Class-E with shunt capacitor and shunt filter.

An active second harmonic injection technique is employed in (Seo et al., 2014) to improve the efficiency and bandwidth for PA design. Multiharmonic load-pull simulations is used to find an optimum third-harmonic termination condition for the active second-harmonic injection to achieve high efficiency PA design. An auxiliary second-harmonic PA is used for injection. A PA was designed using 10-W GaN HEMT for the optimized third harmonic termination, with diplexer and auxiliary PA connected to the drain of the main PA. Based on measurement results, it is learnt that the bandwidth of the PA design improved from 60 MHz to 180 MHz, with PAE of 80%, after the second harmonic injection.

A linear broadband, and efficient PA is essential for Long Term Evolution (LTE) applications. (Huang, He, You, & Hu, 2013) has designed, fabricated and validated a method employing Cree's CGH40010F GaN HEMT for producing high efficiency linear broadband PA design for LTE applications. The research work incorporated a technique by controlling the impedance to find the optimum impedances for Doherty PA design. Third intermodulation distortion (IMD3) is not only depends on fundamental, but also affected by baseband and harmonics. In this work, the author suggested to control baseband and harmonic impedances while maintaining fundamental impedance. A highly efficient

performance across a bandwidth of 1.6–2.6 GHz able to be achieved while showing good linearity with a 5 MHz two-tone signal and a single-carrier 20 MHz LTE signal, respectively.

High quality factor (Q) matching network is required in order to establish high efficiency PA design. This can be a limitation in designing broadband PA. (Shuai, Zhiqun, Kai, & Hui, 2015) proposes microstrip radial stub for Class-EF PA design instead of normal open or short stub. In this design, the output matching network consists of microstrip radial stub and Class-EF harmonic tuning network is adopted to widen the bandwidth of the switch PA. A proof of concept results in 60% of PAE across 1.7-2.55 GHz, with output power of more than 40 dBm.

For less complex circuitry than Class-D topologies and to achieve a wider bandwidth when compared to Class-F and F^{-1} designs, (Tamjid, Ghahremani, Richardson, & Fathy, 2017) chooses Class-E to design high efficiency PA. Input and output matching networks are realized using distributed elements instead of lumped elements to achieve higher efficiency at 2.3 GHz. The design and analysis were conducted using simulation and compared with actual measurement. The design is based on CREE's CGH40025F GaN HEMT and prototype measurement results well correlated with simulation, resulting in more than 57% efficiency across 0.9-2.3 GHz. The improvised PA model provides access to the intrinsic drain waveforms, and based on waveform analysis, non-linearities behavior of the device able to be modeled, which greatly improve the accuracy of the design.

The paper (Chen & Peroulis, 2012) proposes an approach in designing high-frequency broadband harmonic-tuned PA. The author suggested by mode-transferring between continuous Class-F^{-1} (CCF^{-1}) and continuous Class-F (CCF), a broadband PA design can be achieved easily compared to single CCF/CCF^{-1} mode. Specifically, the target fundamental and harmonic impedances can be well matched to the frequency behavior of a three-stage low-pass matching network implemented using transmission lines. The technique

has been validated using 40 dBm GaN transistor, resulting in 87% fractional bandwidth with more than 60% drain efficiency.

The nonlinear device output capacitance is important for wave-shaping the continuous Class-F voltage and current waveforms. This is highlighted in (Tuffy et al., 2012) whereby a simplified method is proposed in designing broadband PA. Wave-shaping by nonlinear device output capacitance, helps to reduce the device sensitivity to second and third harmonics impedance terminations. Thus, the design is reduced to fundamental matching problem by identifying high efficiency regions on the reactance plane. This incomplexity allows wideband PA design by employing RFT. Fabricated PA design exhibits 11 W output power with drain efficiency of 70% from 1.45 – 2.45 GHz.

CHAPTER 3 : RESEARCH METHODOLOGY

3.1 A High-Efficiency Ultra-Broadband Mixed-Mode GaN HEMT Power Amplifier

In this section, a methodology of efficiency enhancement of ultra-broadband RF power amplifier with simple load network approach is discussed. An ultra-broadband 10-W GaN HEMT power amplifier is described having a lossy input matching circuit and a simple lumped load network based on a combination of the reactance compensation technique and third-harmonic tuning to cover a half-decade frequency bandwidth of 0.4 - 2.0 GHz with high operating efficiency. GaN power amplifier device provides higher power, greater efficiency and wider bandwidth (Hamza & Nirmal, 2020).

3.1.1 Reactance Compensation and Third Harmonic Tuning

From the theoretical considerations, it was found out in mid-1960s that the bandwidth response of a parametric amplifier can be improved using multiple-resonant band-pass filters for the signal and idling circuits rather than utilizing simple resonant circuits (DeJager, 1964; Matthaei, 1961). At the same time, it was analytically calculated that the added resonant circuits should have an appropriate Q_L-factor to optimally reduce the rate of change in reactance of both the signal and idling circuits (Humphreys, 1964).

To describe reactance compensation circuit technique, consider the simplified equivalent load networks with a shunt resonant L_pC_p circuit followed by a series resonant L_sC_s circuit, as shown in Figure 3.1. In this case, both resonant circuits are tuned to the fundamental frequency ω_0 and R is the load resistance. The reactance of a resonant circuit varies with frequency. It increases in a series resonant circuit and decreases in a loaded parallel resonant circuit in the vicinity of the resonant frequency. As a result, at near resonant, the positive slope of reactance in the series circuit is compensated with a proportional

negative slope of reactance in a shunt configuration. By diligently choosing the components in the shunt circuit, the rate of change in the reactance with frequency can be made exactly opposite to that of the series circuit, thus producing a nullified variation over a wide frequency bandwidth.

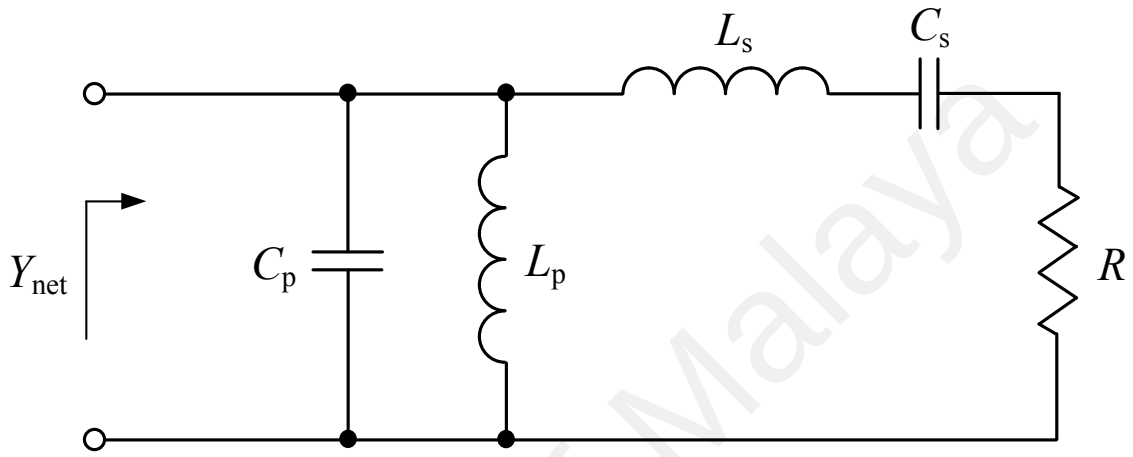

Figure 3.1: Reactance compensation network with lumped elements.

Consider the load network admittance Y_{net} corresponding to a single-reactance compensation circuit shown in Figure 3.1, which can be written as:

$$Y_{net}(\omega) = \left(j\omega C_p + \frac{1}{j\omega L_p} + \frac{1}{R + j\omega' L_s}\right) \tag{3.1}$$

where

$$\omega' = \omega\left(1 - \frac{\omega_0^2}{\omega^2}\right) \tag{3.2}$$

and $\omega_0 = 1/\sqrt{L_s C_s} = 1/\sqrt{L_p C_p}$ is the resonant frequency.

At the resonant frequency when $\omega' = 0$, the load network admittance $Y_{net}(\omega)$ reduces to

$$Y_{net}(\omega) = \left(j\omega C_p + \frac{1}{j\omega L_p} + G\right) \tag{3.3}$$

where $G = 1/R$ is the load conductance.

The frequency bandwidth with zero susceptance will be maximized if, at a resonant frequency ω_0,

$$\left.\frac{dB_{net}(\omega)}{d\omega}\right|_{\omega=\omega_0} = 0 \tag{3.4}$$

where

$$B_{net}(\omega) = ImY_{in}(\omega) = \omega C_p - \frac{1}{\omega L_p} - \frac{\omega\prime L_s}{R^2+(\omega\prime L_s)^2} \tag{3.5}$$

is the load network susceptance.

As a result, an additional equation can be written as

$$C_p + \frac{1}{\omega_0^2 L_p} - \frac{2L_s}{R^2} = 0 \tag{3.6}$$

From (3.6) it follows that the loaded quality factor of the shunt circuit $Q_p = \omega C_p R$ is equal to the loaded quality factor of the series compensating circuit $Q_s = \omega L_s/R$. Figure 3.2 shows the expected frequency behavior of the real and imaginary components of the load-network impedance with a reactance compensation of $Q_p = Q_s = 0.25$ at midband frequency of 1 GHz (R = 50 Ω and C_p = 0.8 pF). The component Re(Z_{net}) shown in Figure 3.2 (*a*) is almost constant with ±2% variation within an octave frequency band, range from 0.7 to 1.4 GHz, whereas the Im(Z_{net}) component shown in Figure 3.2 (*b*) is flat across 0.6 - 1.6 GHz.

However, $Q_p = Q_s = 0.25$ is not an optimum value. A more constant performance for Re(Z_{net}) can achieved with optimized Q_s = 0.15, as shown in Figure 3.3(*a*). In this case, smaller variation of the output power can be achieved over a wide frequency band, and higher efficiency can be achieved using a mixed-mode operation when inductive and capacitive reactances can be present at different bandwidth frequencies. In this case, the load-network reactance changes from the inductive reactance at 0.5 GHz to the capacitive reactance at 2.5 GHz, as shown in Figure 3.3 (*b*).

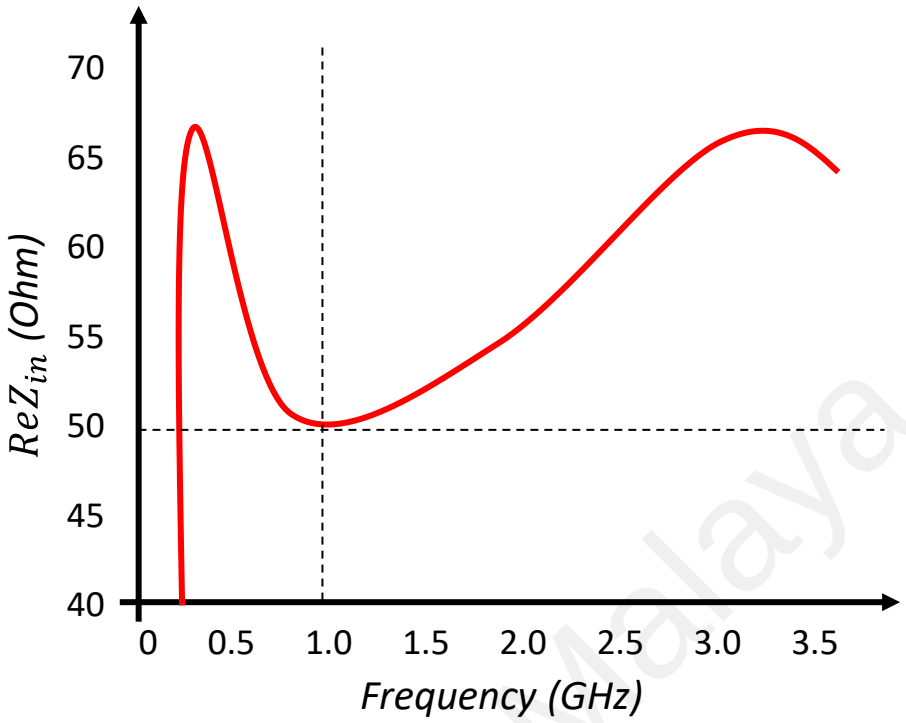

(a)

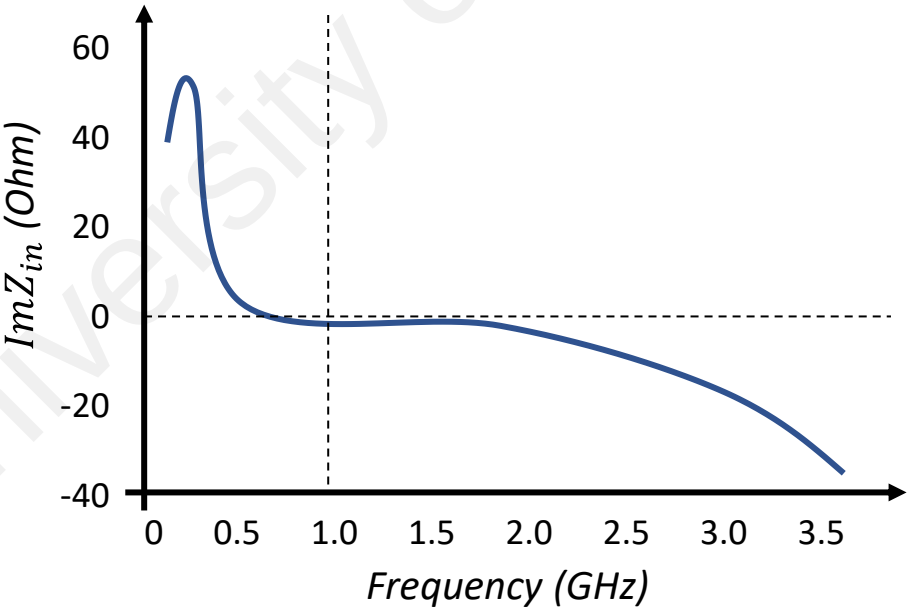

(b)

Figure 3.2: Real (a) and imaginary (b) parts of the input impedance characteristics over a wide frequency band, when Qs = 0.25 at 1 GHz.

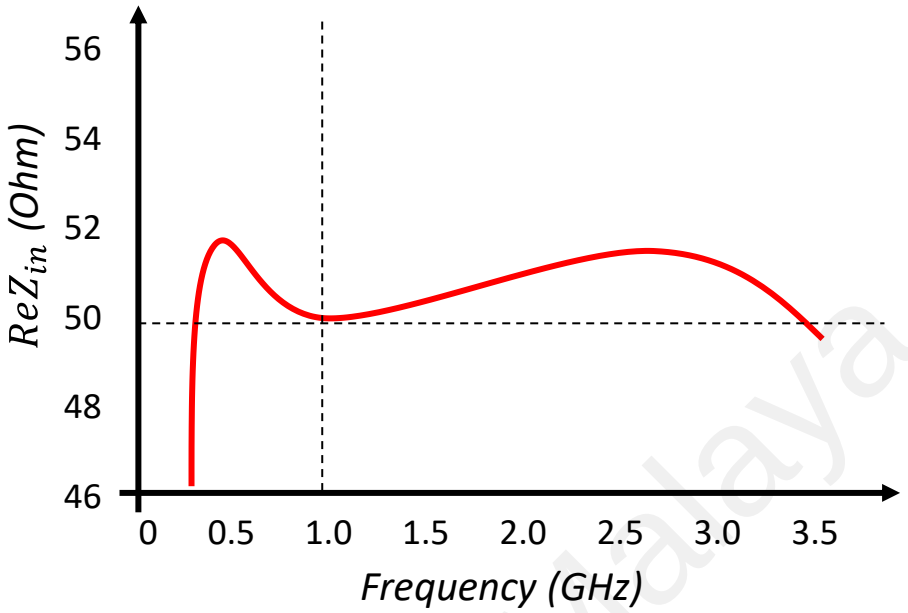

(a)

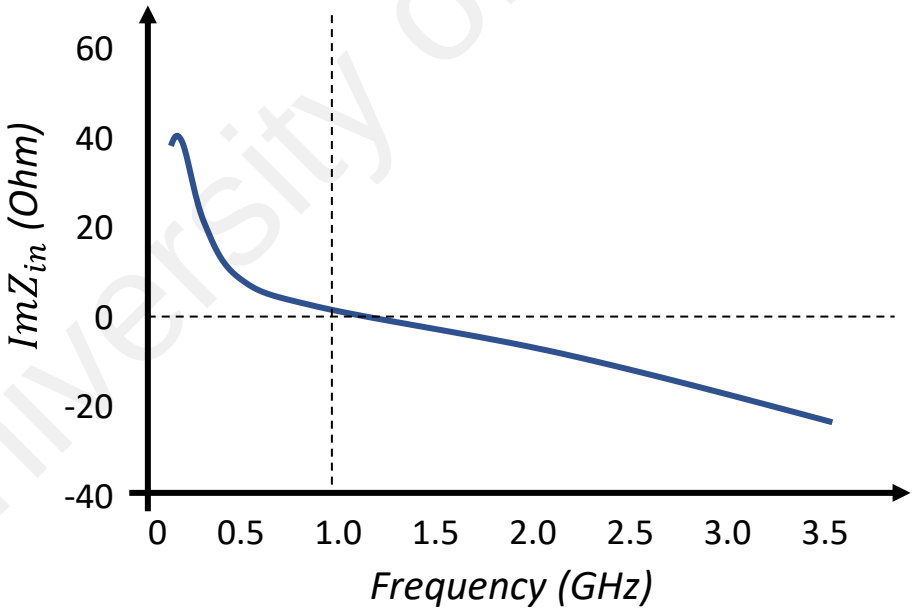

(b)

Figure 3.3: Real (a) and imaginary (b) parts of the input impedance characteristics over a wide frequency band, when Qs = 0.15 at 1 GHz.

Figure 3.4 shows the reactance compensation load network with a low-pass matching section which includes the third-harmonic resonant circuit to approximate Class-F mode of operation at a higher bandwidth of frequency in increasing efficiency (in this case, the third harmonic of lower frequencies is not tuned). The third harmonics resonant circuit $L_{m3}C_{m3}$ provides a capacitive reactance at the fundamental frequency that results in an open-circuit condition at the output. This is due to parallel resonant circuit formed by the shunt capacitor C_p and the equivalent inductor consists of the shunt inductor L_p and the series $L_sC_sL_m$ components.

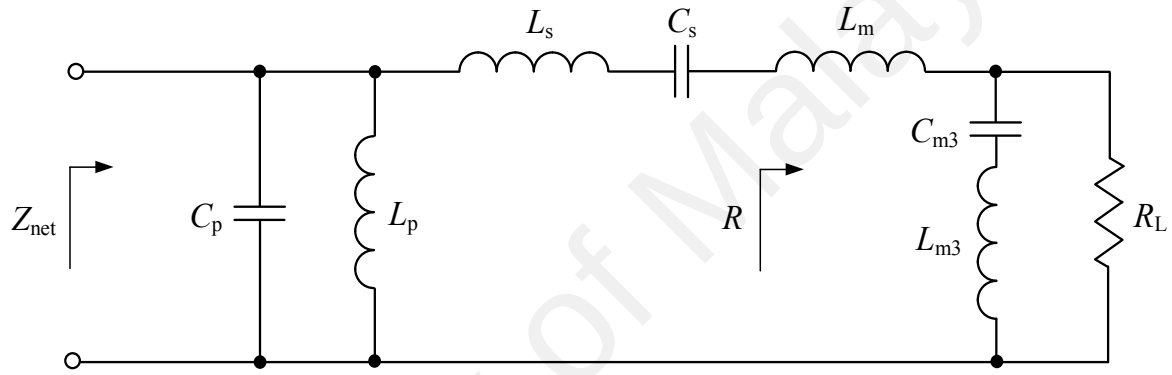

Figure 3.4: Broadband matching network with third-harmonic trap.

The reactive component of the input impedance $\mathrm{Im}(Z_{net})$ should be set to infinite to approximate Class-F mode operation at center bandwidth frequency, ω_0. The third harmonics resonant circuit $L_{m3}C_{m3}$ is tuned to zero at high frequency ω_h, thus resulting in:

$$\omega_h C_p - \frac{L_p + L_m + \frac{8}{9}L_s}{\omega_h L_p\left(L_m + \frac{8}{9}L_s\right)} = 0 \tag{3.7}$$

For the simplified case of equal quality factors when $Q_L = R/\omega L_p = \omega L_s/R = \omega L_m/R$, from Eq. (3.7) it follows that

$$Q_L \cong 0.25 \tag{3.8}$$

the low value of Q_L allows the high efficiency operation over a wide frequency band. The quality factor of 0.25 in Eq. (3.8) corresponds to the theoretical value for reactance compensation circuit for maximally flat reactance as depicted in Eq. (3.4).

3.1.2 Broadband High-Efficiency Power Amplifier Design

A high-efficiency power amplifier is designed using 40 dBm GaN HEMT Cree device CGH40010F (CREE, 2006-2007) with an output shunt capacitance of 1.3 pF at V_{dd} = 28 V. For single reactance compensation circuit, at ω_0, the reactance increases in a series resonant circuit and decreases in a loaded parallel resonant circuit, thus reduces the overall reactance of the load network. This technique can directly be applied to parallel-circuit Class E PA as shown in Figure 3.5, because the load network has the exact same structure (Andrei Grebennikov, 2011).

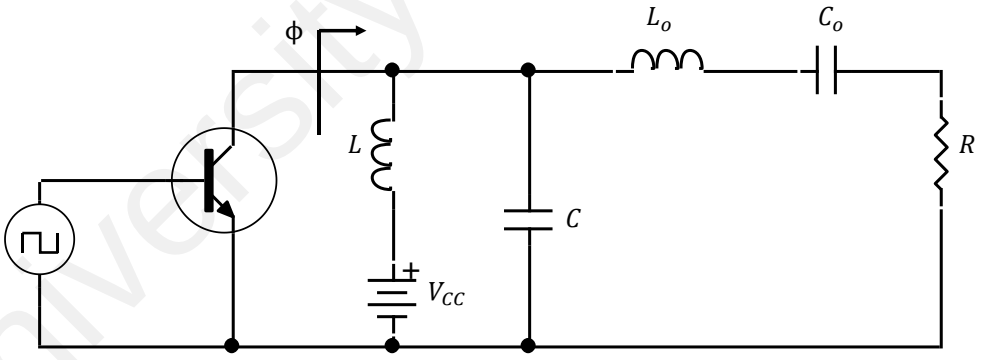

Figure 3.5: Parallel circuit Class E Power Amplifier.

It has been learnt in the previous section that loaded quality factor of the shunt circuit $Q_p = \omega C_p R$ is equal to the loaded quality factor of the series compensating circuit $Q_s = \omega L_s/R$. The shunt capacitance of the device selected is 1.3 pF and the impedance of load network (impedance of the device at 1.0 GHz and load) is 10.3Ω. Therefore,

$$Q_p = \omega_0 C_p R = 2\pi * 1.0\ GHz * 10.3\Omega * 1.3\ pF = \sim 0.1 \quad (3.9)$$

hence,

$$L_p = \frac{R}{\omega_0 Q_p} = 16\ nH \tag{3.10}$$

$$L_s = \frac{Q_s R}{\omega_0} = \sim 0.2\ nH \tag{3.11}$$

$$C_s = \frac{1}{\omega_0 Q_s R} = 155\ pF \tag{3.12}$$

As for third harmonic tuning, circuit C_{m3} and L_{m3} from Figure 3.4 has zero impedance at third harmonic, hence,

$$C_{m3} = \frac{5}{4} C_p = 1.6\ pF \tag{3.13}$$

$$L_{m3} = \frac{1}{5\omega_0^2 C_p} - L_m = 0.6\ nH \tag{3.14}$$

where, ω_0 = 2.1 GHz (high fundamental frequency) and $L_m = L_s$ according.

The third harmonic tuning circuit will behave as parallel tank at the third harmonic combining of shunt capacitive reactance and inductive series reactance having high impedance seeing by the device output. L_m in Figure 3.4 is a series inductance of a low-pass matching section where third-harmonic circuit provides capacitive reactance at lower frequencies within operating frequency range.

To validate the above theories, simulation has been carried as shown in Figure 3.6. The input lossy matching circuit includes a series RC circuit, as well as a shunt RL circuit to provide broadband input matching with minimum input insertion loss. RL circuit connected in parallel to the device or any circuit input having series RC equivalent representation provides broadband reactance compensation when both R are equal, and L and C resonate at midband frequency. R and C are usually either known transistor or circuit parameters, but both R and L can be optimized for better performance over frequency. By using the input matching network shown in Figure 3.6 (including a 1 nF capacitor in series with the parallel

combination of a 5 Ohm resistor and a 10-pF capacitor), the stability is improved at low frequencies (because of the presence of resistor) and the power gain is improved at high frequencies (resistor is bypassed). Increasing the power gain at high frequencies compensates for the lower device gain and improves gain flatness. In this case, the series resonant circuit is tuned to 1.0 GHz, whereas the third-harmonic circuit is optimized to 6.5 GHz (referring to higher fundamental frequency).

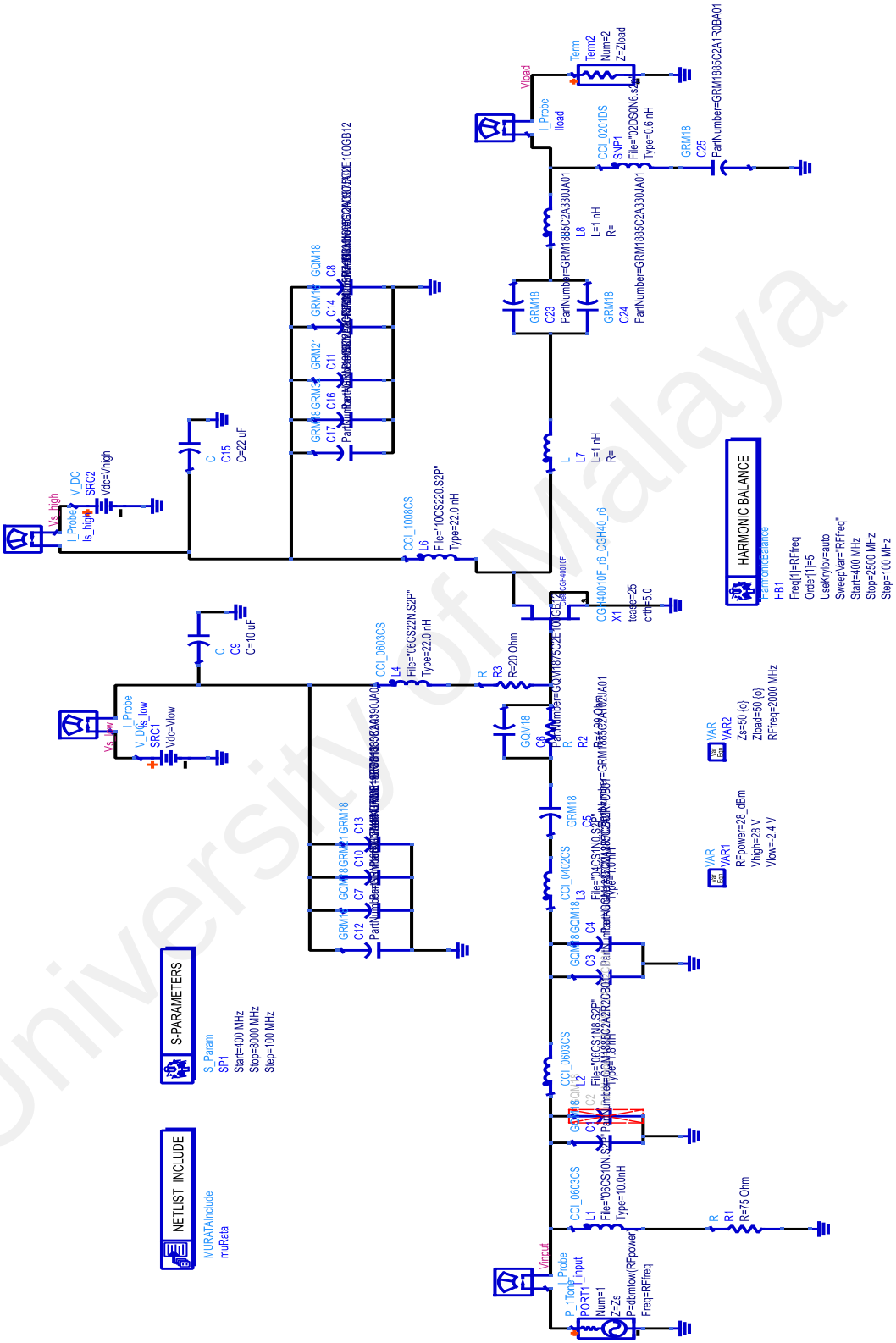

Figure 3.6: Broadband Circuit Design in ADS.

Circuit optimization has been made in simulation in order to achieve desired performance. The interest is to achieve 40 dBm output power with more 60% drain efficiency across the band.

3.1.3 Prototype Development for Ultra-Broadband Mixed-Mode GaN HEMT Power Amplifier

3.1.3.1 Layout Design

Based on the simulation performed and its results, the layout of actual board has been developed as shown in Figure 3.7. The input and output matching network for broadband design is only within a small area, highlighted in yellow box. The extended line at both input and output as shown in red boxes are 50-ohm line connected to SMA connector for measurement purpose. The DC biasing, Vgs and Vds, follows based on the recommendation provided in the datasheet (CREE, 2006-2007). The layout is performed on 2-layer board, with components being populated in first layer and second layer as ground. Ground cut is provided along the matching network to provide better isolation and to avoid parasitic effects, which may cause severe effects at higher frequencies (Rider, Kuhn, & Wolf, 2017). Sufficient ground via-holes are provided to ensure maximum return ground current, especially along the matching network and biasing traces, to avoid high impedance path for current. Six screw holes are provided to mount the board on heat sink. The diameter of the outer radius of screw hole is 9.5mm whereas the inner radius is 5mm diameter. To mount CREE devices and to have direct contact with heat sink, the board is designed with cavity according to the device's dimension. It is very important to ensure heat is dissipated to heat sink and avoid degradation in device's performance.

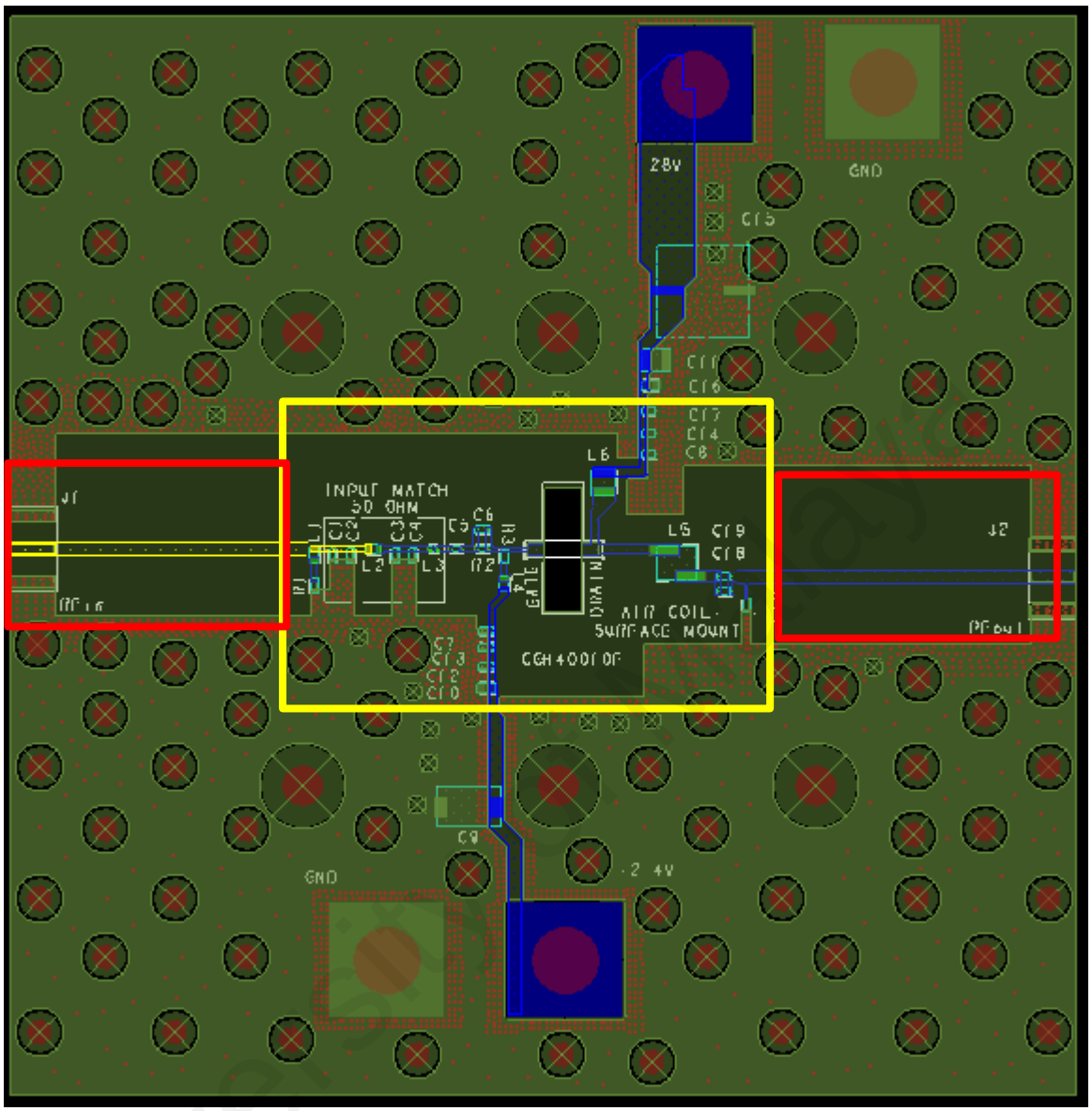

Figure 3.7: Printed Circuit Board (PCB) layout design.

3.1.3.2 Heat sink Design

Heat sink is important for the continuous operation of a power amplifier. It has prominent role to ensure the heat dissipated by the PA device is evenly spread and not trapped under the device. Otherwise the device will become hot and the performance of the PA will be degraded. In fact, improper thermal dissipation design can shorten the amplifier life or even damage it permanently. For every PA device, the manufacturer will specify the maximum temperature specification that it can sustain at device ground or the junction between the device and PCB. This is referred as Junction Temperature. If the junction temperature exceeds the specified limit, it can cause damages to the device or exhibits improper behaviour. Therefore, a heat sink is attached under the PCB in order to allow maximum heat dissipation. A standard aluminium heat sink is used. The heat sink in this work has dimensions of 108.5mm x 74mm with 25mm of thickness. The design of the heat sink top view and side view is shown in Figure 3.8 and Figure 3.9 respectively.

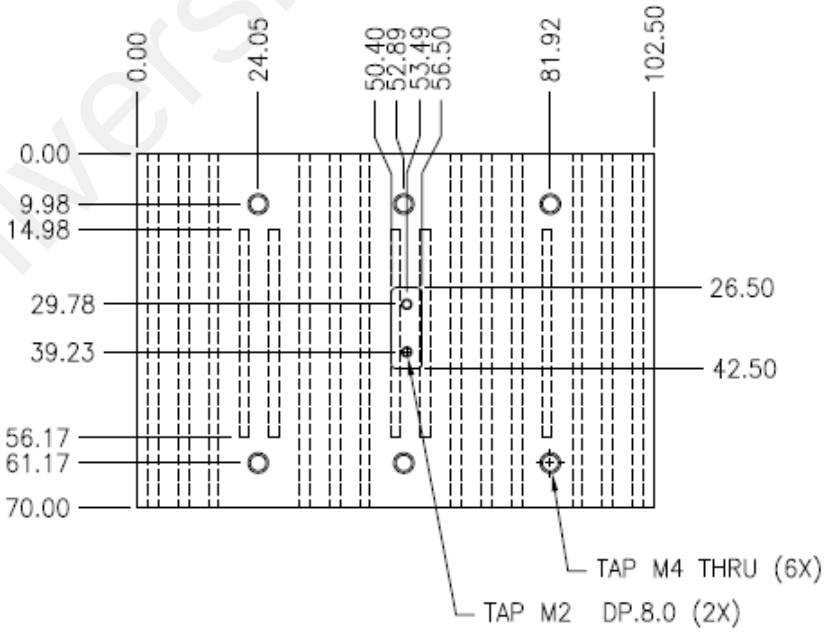

Figure 3.8: Top view of the heat sink.

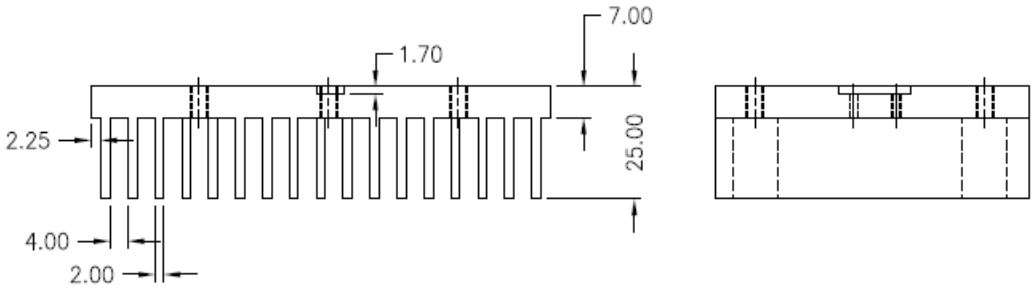

Figure 3.9: Side view of the heat sink.

A small cavity measured with depth of 1.7mm is designed in the area where the device is placed. This is due to a thick gold layer of the CREE transistor which is thicker than the PCB. The cavity will ensure maximum contact between the device and heat sink.

3.1.3.3 Experimental Prototype Development

A prototype board of the design has been developed integrating CREE's CGH40010 GaN HEMT to experimentally verify the proposed broadband power amplifier design method. The board has been fabricated using two-layer Rogers PCB platform, with dielectric constant of 3.66 and substrate thickness of 0.762 mm. The photograph of the prototype board for wideband power amplifier design for top, front and side view are shown in Figure 3.10, Figure 3.11 and Figure 3.12 respectively. The board consists RF input and output ports, two voltage supply feeds for drain voltage and gate voltage, input and output matching networks, consuming an overall size of 120 x 122 mm^2.

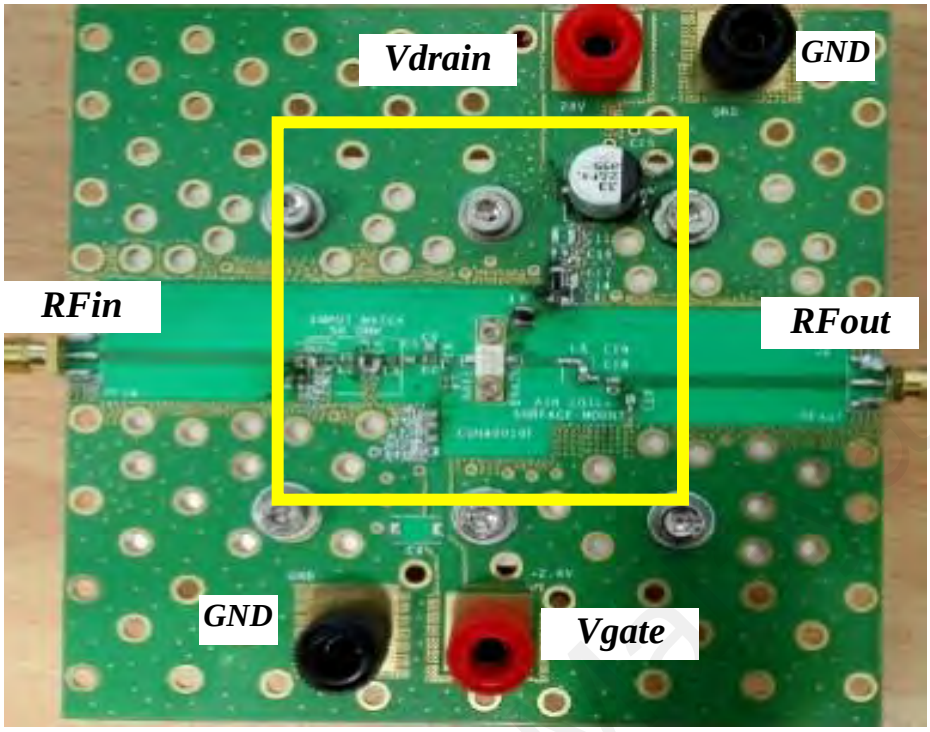

Figure 3.10: Full prototype of broadband power amplifier board (top view)

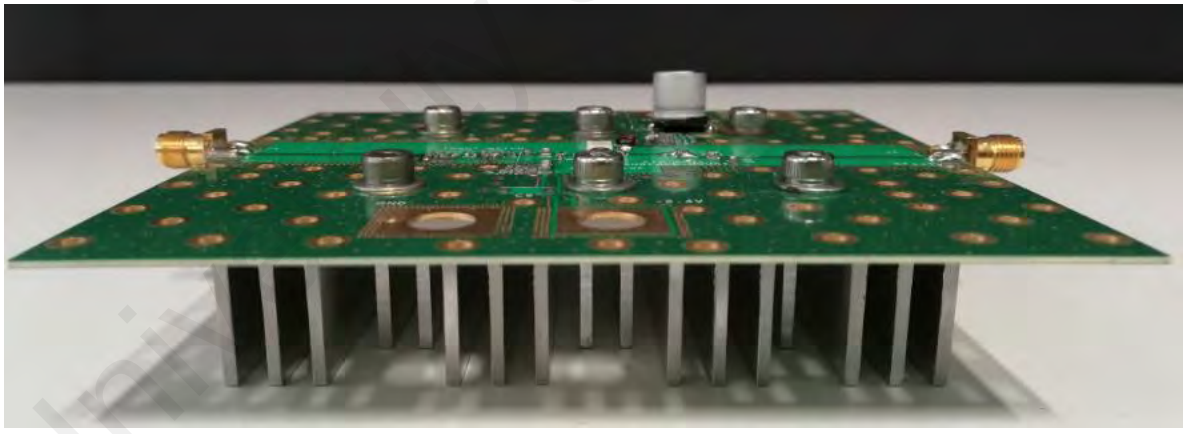

Figure 3.11: Full prototype of broadband power amplifier board (front view)

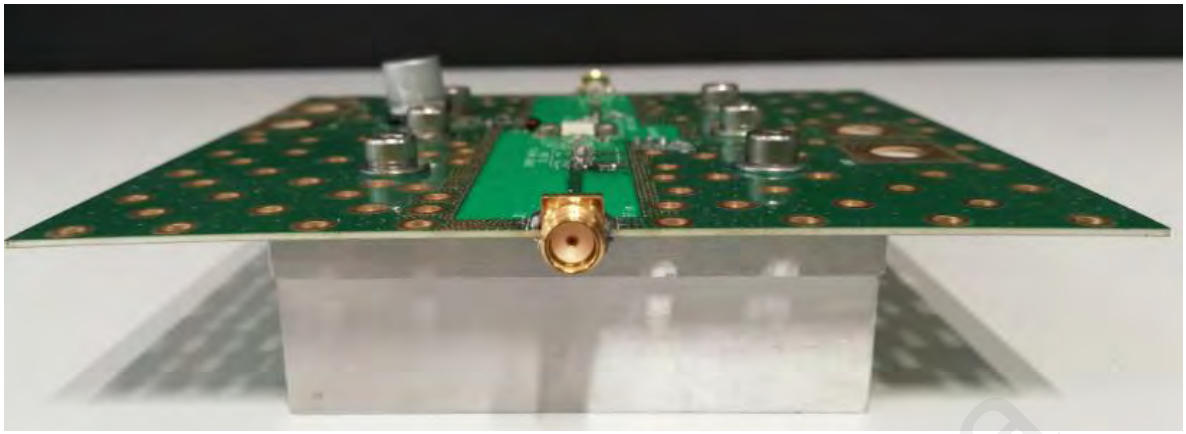

Figure 3.12: Full prototype of broadband power amplifier board (side view)

However, the effective size area relevant to the power amplifier is much smaller, with an area of 55 x 60 mm2 (highlighted in yellow color). The test board is mounted on heatsink using six screws, to provide solid hold between PCB and heatsink. This accommodates good heat dissipation. Several chip capacitors (10 pF, 39 pF and 470 pF) are used to bypass dc gate biasing to ground. The dc-feed lines for the power amplifier consist of high-*Q* air-wound coil inductor.

The board has been designed with well isolated open grounding area, and sufficient via-holes. DC and RF signals are carefully routed so that their coupling is minimized. The width of the DC routing to the drain of the transistor is carefully selected to ensure optimum DC current carrying capacity during operation (Andrei Grebennikov, 2011). For better grounding and to ensure the performance of the power amplifier design, the via-holes are well distributed, with dedicated grounding via-holes for all shunt components.

3.1.4 Measurement Setup for Broadband PA evaluation

Figure 3.13 shows test setup for Power or Gain and Drain efficiency measurement. Rohde and Schwarz SMA 100A signal generator is required to provide input power of 28 dBm to the prototype board. Two power supplies are required; one to supply drain Voltage, Vds and another to bias PA gate, Vgs. The drain supply voltage is 28 V and the quiescent current is set in the range of 40-90 mA. A bias voltage of -2.4 V has been applied to the gate of the power amplifier. Output of the board is connected to a Rohde and Schwarz FSG spectrum analyser to measure the output power level of the prototype across the frequency.

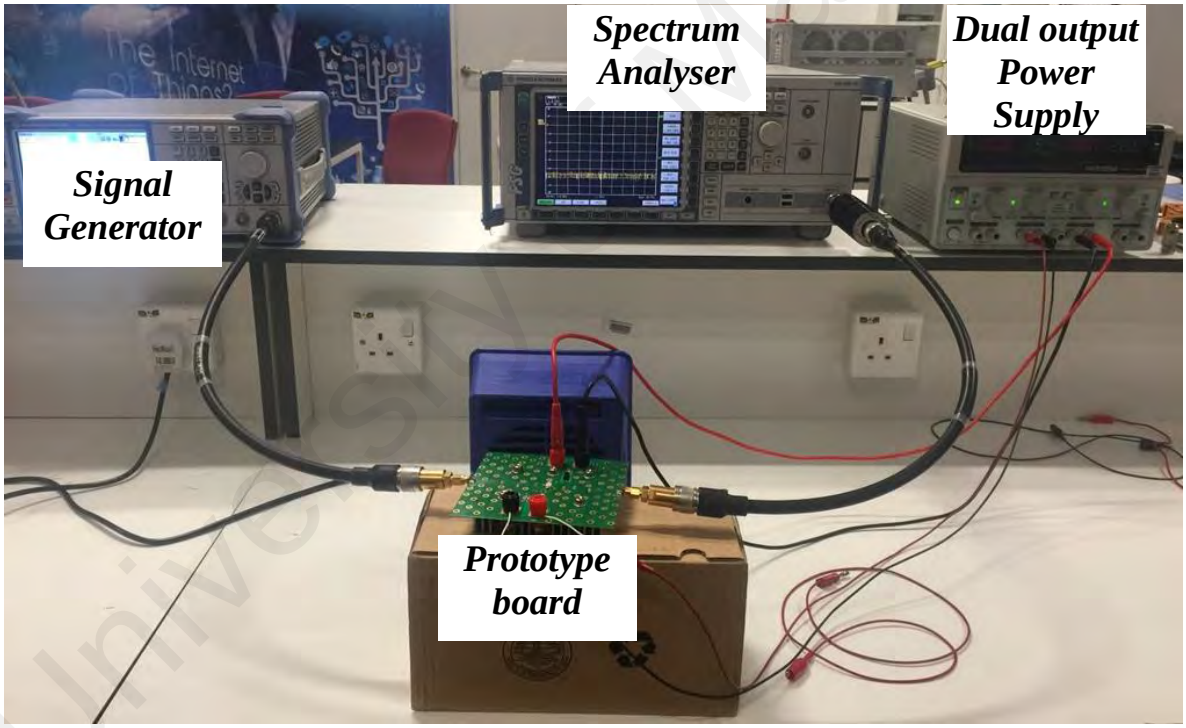

Figure 3.13: Measurement setup for prototype board evaluation

3.2 Broadband RF Power Amplifier Adopting the Combination of Large Signal X-Parameter and Real Frequency Techniques (RFT)

In this section, a new design approach of broadband RF power amplifier (PA) is introduced in this work with combination of large signal X-parameter and Real-Frequency Technique (RFT). A theoretical analysis of large signal X-parameter is revisited, and a simplification method is introduced to determine the optimum large signal impedances of a Gallium Nitride HEMT (GaN HEMT) device. With the optimum impedance extraction over the wide frequency range (0.3 to 2.0 GHz), a wideband matching network is constructed employing RFT and the final design is implemented with practical mixed-lumped elements.

3.2.1 Large Signal X-Parameter Impedance Extraction

Concept of X-parameters is based on Poly Harmonic Distortion (PHD) modelling technique (Biernacki et al., 2017; Joujili et al., 2016; Pichler, Leder, Magerl, & Arthaber, 2017; Wang, Nielsen, Jensen, & Larsen, 2014). It is simply an extension of S-parameters under large signal conditions. For active and passive devices, S-parameters merely describes a linear relationship between input and output ports in terms of incident and reflected wave parameters. On the other hand, PHD approach, assumes the presence of discrete tone signals (multisines) for the incident as well as for the scattered waves (Verspecht & Root, 2006). Detailed explanation is provided in section 2.6.

The basic PHD model (2.26) simply describes that the B-waves result from a linear mapping of the A-waves, similar to the classic S-parameters. However, in large signal, A_{11} wave creates a phase reference point for all of the other incident A-waves, and the contribution to the B-waves of a particular A-wave depends on the phase relationship between this particular A-wave and the large signal A_{11} wave. This relative phase dependency is expressed in (2.26) through the presence of the conjugate A-wave terms. This

is clarified with the following example. Consider (2.26) restricted to the simple case of a B_{21} (fundamental at the output) depending on A_{21} (reflected fundamental at the output) and A_{11} (fundamental incident at the input). In this case, (2.26) is reduced to

$$B_{21} = S_{21,11}(|A_{11}|)A_{11} + S_{22,11}(|A_{11}|)A_{21} + T_{22,11}(|A_{11}|)P^2 conj(A_{21}) \quad (3.15)$$

By only considering 2nd and 3rd terms of (3.15) yields below:

$$\frac{\Delta_{21}B_{21}}{A_{21}} = S_{22,11}(|A_{11}|) + T_{22,11}(|A_{11}|)e^{-j2(\varphi(A_{21})-\varphi(A_{11}))} \quad (3.16)$$

The first term in (3.16) is a function of the amplitude of A_{11} only and behaves exactly like a classic S_{22} (except for the fact, of course, that it depends on the input signal amplitude). The second term depends not only on the input signal amplitude through the function $T_{22,11}(|A_{11}|)$ but also on the phase difference between A_{21} and A_{11} through the complex exponential. Note that it is not dependent on the amplitude of A_{21}.

3.2.1.1 Transmission Line Theory for Large Signal Impedance Extraction

This work has been further developed using (3.16), therefore, $S_{22,11}(|A_{11}|)$ information is sufficient to extract large signal device output impedance and similar derivation will also yield large signal $S_{11,11}(|A_{11}|)$ for input port, hence, large signal input impedance of the device can be extracted as well.

High power device impedance with optimum power performance is extracted as represented in Figure 3.14. Transmission line with optimum characteristic impedance, $Z_{o(1 \text{ or } 2)}$ and electrical length, $\theta_{(1 \text{ or } 2)}$, are essential between source and device input, and load and device output, to match the device to the source and load respectively, hence, delivering optimum power with good efficiency. Large signal device input and output impedances can be obtained with reflection coefficient information. For instance, load reflection coefficient, Γ_out (x) at distance x can be expressed as:

$$\Gamma_{out}(x) = B_{21}e^{j\beta x}/A_{21}e^{-j\beta x} \tag{3.17}$$

where, incident and reflected waves are denoted as $Ae^{-j\beta x}$ and $Be^{j\beta x}$ respectively. In this case βx is electrical length of the transmission line, or $\theta_{(1 \text{ or } 2)}$ as stated above.

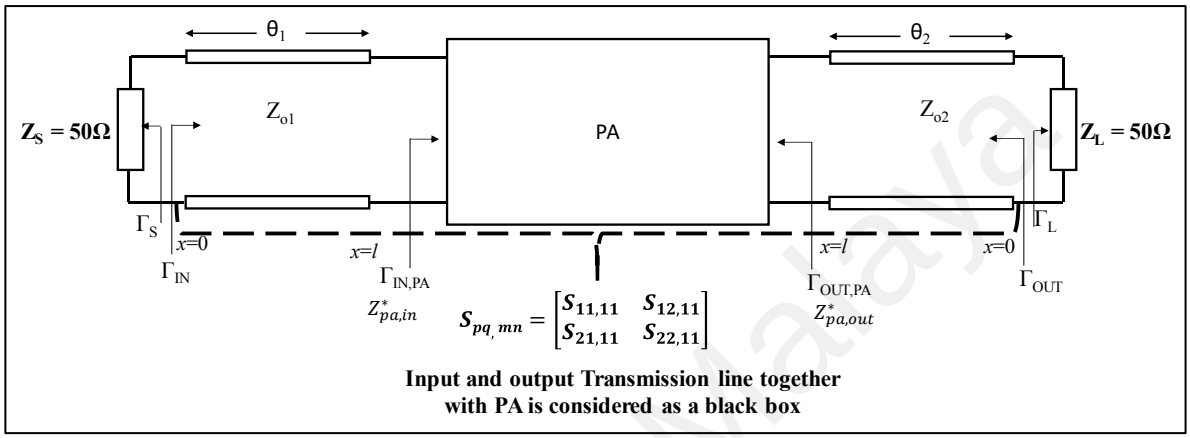

Figure 3.14: Simplified large signal device impedance extraction under 2-port network condition

Output reflection coefficient, Γ_{OUT} of the board in Figure 3.14 can be expressed as:

$$\Gamma_{OUT} = S_{22,11} + \frac{S_{12,11}\,\Gamma_S\,S_{21,11}}{1-\Gamma_S S_{11,11}} \tag{3.18}$$

When the device is well matched at source, Γ_S is assumed to be zero, hence based on (3.18)

$$\Gamma_{OUT} = S_{22,11} = \Gamma_{out}(0) \tag{3.19}$$

However, the interest lies in obtaining $\Gamma_{OUT,PA}$, to determine large signal output impedance of the device. This can be obtained as below,

$$\Gamma_{out}(l) = \Gamma_{OUT}e^{2j\theta_2} = \Gamma_{OUT,PA} \tag{3.20}$$

Hence, large signal device output impedance, $Z^*_{pa,out}$ simply can be obtained via equation below,

$$Z^*_{pa,out} = Z_{o2}\frac{1+\Gamma_{OUT,PA}}{1-\Gamma_{OUT,PA}} \tag{3.21}$$

The input large signal impedance, $Z^*_{pa,in}$ can be determined with similar concept.

3.2.1.2 Proof of Concept via Simulation

Based on Figure 3.14, as a proof of concept, a test bench evaluated to validate above theory, to deliver 40 dBm output power with efficiency of more than 65% over a wide bandwidth, 0.3 – 2.0 GHz. This is established via simulation, where characteristic impedance, $Z_{o(1 \text{ or } 2)}$ and electrical length, $\theta_{(1 \text{ or } 2)}$ are carefully optimized to obtain desired output power and maximum efficiency for 0.5 GHz, 1.0 GHz, 1.5 GHz and 2.0 GHz independently, while maintaining Z_S and Z_L equals to 50 Ω. The optimized transmission line and active device (DUT) is considered as a 'single black box'. Its X-parameter data, Γ_{OUT} and Γ_{IN}, are extracted via simulation under 50 Ω condition too.

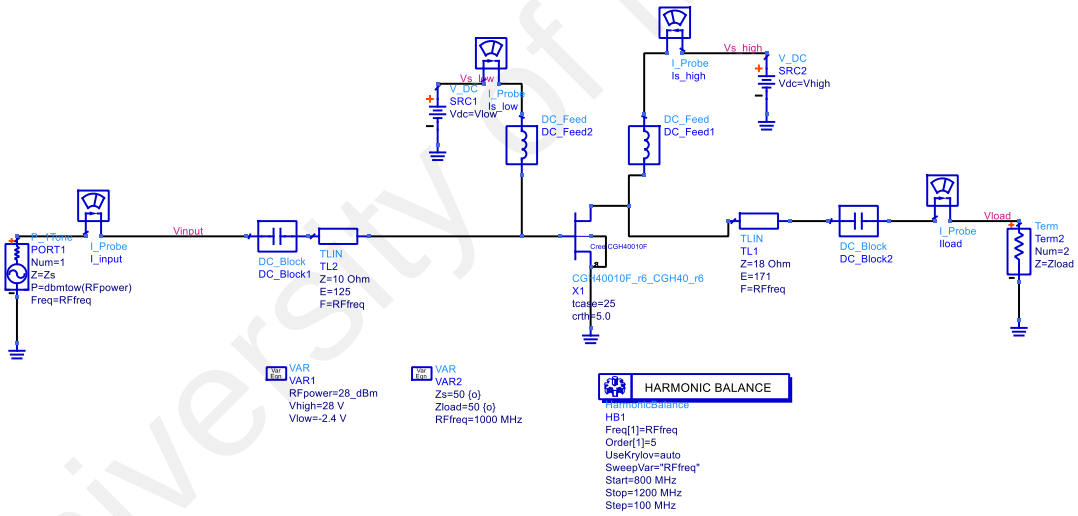

Figure 3.15: GaN PA with optimum input and output transmission line at 1 GHz.

Figure 3.15 shows GaN PA is simulated at 1 GHz to deliver desired 40 dBm output power with almost 70% efficiency. Both the input and output of the device are terminated to 50 Ω load. The input and output transmission lines are optimized to achieve the said performance.

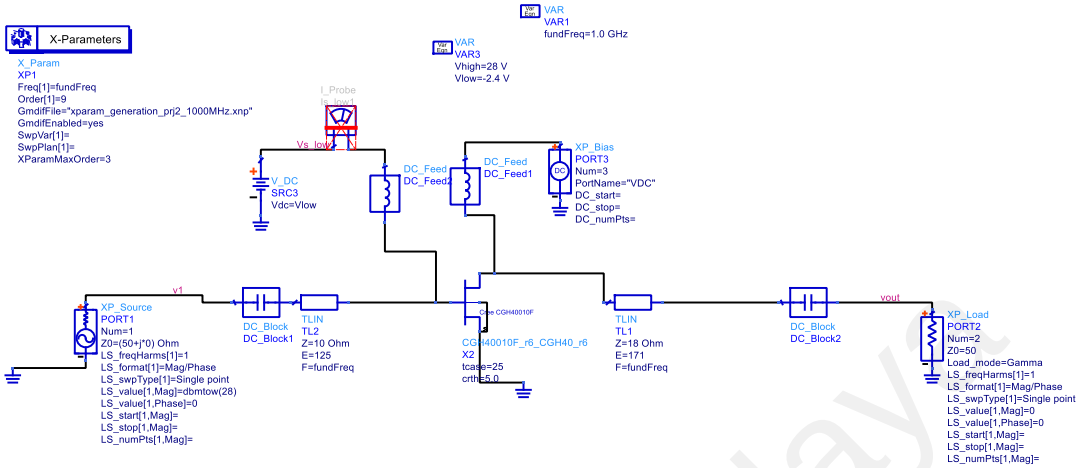

Figure 3.16: Simulation schematic to extract large signal Γ_{OUT} and Γ_{IN} at 1 GHz.

The schematic with optimum input and output transmission line as in Figure 3.15, is further simulated using X-parameter to retrieve its corresponding Γ_{IN} and Γ_{OUT} as depicted in Figure 3.16. The extracted X-parameter data will be used in (3.20), hence, the device large signal input and output impedance can be obtained based on (3.21). The whole process is repeated for each frequency point 0.5 GHz, 1.5 GHz and 2.0 GHz dedicatedly. The impedances obtained will be used in following section, to develop broadband matching network using RFT.

3.2.2 Broadband Matching Network Development using RFT

In this section, a broadband matching development methodology based on the large signal impedance data extracted in previous section will be discussed. Assuming $S_{12,11}$ is small enough, RFT-Single is adopted in this work to establish a solution for wideband matching network. The bandwidth operation of this work is to comply an operational frequency range from 0.3-2.0 GHz. The maximum power about 40 dBm and a minimum drain efficiency of 65% is targeted. The supply voltage requirement is 28 V, therefore the suitable device technology to meet the power performance (max. power and efficiency) is GaN HEMT technology from CREE Inc. (CGH40010H) (CREE, 2006-2007).

3.2.2.1 Initial matching network construction using RFT MATLAB tool

For initial stage, MATLAB tool based on RFT algorithm as discussed in section 2.7 has been developed by Prof. Siddik Yarman. Initial matching network construction will be developed in this tool by entering the desired value for each parameter. User will be prompt by the command window for parameter insertion, which will result in the network development and optimization process by the algorithm. Eventually, the structure of the input and output matching network and the graph of TPG will be shown. In Table 3.1, each of the command prompt for input parameter will be explained briefly.

Table 3.1: MATLAB input parameter description

f_o	1500 MHz; Normalized frequency in MHz.
T_o *(dB)*	0.8; Targeted flat gain level
ntr	0; Control flag which is set according to designer's desire. When *ntr*=1, ideal transformer would be included into the design; for *ntr*=0, designer must work with low-pass prototype with no ideal transformer
k	0; Order of transmission zeros in DC
$h= [h_1, h_2, h_3, \ldots, h_o]$	[1111111]; Input of coefficients for h to determine the elements of matching circuits. An ad hoc direct choice for the coefficients (h= ±1) would provide satisfactory initialization to start RFT algorithm (Binboga Siddik Yarman, 2008)
w_{low}	300 MHz; Low end of optimization frequency (normalized respect to selected frequency)
w_{high}	2000 MHz; High end of optimization frequency (normalized respect to selected frequency)
# N_opt	80; Sample points of optimization

When the MATLAB tool is set to run, it will prompt the user to insert desired value for each parameter, as given in Table 3.1. The algorithm of RFT will perform its task according to the parameters that have been entered in the command. The RFT tool will extract a file containing input and output impedances which was obtained in using large signal X-parameter in previous section. The optimization process will be executed by the algorithm according to the specification included for matching network. The tool will display a schematic diagram as shown in Figure 3.17 and its corresponding TPG graph as shown in Figure 3.18, once the whole algorithm process is completed. The values provided in the schematic diagram is not final, but this will serve as initial value for matching network development. The TPG graph indicates the performance of the matching network developed by the tool. The TPG of the matching network obtained is preferable to be as flat as possible. Furthermore, it is advisable that the graph obtain should be in the range of 0 to -1 (Aridas et al., 2014). The input coefficient of h is the coefficient that based on the ad hoc choices (±1). The number of elements (inductor and capacitor) presented are based on the number of coefficients, e.g. [1 1 1 1 1] represents 4 elements and the last value represents the termination of 50 Ω.

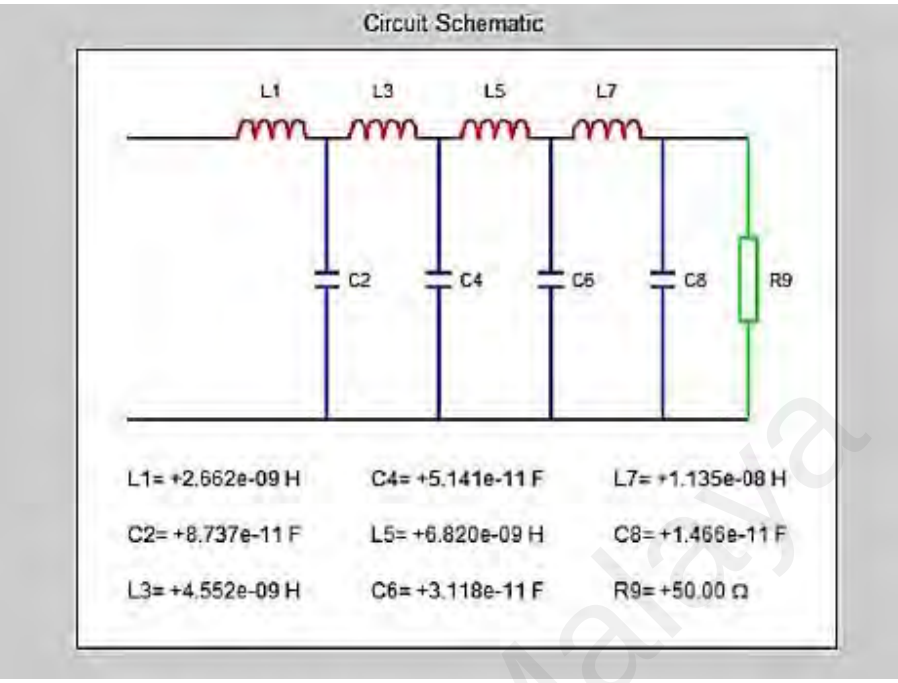

Figure 3.17: Example of output matching network obtained using RFT MATLAB tool.

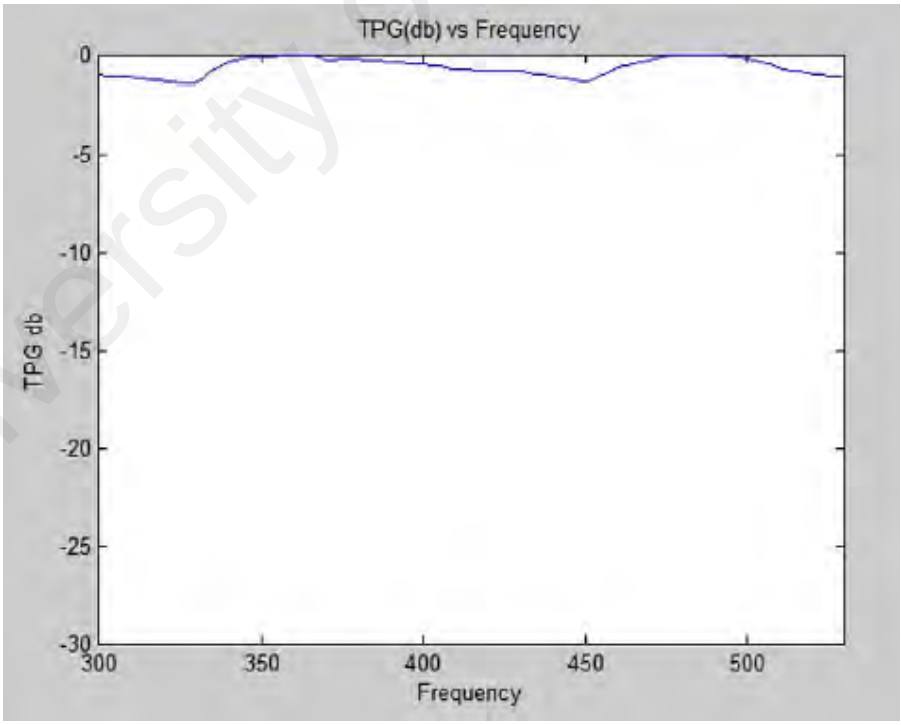

Figure 3.18: Example of TPG graph for output matching network obtained using RFT MATLAB tool.

3.2.3 Simulation of Complete Broadband PA design

As discussed in above section, initial values for input and output broadband matching network that provide TPG in the range of 0 to -1 are retrieved using MATLAB tool. Figure 3.19 and 3.20 provides the input and output matching values respectively.

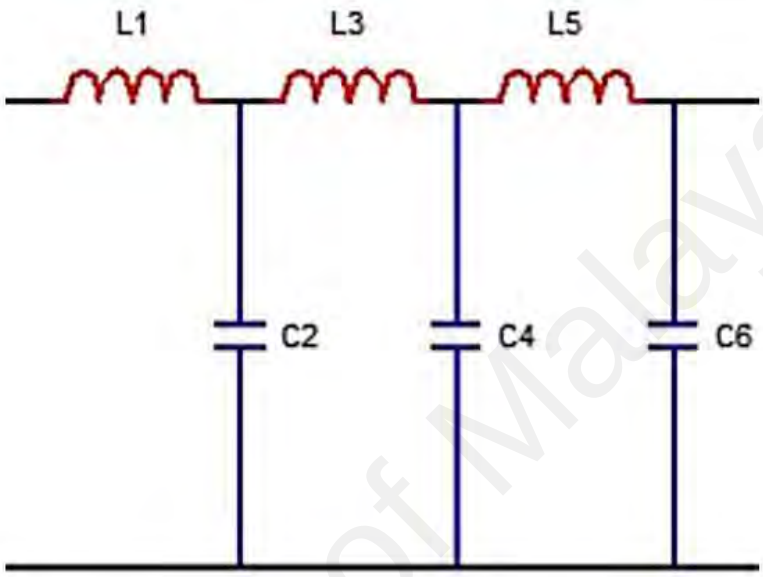

Components	Value
L1	1.79 nH
L3	1.65 nH
L5	2.36 nH
C2	1.5 pF
C4	1.2 pF
C6	1.8 pF

Figure 3.19: Input matching network obtained using RFT MATLAB tool.

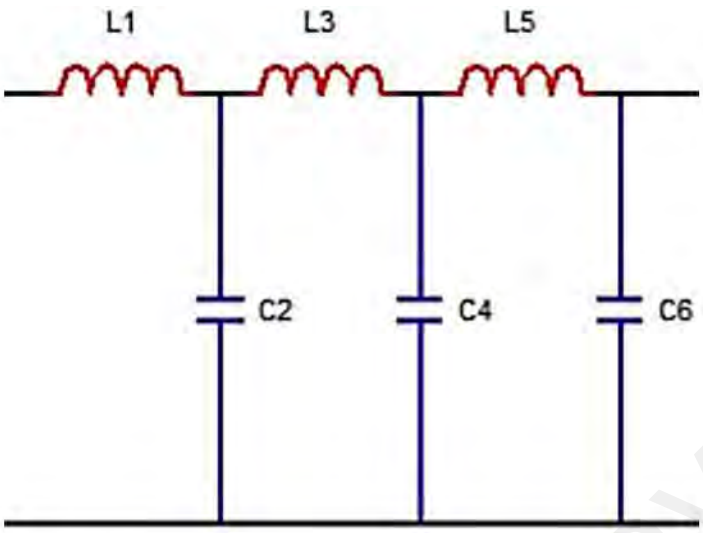

Components	Value
L1	1.70 nH
L3	3.30 nH
L5	2.71 nH
C2	1.2 pF
C4	1.6 pF
C6	1.5 pF

Figure 3.20: Output matching network obtained using RFT MATLAB tool.

The inductor values for both input and output matching network is represented by Coplanar Waveguide (CPWG) transmission line to provide optimum performance in broadband design. In order to translate all these values to CPWG, firstly, the characteristic impedance, Z_0 and electrical length, θ for each inductor need to be calculated. Mathematical equation of reactance, X for each inductor L is expressed as below:

$$X = 2\pi fL = Z_0 sin\theta \tag{3.22}$$

where, f represents the desired frequency.

Based (3.22), the values θ for corresponding L have been tabulated in Table 3.2 for both input and output matching network. Characteristic impedance, Z_0 is fixed at 50 Ω at f =1.5 GHz.

Table 3.2: Input and output CPWG θ

Input		Output	
L	θ	L	θ
L1	20°	L1	19°
L3	18°	L3	38°
L5	27°	L5	30°

Once the values are obtained, these Z_0 and θ are inserted in ADS LineCalc tool to synthesize the width, w and length l for the coplanar waveguide as shown in Figure 3.21. In order to ensure the transmission line maintains approximately 50 Ω for Z_0, w and g is fixed as 1.5 mm and 0.9 mm respectively. Hence, only l need be computed using the tool.

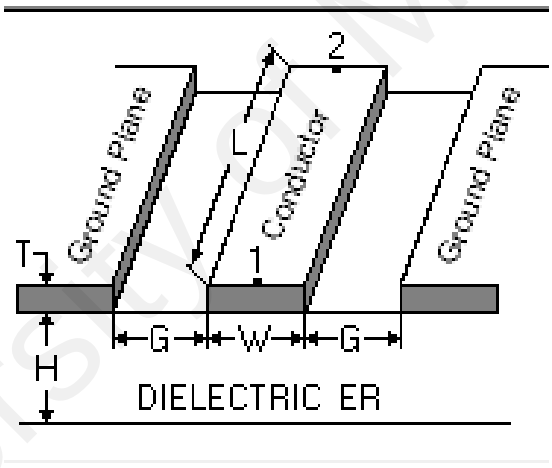

Figure 3.21: CPWG graphical representation

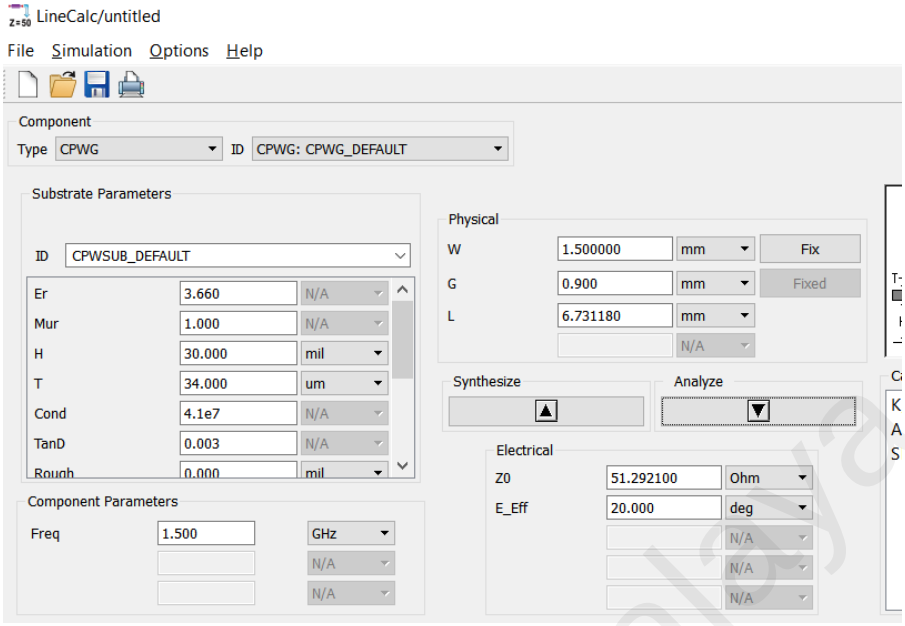

Figure 3.22: ADS LineCalc tool.

Figure 3.22 shows the ADS LineCalc tool used to calculate the length, *l* of CPWG. Besides *w* and *g*, dielectric constant, ε_r is fixed as 3.66 and substrate thickness, *h* as 0.762 mm (30 mil) based on the 2-layer Rogers 4350B PCB material that will be used for actual prototype board. Table 3.3 display the computed value for length of CPWG for both input and output matching network respectively.

Table 3.3: Input and output CPWG *l*

Input		Output	
L	*l* (mm)	L	*l* (mm)
L1	6.73118	L1	6.39462
L3	6.05806	L3	12.7892
L5	9.08709	L5	10.0968

Based on the values obtained from RFT MATLAB and ADS LineCalc tools, complete broadband PA design is simulated using ADS. Figure 3.23 shows the complete schematic of the PA design. Minor optimization performed to obtain optimum performance via simulation.

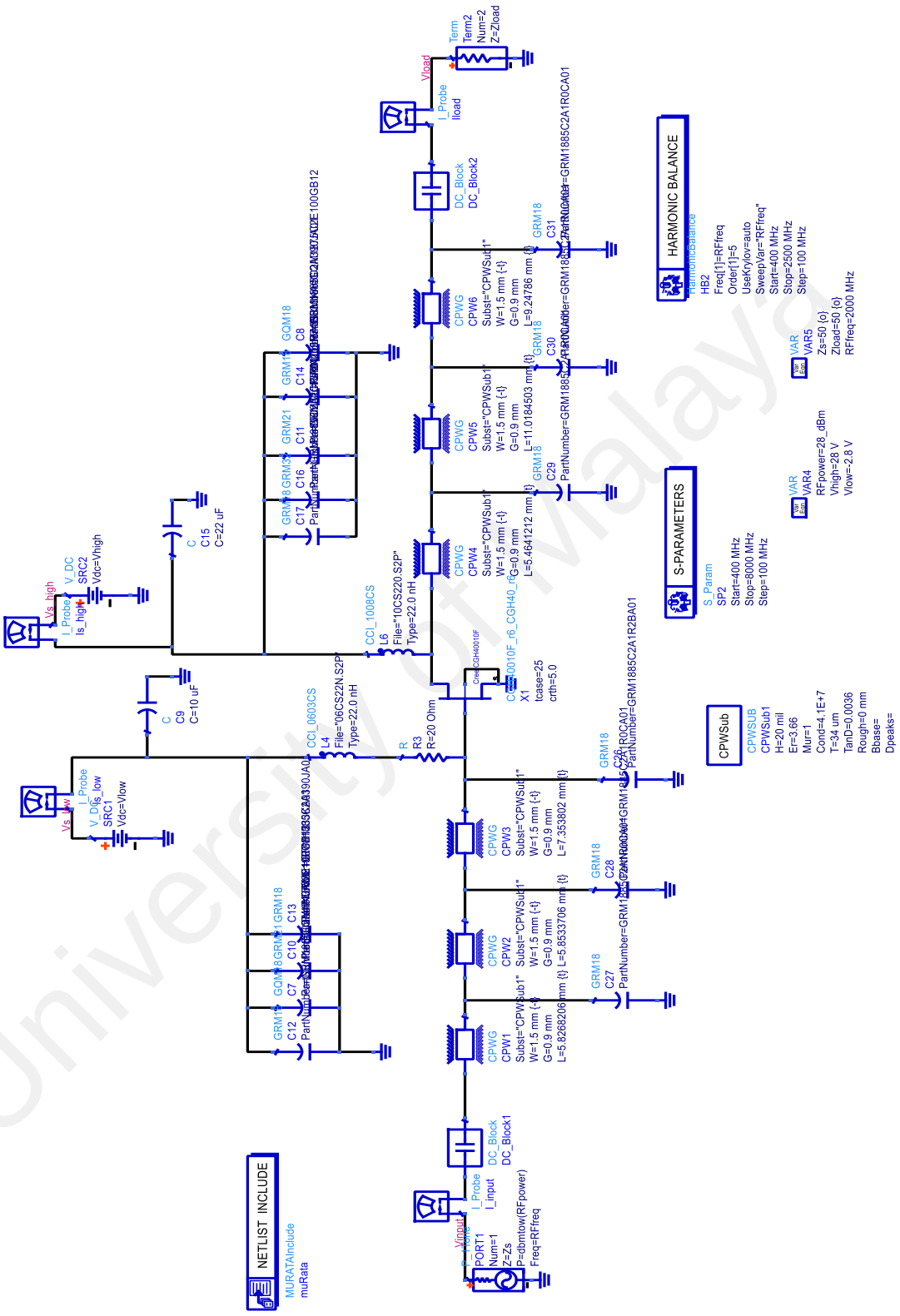

Figure 3.23: Complete broadband PA schematic simulated using ADS.

3.2.4 Prototype Development for Wideband Large Signal GaN HEMT Power Amplifier

3.2.4.1 Layout Design

The layout for prototype board of the design has been developed as shown in Figure 3.24. The input and output matching network for broadband design are based on CPWG as discussed in previous section. Both input and output terminated with 50-ohm SMA connector for measurement purpose. The DC biasing, Vgs and Vds, follows based on the recommendation provided in the datasheet (CREE, 2006-2007). The layout is performed on 2-layer board, with components being populated in first layer and second layer as ground. Sufficient ground via-holes are provided to ensure maximum return ground current, especially along the matching network and biasing traces (Rider, Kuhn, & Wolf, 2017). Six screw holes are provided to mount the board on heat sink. To mount CREE device and to have direct contact with heat sink, the board is designed with cavity according to the device's dimension. This is very important to ensure heat is dissipated to heat sink and avoid degradation in device's performance. Heat sink used for this prototype is the same as discussed in section 3.1.3.2.

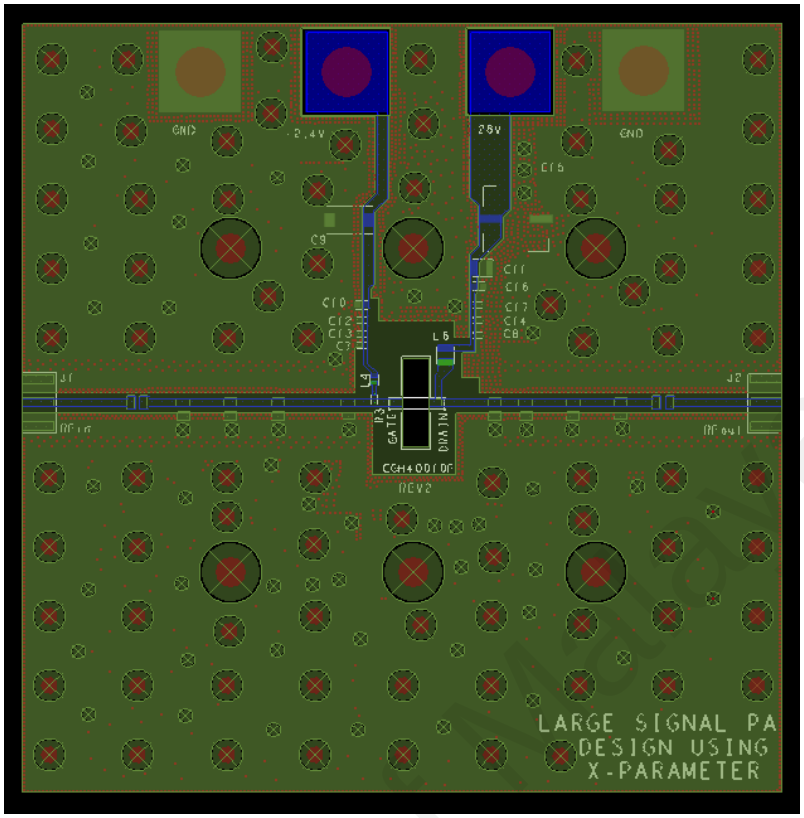

Figure 3.24: Layout design for broadband PA application.

3.2.4.2 Experimental Prototype Development

A prototype board of the design has been developed integrating CREE's CGH40010 GaN HEMT. The board is fabricated using 2-layer Rogers 4350B PCB material to experimentally verify the proposed broadband PA design methodology. Dielectric constant, ε_r of PCB is 3.66 and the substrate thickness is 0.762 mm. The photograph of the prototype board for wideband power amplifier design is shown in Figure 3.25. The board is supplied with drain voltage of 28 V and the quiescent current is set in the range of 40-90 mA. At the gate, -2.4 V has been applied to bias the power amplifier. For proper grounding, the board is designed with well distributed large number of via-holes. DC-to-RF routing are well isolated between each other to achieve minimum spurious as possible. To ensure DC current to the drain is optimum, the width of the routing is maximized, and this will guarantee drain

efficiency will not be affected during operation (Andrei Grebennikov, 2011). For optimum heat dissipation during operation, the board is mounted on heatsink using six screws, providing solid hold between PCB and heatsink. Tantalum and ceramic types of capacitors are used. Several chip capacitors (10 pF, 39 pF and 470 pF) are used to bypass dc gate biasing to ground. The dc-feed lines for the power amplifier consist of high-Q air-wound coil inductor.

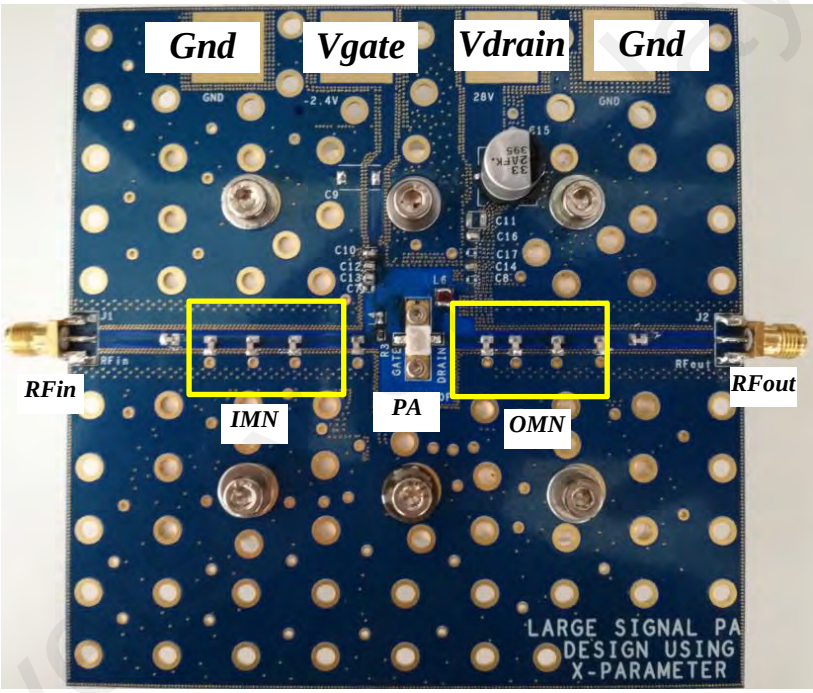

Figure 3.25: Complete broadband PA prototype board based on large signal impedance and RFT (top view).

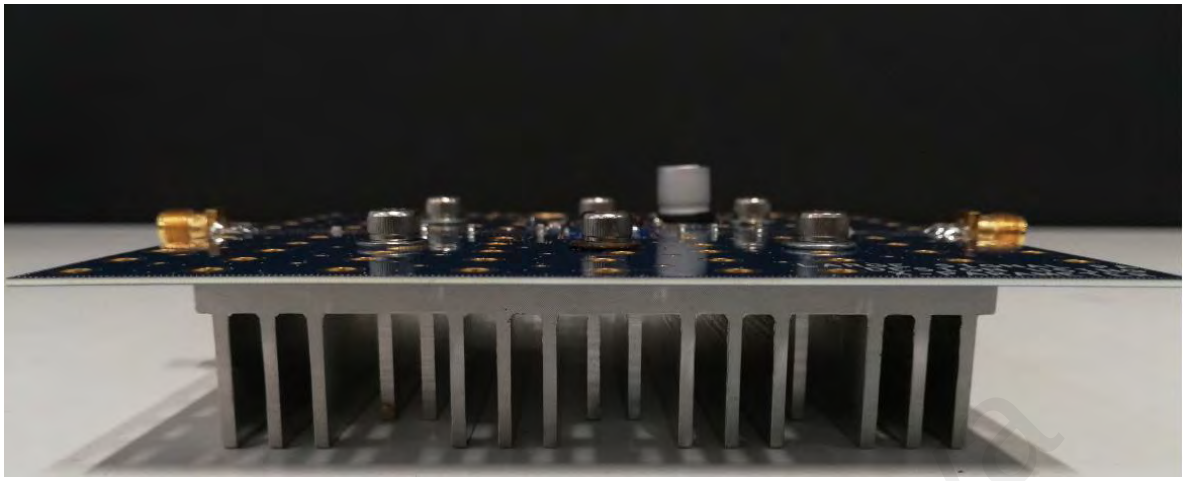

Figure 3.26: Complete broadband PA prototype board based on large signal impedance and RFT (front view).

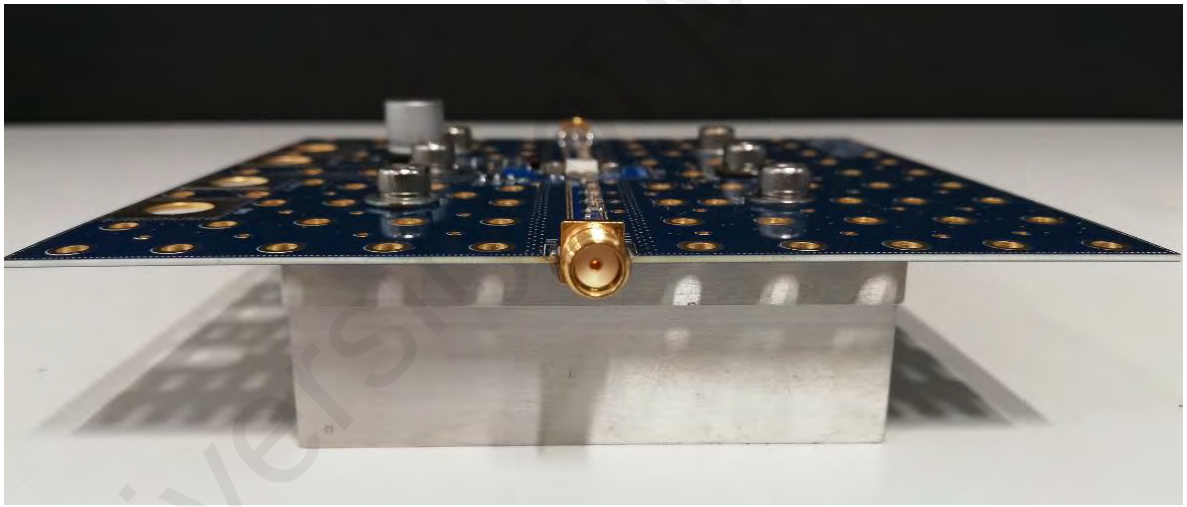

Figure 3.27: Complete broadband PA prototype board based on large signal impedance and RFT (side view).

For measurement setup, please refer to section 3.1.4.

CHAPTER 4 : RESULTS AND DISCUSSION

4.1 Ultra-Broadband Mixed-Mode GaN HEMT Power Amplifier Results

In this section, simulation and measurement results of high efficiency ultra-broadband RF power amplifier is discussed. This design is able to deliver 40 dBm output power over a half-decade frequency bandwidth of 0.4 - 2.0 GHz with high operating efficiency.

4.1.1 Simulation Results

Simulation has been carried out as shown in Figure 3.6 to validate the theory discussed in section 3.1.2. Circuit optimization has been made in simulation in order to achieve the desired performance. The interest is to achieve 40 dBm output power with more than 60% drain efficiency across the bandwidth.

4.1.1.1 Simulated Output Power, Efficiency and Gain

In this work, high importance is given to the output power, PAE and the gain of the design across the broad bandwidth. Simulation results for all these key parameters are shown in Figure 4.1, Figure 4.2 and Figure 4.3 respectively.

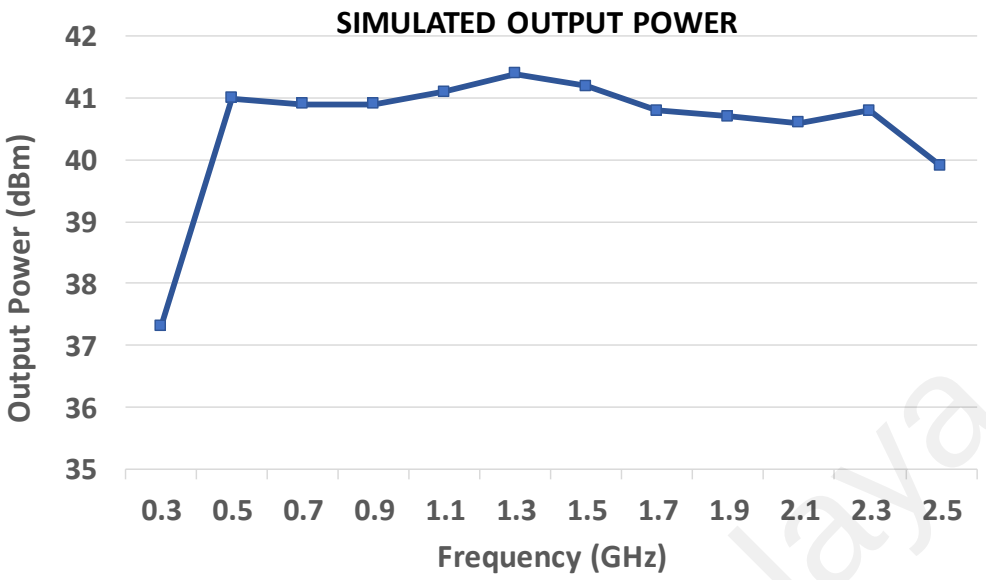

Figure 4.1: Complete broadband PA: simulated Output Power.

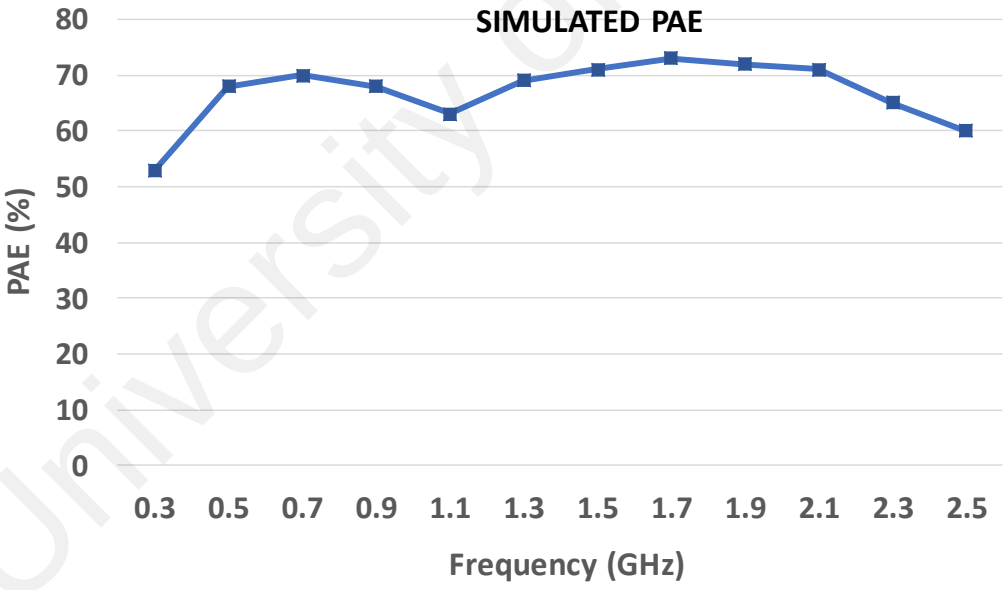

Figure 4.2: Complete broadband PA: simulated PAE.

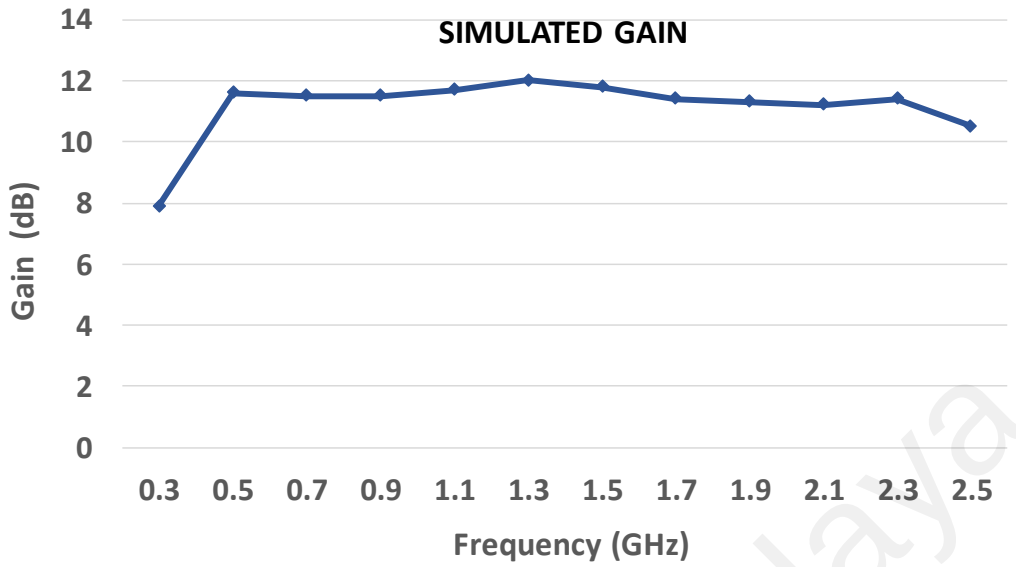

Figure 4.3: Complete broadband PA: simulated Gain.

In general, the performances of the broadband PA based on simulation meets the design goal. The design is able to achieve 40 dBm output power across 0.4 – 2.0 GHz bandwidth, with PAE better than 60%. The device shows a stable gain of 10 to 12 dB across the desired frequency range. These results met the design goal and can be considered as benchmark to proceed for actual prototype development.

4.1.2 Measurement Results

Based on simulation results, the actual prototype board is developed using CREE's CGH40010 GaN HEMT. The board is fabricated using 2-layer Rogers 4350B PCB material to validate the proposed broadband PA design. Dielectric constant, ε_r of PCB is 3.66 and the substrate thickness is 0.762 mm.

4.1.2.1 Measured Output Power, Efficiency and Gain

In this section, for better comparison and discussion, both simulated and measured results for output power, PAE and gain are shown in Figure 4.4, Figure 4.5 and Figure 4.6 respectively.

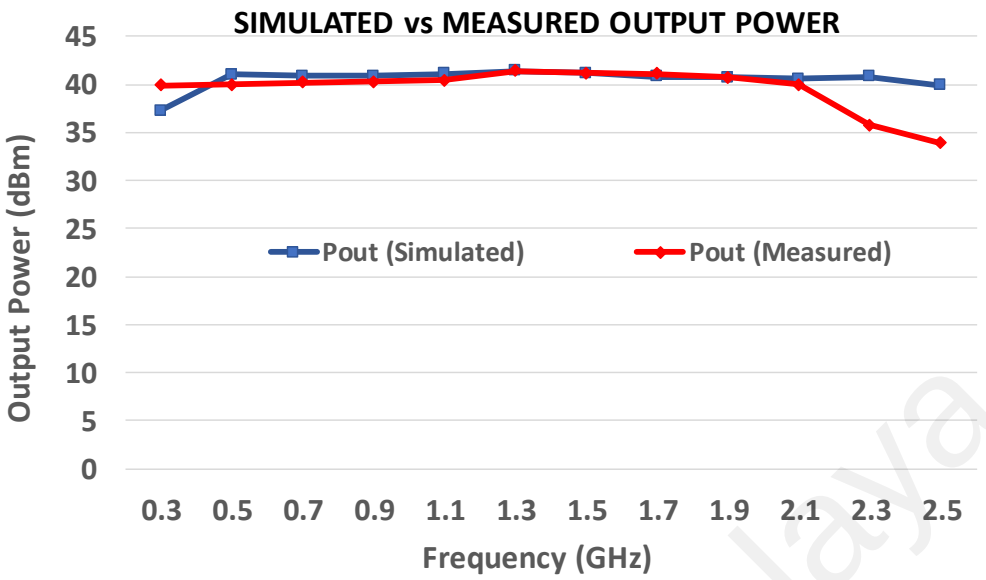

Figure 4.4: Complete broadband PA: simulated vs measured Output Power.

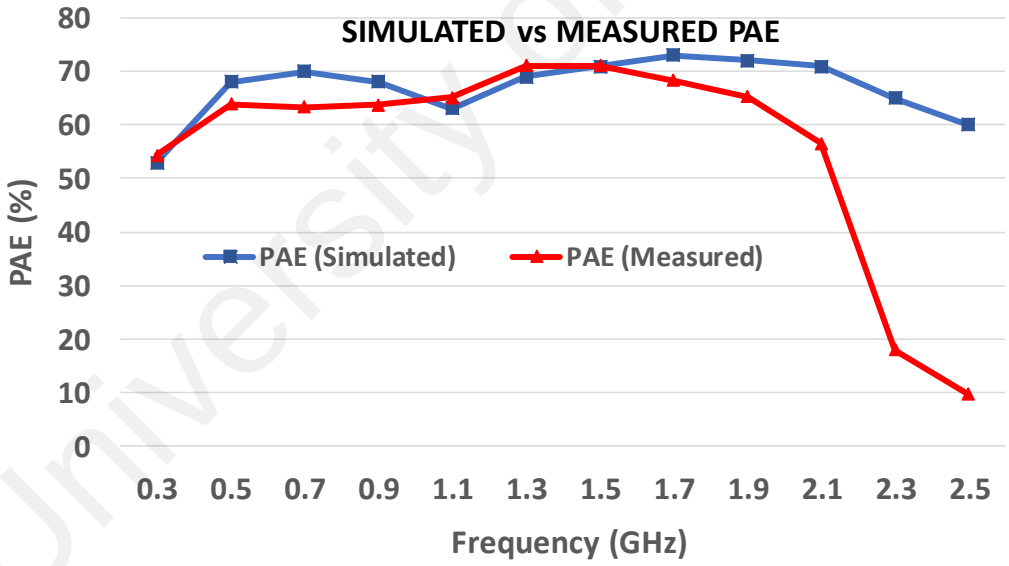

Figure 4.5: Complete broadband PA: simulated vs measured PAE.

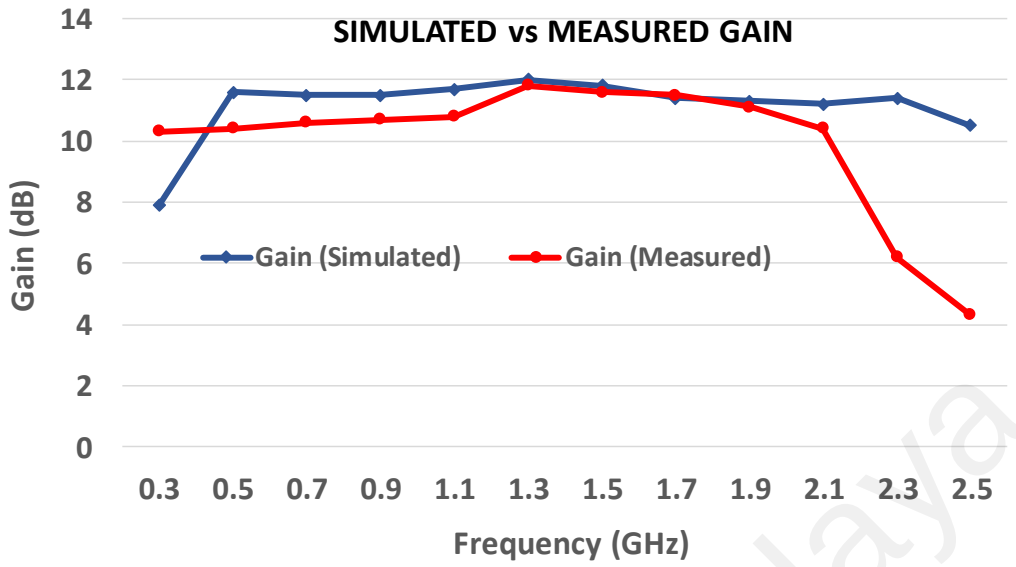

Figure 4.6: Complete broadband PA: simulated vs measured Gain.

In the simulation stage, actual passive component models have been used to simulate proposed design. As shown in Figure 4.4, comparison between output power for both simulation and measurement results yield that the proposed design is able to achieve the desired output power, 40 dBm across the bandwidth, from 0.4 – 2.0 GHz. The measurement results were obtained with very minimum tuning or optimization on the prototype board. In fact, the prototype board is able to exhibit 40 dBm output power at 0.3 GHz, but not in simulation. This could be due to PCB parasitic capacitance effect that have contributed to additional capacitance, causing the frequency response to be shifted slightly to lower end of the bandwidth. However, due to same effect, higher end of the bandwidth, beyond 2.1 GHz, are far off the simulation results. At these frequencies, the effect of PCB substrate is more severe due to distributed elements. To ensure that this effect is very minimal, as rule of thumb, the ground keep-out (separation between microstrip and top layer ground) is maximized wherever possible as shown in Figure 3.10 (Rider, Kuhn, & Wolf, 2017). In

general, the simulation and measurement results are in good agreement (with less than 10% error) within 0.4 – 2.0 GHz.

Figure 4.5 shows high efficiency over the wide frequency bandwidth can be obtained for both simulation and measurement. The overall power added efficiency (PAE) correlated well between simulated and measurement results, error not more than 10%, from 0.4 – 2.0 GHz, making both the results meeting the design goal of more than 60%. The error in correlation possibly due to PCB substrate on prototype board and the limited modeling accuracy of the components used in simulation. In addition, it is observed the efficiency at lower end and higher end of the frequencies are lower compared to mid frequencies. This possibly could be due to several assumptions. The lower end frequencies harmonics are within the bandwidth of operation therefore it could be slightly worse compared to mid frequencies. The third harmonic tuning circuit response may have shifted slightly lower on actual PCB board making the mid-range has better efficiency compared to high end.

However, to ensure high efficiency achieved on actual measurement, few measures have been taken. One of the PCB layout design rule has been applied. Wide trace is used to provide supply to the transistor. Wide DC routing will prevent unwanted losses, hence prevent voltage drop (Andrei Grebennikov, 2011). Besides, proper heat dissipation is a must to ensure high efficiency throughout the operation. Without robust design, heat generated by transistor during operation will be trapped. This will cause more power to be dissipated, hence leading to poor efficiency. Therefore, the PCB board is mounted on heat sink, providing maximum contact for transistor via through hole to the heat sink. The approach allows the heat to be equally distributed and avoid excessive heat to be generated, thus not only avoiding degradation in efficiency, but also will prevent from damaging the device.

The measured power gain of the designed prototype board agrees well with simulated results, ranging from 10 to 12 dB for the desired bandwidth as shown in Figure 4.6.

4.1.3 Comparison of performances with various work

The comparison Table 4.1 shows the performance summary of various state-of-art broadband power amplifiers implemented with GaN HEMT technology. In this work, high efficiency greater than 60% was achieved across wide frequency bandwidth of 0.4 - 2.0 GHz with reasonable high-gain operation of more than 11 dB, which is a significant achievement using a simple approach, suitable for two-way radio product implementations.

Table 4.1: Performance Summary of Broadband High-Efficiency Power Amplifiers

Frequency (GHz)	Fractional Bandwidth (%)	PAE (%)	Output power (dBm)	Power gain (dB)	Device Technology	Work
0.5-0.9	57.1	75-81	40-41	14-17	GaN	(Sharma et al., 2016)
1.7-2.8	49	60-80	40-42.6	14	GaN	(Y. Sun et al., 2015)
0.88-1.06	19	80-87	40-41	10	GaN	(Seo et al., 2014)
0.16-0.32	67	60-85	38-42.5	10-14.5	GaN	(Beltran, 2015)
0.4-2.0	133%	61-72	40-42	11-12	GaN	This Work

In first work presented in Table 4.1, (Sharma et al., 2016) has designed a high efficiency broadband PA with second harmonic manipulation. Initiated from ideal Class-F^{-1} condition, a series of voltage and current waveforms that is better than Class-B RF performance, including Class-F^{-1}, is identified in proposed methodology. A contiguous design space is created by extending these waveforms via continuous-mode concept. Within this expanded design space, fundamental and second harmonic matching trajectory for wider bandwidth for

highly efficient PA can be extracted. Actual measurement results show that more than 75% of PAE can be achieved for fractional bandwidth of 57%. (Y. Sun et al., 2015) proposed a controllable dual-mode PA with Class-F-1 and Class-J. This is achieved with comprehensive analysis on frequency response of the low pass matching and parasitic circuit. The design yields broadband PA design with fractional bandwidth of 49%, covering from 1.7 – 2.8 GHz. The design exhibits output power of more than 40 dBm and PAE of more than 60% across the bandwidth. (Seo et al., 2014) suggest to improve the efficiency and bandwidth for PA design by employing an active second harmonic injection technique. A PA was designed using 10-W GaN HEMT for the optimized third harmonic termination, with diplexer and auxiliary PA connected to the drain of the main PA. With the proposed technique, the PA design able to deliver more than 40 dBm output power from 0.88 – 1.06 GHz with PAE of 80% from. (Beltran, 2015) proposes a technique that provide both broadband reactance compensation and impedance matching concurrently by using broadband lumped-element network. The proposed method able to achieve PAE of 60 – 85 % with an output power of more than 38 dBm, and fractional bandwidth less than 70%.

4.2 Broadband RF Power Amplifier Adopting the Combination of Large Signal X-Parameter and Real Frequency Techniques (RFT) Results

In this section, simulation and measurement results of broadband RF power amplifier adopting the combination of large signal X-parameter and RFT is discussed. This design able to deliver 40 dBm output power covering a wide bandwidth of 0.3 - 2.0 GHz with high operating efficiency.

4.2.1 Large Signal Impedance Extraction using Transmission Line theory

As a proof of concept, a test bench is evaluated to validate theory discussed in section 3.2.1, to deliver 40 dBm output power with efficiency of more than 65% over a wide bandwidth, 0.3 – 2.0 GHz. This is established via simulation, whereby, the characteristic impedance, Z_o, and electrical length, θ, of both input and output transmission line have been carefully optimized to achieve above mentioned performance. Large signal X-parameter data, Γ_{OUT} and Γ_{IN}, for simulated design have been extracted as well. By using (3.21) and similar equation for input, the large signal device impedances can be obtained, and the results are shown in Figure 4.7, whereby both input and output impedances are compared with manufacturer's recommended datasheet impedances (CREE, 2006-2007).

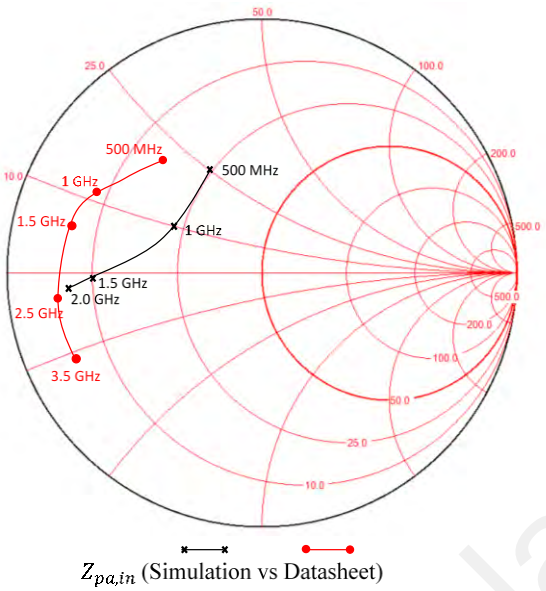

(a)

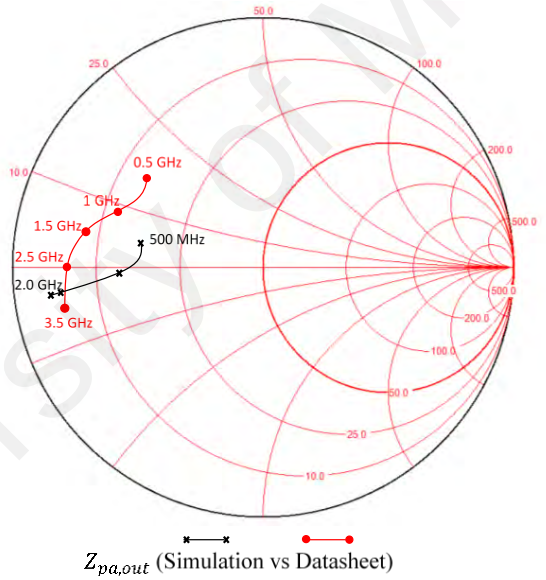

(b)

Figure 4.7: Simulated PA input (a) and output (b) impedance vs datasheet.

4.2.1.1 Complete PA Simulated Output Power, Efficiency and Gain

RFT is adopted in this work to establish wideband matching network for large signal impedance simulated in previous section. A complete broadband PA line up is simulated and validated prior to actual board fabrication. In this work, high importance is given to the output

power, PAE and the gain of the design across the broad bandwidth. Simulation results for all these key parameters are shown in Figure 4.8, Figure 4.9 and Figure 4.10 respectively.

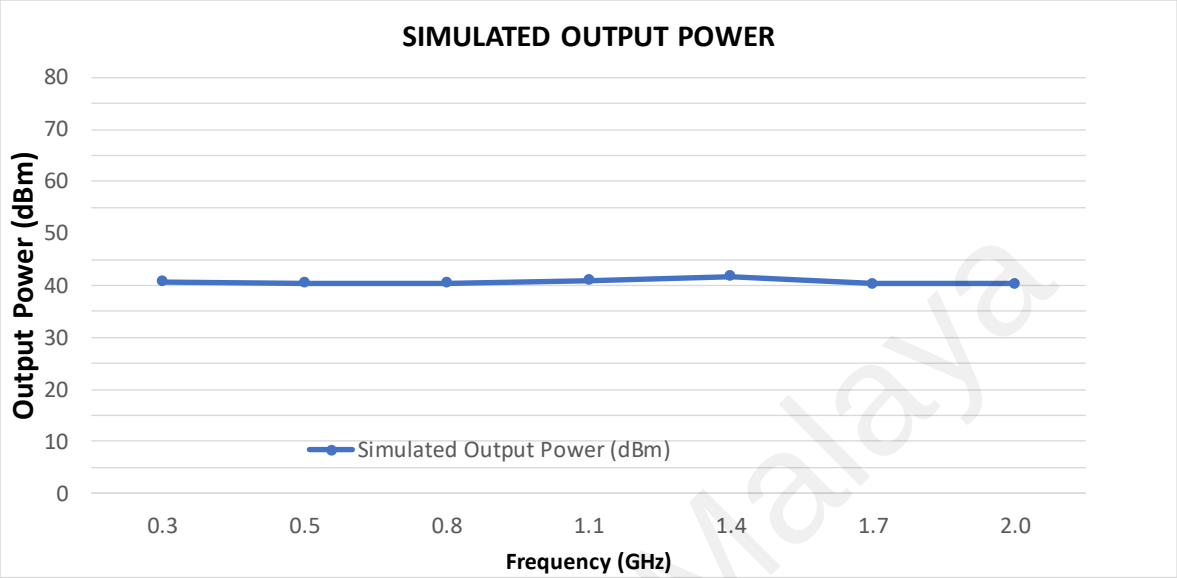

Figure 4.8: Complete broadband PA: simulated Output Power.

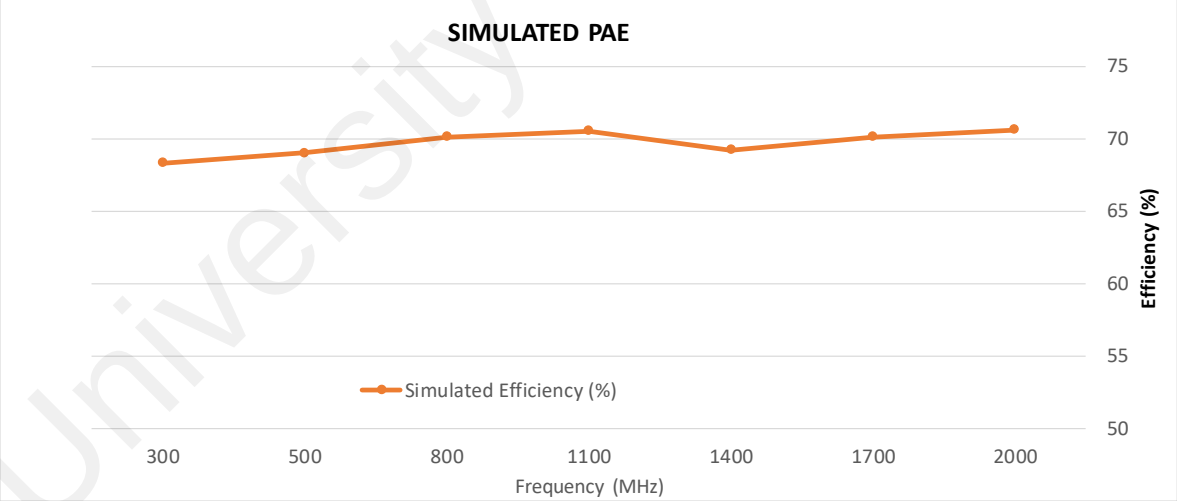

Figure 4.9: Complete broadband PA: simulated PAE.

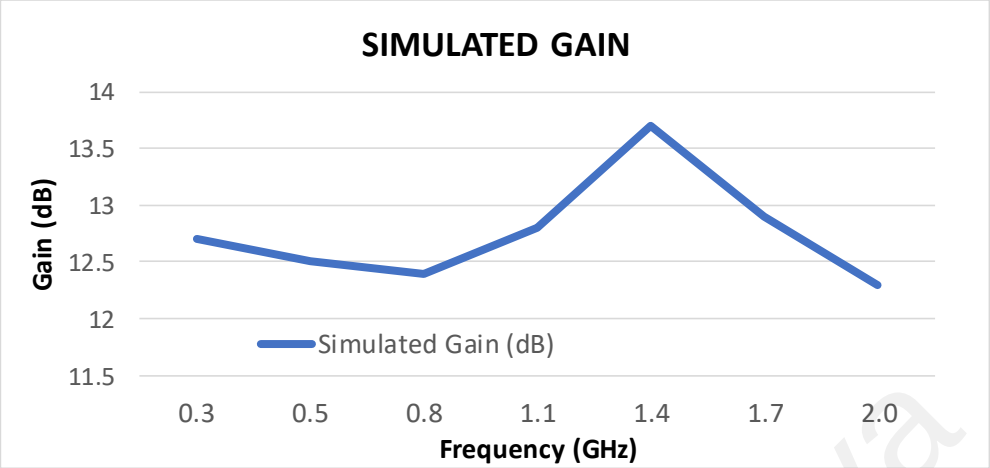

Figure 4.10: Complete broadband PA: simulated Gain.

In general, the performances of the broadband PA based on simulation meet the design goal. The design is able to achieve output power approximately 40 dBm across 0.3 – 2.0 GHz bandwidth, with PAE more than 65%. The device shows gain of more than 12 dB across the desired frequency range.

4.2.2 Measurement Results

Based on simulation results, the actual prototype board is developed using CREE's CGH40010 GaN HEMT. The board is fabricated using 2-layer Rogers 4350B PCB material to validate the proposed broadband PA design. Dielectric constant, ε_r of PCB is 3.66 and the substrate thickness is 0.762 mm.

4.2.2.1 Measured Output Power, Efficiency and Gain

In this section, for better comparison and discussion, both simulated and measured results for output power, PAE and gain are shown in Figure 4.11, Figure 4.12 and Figure 4.13 respectively.

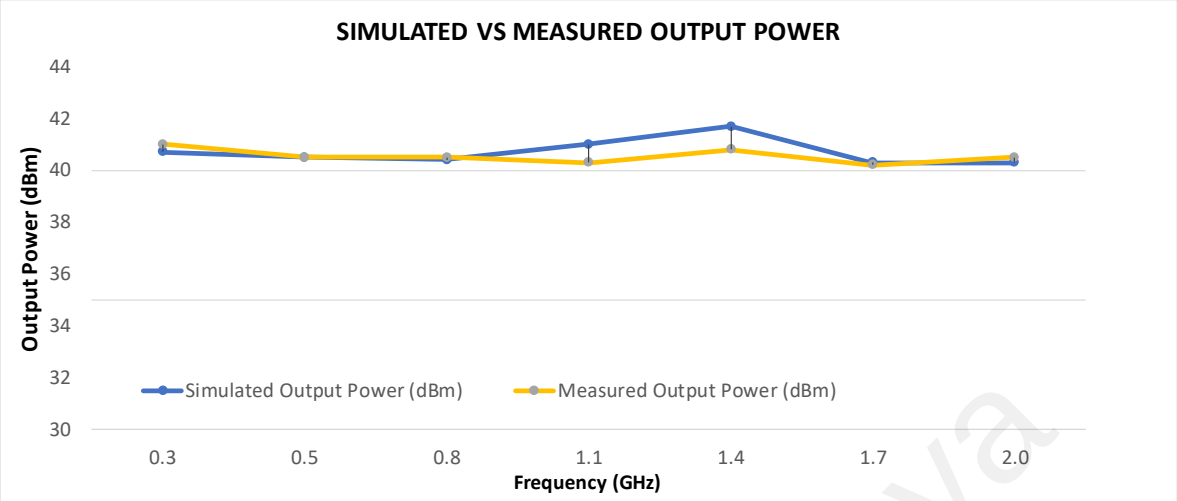

Figure 4.11: Complete broadband PA: simulated vs measured Output Power.

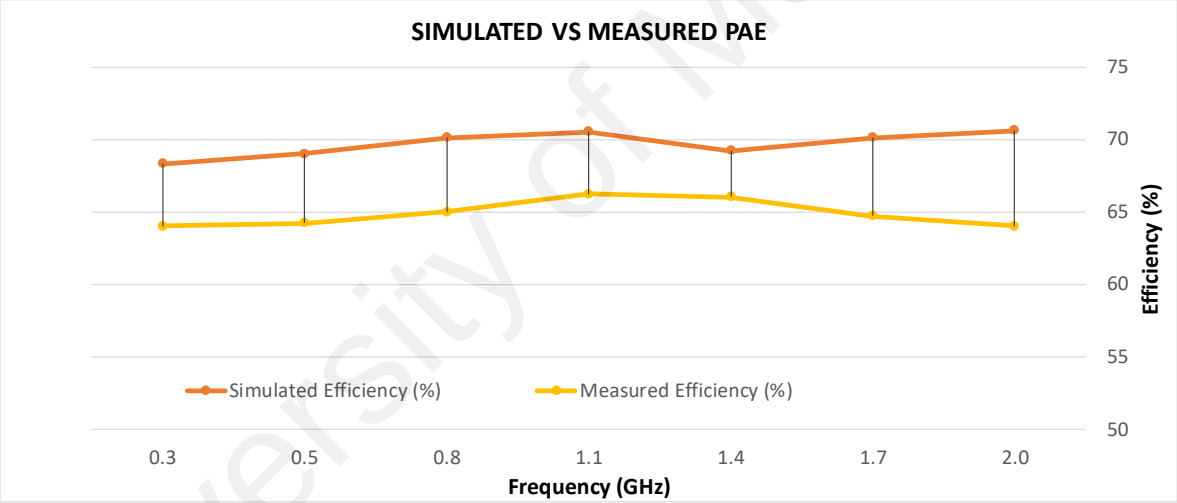

Figure 4.12: Complete broadband PA: simulated vs measured PAE.

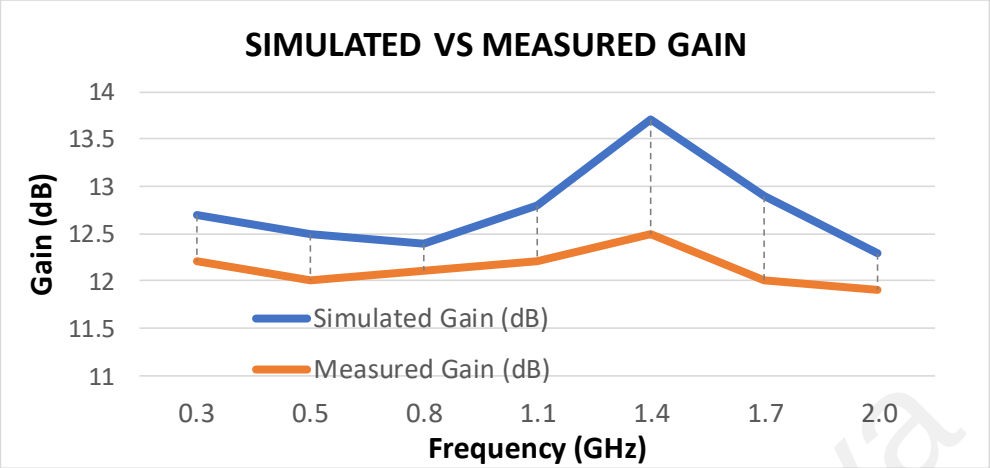

Figure 4.13: Complete broadband PA: simulated vs measured Gain.

As shown in Figure 4.11 and 4.12, the simulation and measurement results of the prototype board are well correlated. The concept board able to achieve 40 dBm output across wide bandwidth from 0.3 – 2.0 GHz with drain efficiency more than 63%. On the other hand, Figure 4.13 shows measured gain is almost correlated with simulated gain. These results achieved with very minimum optimization on the actual board, hence proving the proposed methodology works well. For simulation, as explained in section 3.2.1.2, narrowband transmission line has been developed for each dedicated frequency points to achieve desired output power and efficiency, hence could be possible reason behind slight degradation in actual wideband design.

Differences of 5% in efficiency and 1 dB in gain are considered a good achievement because these differences could be owed by several factors. The accuracy of device model vs the actual device used during measurement could be one of the factors. Simulation is based on the model of internal device and external package parameters such as leads are not included. Besides, variations in the load network parameters such as output lead of the transistor and parasitic inductances of grounded chip capacitors, will result in efficiency degradation, even if simulations were carried out using S-parameter capacitor models, which

do not include any connecting pads. Thus, these small variations in gain and efficiency indicate that the proposed method combining the concept of X-parameters and Real-Frequency Technique is suitable to predict the ultra-wideband PA performance with sufficient accuracy over the entire bandwidth.

4.2.3 Comparison of performances with various work

A comparison Table 4.2 shows the performance summary of various state-of-art broadband power amplifiers design.

Table 4.2: Performance Summary of Broadband High-Efficiency Power Amplifiers

Frequency (GHz)	Fractional Bandwidth (%)	PAE (%)	Output power (dBm)	Power gain (dB)	Device Technology	Work
0.5-0.9	57.1	75-81	40-41	14-17	GaN	(Sharma et al., 2016)
1.35-2.5	60	68-82	41-42.5	15-17	GaN	(Yang et al., 2016)
1.4-2.7	63	68	41	9	GaN	(A. Grebennikov, 2016)
1.8-2.7	40	57-73	40-41	9-14	GaN	(Zhou et al., 2017)
1.5-2.6	54	40-45	40-41.8	18 - 20	GaN	(Khan et al., 2018)
0.3-2.0	147	63-66	40	12	GaN	This Work

As discussed in section 4.1.3, (Sharma et al., 2016) has designed a high efficiency broadband PA with second harmonic manipulation. The proposed work yield output power of more than 40 dBm across the bandwidth from 0.5 – 0.9 GHz with PAE more than 75%. Alternatively, (Yang et al., 2016) proposed a technique that covers fractional bandwidth of 60%. The work

suggests implementing a modified elliptical low pass filter at the output matching network, which provides sharp roll off between highest fundamental frequency and second harmonic of the lowest frequency. A design with an output power more than 41 dBm and efficiency more than 68% is achieved. (A. Grebennikov, 2016) proposes a technique which uses shunt filter instead of series filter, achieving new load network which provides broadband capabilities on top of high efficiency. A test board using GaN HEMT is able to achieve 41 dBm across the frequency band from 1.4 – 2.7 GHz with average drain efficiency of 68%. (Zhou et al., 2017) developed a Doherty power amplifier prototype using a second-harmonic short-circuit network (SHSN) with mutual coupling to achieve high efficiency design without sacrificing its bandwidth. The technique able to deliver 40 dBm of output power with efficiency more than 50% across 1.8 – 2.7 GHz frequency bandwidth. Another broadband Doherty power amplifier design proposed by (Khan et al., 2018) able to achieve 40% of efficiency with fractional bandwidth of 54%, exhibiting maximum output power of 41.8 dBm.

Comparison with recent research work shows that broadband RF power amplifier adopting the combination of large signal X-Parameter and RFT proposed in this thesis able to achieve 40 dBm output power across even a wider bandwidth, from 0.3 – 2.0 GHz, or fractional bandwidth of 147% while maintaining high efficiency of more than 63%.

CHAPTER 5 : CONCLUSION

5.1 Overall Conclusion

The objective of this research work is to design a wideband power amplifier for large signal application especially for operation bandwidth covering more than one octave. The broadband 40 dBm power transmitter must be able to deliver flat desired output power across wide bandwidth with high efficiency. It is learnt that this could be quite challenging especially taking some factors into considerations. The PA needs to be well matched to input and output port across the bandwidth in order to transfer maximum power while maintaining high drain efficiency. In addition, the design should also emphasize in maintaining flat gain across the bandwidth.

Small signal analysis to design matching network will not yield a good design. The signal behaves nonlinearly under large signal conditions, at which, harmonics will be generated. Nonlinear characterization is important in order to extract large signal impedances hence, to design an optimum matching network across the bandwidth. However, it is tedious and time-consuming process to extract large signal impedances. A simple process is required to minimize design cycle time.

An ultra-broadband GaN HEMT power amplifier with combination of reactance compensation technique and third-harmonic resonant circuit is designed. Both parallel and series resonant circuits are tuned to the fundamental frequency ω_0 hence producing a nullified variation over a wide frequency bandwidth. This can be achieved when the rate of change in the reactance with frequency of shunt resonant circuit is exactly opposite to that of the series circuit. Higher frequencies third harmonic resonant circuit that approximate Class-F mode of operation is combined in this design. The circuit helps to provide a capacitive reactance at the fundamental frequency that results in an open-circuit condition at the output. This is not

applicable for lower band frequencies due to the in-band third harmonics. Theoretically, combination of both reactance compensation and third harmonic tuning at higher frequencies, provides broadband PA design with high drain efficiency. This is proven with a prototype design using CREE's CGH40010 GaN HEMT device. Measurement results yields output power of 40 dBm across 0.4 – 2.0 GHz. Comparison with other recent works proves that this research work able to achieve more than 60% of drain efficiency, making one of the high efficiency broadband PA design.

Another design approach is introduced in this research work too. Poly Harmonic Distortion (PHD) modelling based X-parameter concept is used in this approach. S-parameter characterization is only based on small signal analysis. Therefore, it may not be suitable to represent large signal impedances. On the other hand, X-parameters are able to characterize an active device under large signal condition hence, able to provide large signal devices impedances. However, in order to extract these impedances, a simplified method has been introduced using narrowband transmission line theory. The approach is analysed using CAD tool and the results is simulated. The resultant impedances are compared with CGH40010 GaN HEMT device manufacturer's datasheet. The extracted impedances are used with Real Frequency Technique (RFT) to develop broadband matching network. A layout design is developed based on simulated circuit and actual PCB board fabricated. Actual board design able to achieve 40 dBm output power with efficiency more than 63% across 0.3-2.0 GHz.

Both approaches presented in this research work are able to achieve desired output power across wideband frequencies. These high efficiency designs are suitable to be used for commercial software defined mobile radio application. In the case of large signal device impedances are not known, the second approach which is broadband RFPA adopting the combination of large signal X-Parameter and RFT will be more suitable. The suggested

approach is less complex and helps to reduce time consuming process in extracting large signal impedances, hence reducing overall design cycle time.

5.2 Future Work

Number of mobile users have increased tremendously over the last decade. Not only that, today the world has become more data driven, where huge amount of data is needed to be transferred, processed and etc. This eventually has led to the move toward 5G, millimetre wave or higher frequency of operation for mobile communication; more than 10 GHz. Higher frequencies provide better throughput hence it supports the need of higher and faster data processing. A lot of research being done in this context and designing a broadband power amplifier for 5G operation definitely will add value in future. Proposed two methodologies in this research work have proven able to produce high efficiency PA design in ISM band. Perhaps, these research work can be further enhanced to design broadband PA for 5G operation. However, main caution will be taking the distributed elements into consideration since in mmWave, transmission line and components are no longer considered as lumped.

REFERENCES

Afanasyev, P., Grebennikov, A., Farrell, R., & Dooley, J. (2020, 16-19 June 2020). *Broadband Operation of Class-E Power Amplifier with Shunt Filter.* Paper presented at the 2020 18th IEEE International New Circuits and Systems Conference (NEWCAS).

Aggrawal, E., Rawat, K., & Roblin, P. (2017). Investigating Continuous Class-F Power Amplifier Using Nonlinear Embedding Model. *IEEE Microwave and Wireless Components Letters, 27*(6), 593-595.

Aridas, N. K., Yarman, B. S., & Chacko, P. (2014). Wideband power amplifier for two-way radio applications via real-frequency technique. *Electronics Letters, 50*(23), 1762-1764.

Barmuta, P., Ferranti, F., Lewandowski, A., Knockaert, L., & Schreurs, D. (2014). Efficient Generation of X-Parameters Transistor Models by Sequential Sampling. *IEEE Microwave and Wireless Components Letters, 24*(8), 530-532.

Beltran, R. A. (2015, 17-22 May 2015). *Broadband class-E power amplifier designed by lumped-element network transforms and GaN FETs.* Paper presented at the 2015 IEEE MTT-S International Microwave Symposium.

Biernacki, R. M., Marcu, M., & Root, D. E. (2017, 4-9 June 2017). *Circuit optimization with X-parameter models.* Paper presented at the 2017 IEEE MTT-S International Microwave Symposium (IMS).

Carlin, H. (1977). A new approach to gain-bandwidth problems. *IEEE Transactions on Circuits and Systems, 24*(4), 170-175.

Ceylan, O., Yagci, H. B., & Yarman, S. B. (2010, 25-27 Aug. 2010). *Wideband matching circuit design for differantial output systems by using real frequency technique.* Paper presented at the 2010 10th Mediterranean Microwave Symposium.

Chen, K., & Peroulis, D. (2011). Design of Highly Efficient Broadband Class-E Power Amplifier Using Synthesized Low-Pass Matching Networks. *IEEE Transactions on Microwave Theory and Techniques, 59*(12), 3162-3173.

Chen, K., & Peroulis, D. (2012). Design of Broadband Highly Efficient Harmonic-Tuned Power Amplifier Using In-Band Continuous Class-F^{-1}/F Mode Transferring. *IEEE Transactions on Microwave Theory and Techniques, 60*(12), 4107-4116.

CREE, I. (2006-2007). RF Power GaN HEMT *CGH40010 Data Sheet*. 4600 Silicon Driv Durham, NC 27703.

Dai, Z., He, S., You, F., Peng, J., Chen, P., & Dong, L. (2015). A New Distributed Parameter Broadband Matching Method for Power Amplifier via Real Frequency Technique. *IEEE Transactions on Microwave Theory and Techniques, 63*(2), 449-458.

DeJager, J. T. (1964). Maximum Bandwidth Performance of Non- degenerate Parametric Amplifier with Single-Tuned Idler Circuit. *IEEE Transactions on Microwave Theory and Techniques, 12*(4), 459-467.

Demenitroux, W., Maziere, C., Gasseling, T., Gustavsen, B., Campovecchio, M., & Quere, R. (2010, 28-30 Sept. 2010). *A new multi-harmonic and bilateral behavioral model taking into account short term memory effect.* Paper presented at the The 40th European Microwave Conference.

Dong, Y., Mao, L., & Xie, S. (2017). Extended Continuous Inverse Class-F Power Amplifiers With Class-AB Bias Conditions. *IEEE Microwave and Wireless Components Letters, 27*(4), 368-370.

Doudorov, G. (2003). *Evaluation of Si-LDMOS Transistor for RF Power Amplifier in 2 - 6 GHz Frequency Range.* (Masters), Linkoping University, Sweden, Sweden. (LiTH-ISY -EX-3435-2003)

Du, X., Nan, J., Chen, W., & Shao, Z. (2014). 'New' solutions of Class-E power amplifier with finite dc feed inductor at any duty ratio. *IET Circuits, Devices & Systems, 8*(4), 311-321.

Gonzalez, G. (1996). *Microwave Transistor Amplifiers: Analysis and Design* (2nd ed.): Prentice Hall

Gonzalez, G. (2008). *Microwave transistor amplifiers : analysis and design*. Taipei: Pearson Education.

Gou, Y., Lin, M., Wu, Q., & Fu, J. (2015). Analytical Reflection Coefficient Expressions Utilizing Load-Dependent X-Parameters. *IEEE Transactions on Microwave Theory and Techniques, 63*(10), 3142-3152.

Grebennikov, A. (2011). *RF and microwave transmitter design*. Hoboken NJ: Wiley.

Grebennikov, A. (2016). High-Efficiency Class-E Power Amplifier With Shunt Capacitance and Shunt Filter. *IEEE Transactions on Circuits and Systems I: Regular Papers, 63*(1), 12-22.

Grebennikov, A., Sokal, N. O., & Franco, M. J. (2012). Switchmode RF and microwave power amplifiers, second edition.

Grebennikov, A., & Wong, J. (2012). A Dual-Band Parallel Doherty Power Amplifier for Wireless Applications. *IEEE Transactions on Microwave Theory and Techniques, 60*(10), 3214-3222.

Guo, Q., Zhang, X. Y., Xu, J., Li, Y. C., & Xue, Q. (2017). Bandpass Class-F Power Amplifier Based on Multifunction Hybrid Cavity–Microstrip Filter. *IEEE Transactions on Circuits and Systems II: Express Briefs, 64*(7), 742-746.

Hamza, K. H., & Nirmal, D. (2020). A review of GaN HEMT broadband power amplifiers. *AEU-International Journal of Electronics and Communications, 116*, 153040.

Hayati, M., Roshani, S., Kazimierczuk, M. K., & Sekiya, H. (2016). Analysis and design of class E power amplifier considering MOSFET parasitic input and output capacitances. *IET Circuits, Devices & Systems, 10*(5), 433-440.

Hayati, M., Roshani, S., Roshani, S., Kazimierczuk, M. K., & Sekiya, H. (2018). Design of Class E Power Amplifier with New Structure and Flat Top Switch Voltage Waveform. *IEEE Transactions on Power Electronics, 33*(3), 2571-2579.

Hayati, M., Sheikhi, A., & Grebennikov, A. (2015). Class-F Power Amplifier With High Power Added Efficiency Using Bowtie-Shaped Harmonic Control Circuit. *IEEE Microwave and Wireless Components Letters, 25*(2), 133-135.

Horn, J., Gunyan, D., Betts, L., Gillease, C., Verspecht, J., & Root, D. E. (2008, 13-14 May 2008). *Measurement-based large-signal simulation of active components from automated nonlinear vector network analyzer data via X-parameters.* Paper presented at the 2008 IEEE International Conference on Microwaves, Communications, Antennas and Electronic Systems.

Huang, C., He, S., You, F., & Hu, Z. (2013). Design of Broadband Linear and Efficient Power Amplifier for Long-Term Evolution Applications. *IEEE Microwave and Wireless Components Letters, 23*(12), 653-655.

Humphreys, B. L. (1964). Characteristics of broadband parametric amplifiers using filter networks. *Proceedings of the Institution of Electrical Engineers, 111*(2), 264-274.

Joujili, H. G., Mivehchy, M., & Habibi, M. (2016). A Novel Analytical Design Approach for Determining the Optimum Load to Minimize Harmonic Output Power Based on X-Parameters. *IEEE Transactions on Microwave Theory and Techniques, 64*(11), 3492-3500.

Khan, M. S., Zhang, H., Wang, X., Ullah, R., Ahmad, I., Shahzad, S., . . . Tunio, M. Z. (2018). A Novel Two-Stage Broadband Doherty Power Amplifier for Wireless Applications. *IEEE Microwave and Wireless Components Letters, 28*(1), 40-42.

Kumar, N., Prakash, C., Grebennikov, A., & Mediano, A. (2008). High-Efficiency Broadband Parallel-Circuit Class E RF Power Amplifier With Reactance-Compensation Technique. *IEEE Transactions on Microwave Theory and Techniques, 56*(3), 604-612.

Lee, C., Lin, Y., & Lin, W. (2016). Large-Signal Characterization of pHEMT Under Different Load Conditions by Using X-Parameters. *IEEE Microwave and Wireless Components Letters, 26*(2), 125-127.

Lee, C., Lin, Y., Lin, W., & Lee, C. (2016, 24-26 Aug. 2016). *A simple and fast de-embedding procedure of X-parameter measurement for RF transistor characterization in the large-signal operating region.* Paper presented at the 2016 IEEE International Symposium on Radio-Frequency Integration Technology (RFIT).

Lin, C., & Chang, H. (2010). A High Efficiency Broadband Class-E Power Amplifier Using a Reactance Compensation Technique. *IEEE Microwave and Wireless Components Letters, 20*(9), 507-509.

Liu, S., Liu, M., Yang, S., Ma, C., & Zhu, X. (2017). A Novel Design Methodology for High-Efficiency Current-Mode and Voltage-Mode Class-E Power Amplifiers in Wireless Power Transfer systems. *IEEE Transactions on Power Electronics, 32*(6), 4514-4523.

Ma, L., Zhou, J., & Yu, Z. (2015, 6-9 Dec. 2015). *Design of a high-efficiency dual-band harmonic-tuned power amplifier via simplified real frequency technique.* Paper presented at the 2015 Asia-Pacific Microwave Conference (APMC).

Mass, S. A. (2003). *Nonlinear Microwave and RF Circuits* (2nd ed.).

Matthaei, G. L. (1961). A Study of the Optimum Design of Wide-Band Parametric Amplifiers and Up-Converters. *IRE Transactions on Microwave Theory and Techniques, 9*(1), 23-38.

Meng, F., Zhu, X., Xia, J., & Yu, C. (2018). A New Approach to Design a Broadband Doherty Power Amplifier via Dual-Transformation Real Frequency Technique. *IEEE Access, 6*, 48588-48599.

Mindan, B., & Hong, L. (2010, 16-18 July 2010). *The Analysis of Impedance Matching Problem in RF Circuit Design.* Paper presented at the 2010 International Forum on Information Technology and Applications.

Nielsen, T. S., Dieudonne, M., Gillease, C., & Root, D. E. (2012, 14-17 Oct. 2012). *Doherty Power Amplifier Design in Gallium Nitride Technology Using a Nonlinear Vector Network Analyzer and X-Parameters.* Paper presented at the 2012 IEEE Compound Semiconductor Integrated Circuit Symposium (CSICS).

Ozalas, M. T. (2005, 6-7 April 2005). *High efficiency class-F MMIC power amplifiers at ku-band.* Paper presented at the The 2005 IEEE Annual Conference Wireless and Micrwave Technology, 2005.

Pedro, J. C., Nunes, L. C., & Cabral, P. M. (2015). A Simple Method to Estimate the Output Power and Efficiency Load–Pull Contours of Class-B Power Amplifiers. *IEEE Transactions on Microwave Theory and Techniques, 63*(4), 1239-1249.

Pelaez-Perez, A. M., Woodington, S., Fernandez-Barciela, M., Tasker, P. J., & Alonso, J. I. (2012). Large-Signal Oscillator Design Procedure Utilizing Analytical X-Parameters Closed-Form Expressions. *IEEE Transactions on Microwave Theory and Techniques, 60*(10), 3126-3136.

Pichler, B., Leder, N., Magerl, G., & Arthaber, H. (2017, 25-28 Sept. 2017). *Experimental study on load dependent X-parameter models for PA design.* Paper presented at the 2017 IEEE Radio and Antenna Days of the Indian Ocean (RADIO).

Raab, F. H. (2001). Class-E, Class-C, and Class-F power amplifiers based upon a finite number of harmonics. *IEEE Transactions on Microwave Theory and Techniques, 49*(8), 1462-1468.

Raab, F. H., Asbeck, P., Cripps, S., Kenington, P. B., Popovic, Z. B., Pothecary, N., . . . Sokal, N. O. (2002). Power amplifiers and transmitters for RF and microwave. *IEEE Transactions on Microwave Theory and Techniques, 50*(3), 814-826.

Rider, T., Kuhn, W. B., & Wolf, A. (2017, 7-11 Aug. 2017). *Crosstalk and EMI in mixed-signal / microwave multi-layer pc boards.* Paper presented at the 2017 IEEE International Symposium on Electromagnetic Compatibility & Signal/Power Integrity (EMCSI).

Root, D. E., Marcu, M., Horn, J., Xu, J., Biernacki, R. M., & Iwamoto, M. (2012, 17-22 June 2012). *Scaling of X-parameters for device modeling.* Paper presented at the 2012 IEEE/MTT-S International Microwave Symposium Digest.

Seo, M., Lee, H., Gu, J., Kim, H., Ham, J., Choi, W., . . . Yang, Y. (2014). High-Efficiency Power Amplifier Using an Active Second-Harmonic Injection Technique Under Optimized Third-Harmonic Termination. *IEEE Transactions on Circuits and Systems II: Express Briefs, 61*(8), 549-553.

Sharma, T., Darraji, R., & Ghannouchi, F. (2016). A Methodology for Implementation of High-Efficiency Broadband Power Amplifiers With Second-Harmonic Manipulation. *IEEE Transactions on Circuits and Systems II: Express Briefs, 63*(1), 54-58.

Shuai, C., Zhiqun, C., Kai, W., & Hui, W. (2015, 18-20 Oct. 2015). *Broadband switch power amplifier design.* Paper presented at the 2015 IEEE 16th International Conference on Communication Technology (ICCT).

Simpson, G., Horn, J., Gunyan, D., & Root, D. E. (2008, 9-12 Dec. 2008). *Load-pull + NVNA = enhanced X-parameters for PA designs with high mismatch and technology-independent large-signal device models.* Paper presented at the 2008 72nd ARFTG Microwave Measurement Symposium.

Sun, G., & Jansen, R. H. (2012). Broadband Doherty Power Amplifier via Real Frequency Technique. *IEEE Transactions on Microwave Theory and Techniques, 60*(1), 99-111.

Sun, Y., Zhu, X., Zhai, J., Zhang, L., & Meng, F. (2015). Highly Efficient Concurrent Power Amplifier With Controllable Modes. *IEEE Transactions on Microwave Theory and Techniques, 63*(12), 4051-4060.

Tamjid, F., Ghahremani, A., Richardson, M., & Fathy, A. E. (2017, 15-18 Jan. 2017). *A novel approach to the design of a broadband high efficiency Class-E power amplifier with over 87% bandwidth.* Paper presented at the 2017 IEEE Topical Conference on RF/Microwave Power Amplifiers for Radio and Wireless Applications (PAWR).

Tuffy, N., Guan, L., Zhu, A., & Brazil, T. J. (2012). A Simplified Broadband Design Methodology for Linearized High-Efficiency Continuous Class-F Power Amplifiers. *IEEE Transactions on Microwave Theory and Techniques, 60*(6), 1952-1963.

Verspecht, & Root, D. E. (2006). Polyharmonic distortion modeling. *IEEE Microwave Magazine, 7*(3), 44-57.

Verspecht, J., Williams, D. F., Schreurs, D., Remley, K. A., & McKinley, M. D. (2005). Linearization of large-signal scattering functions. *IEEE Transactions on Microwave Theory and Techniques, 53*(4), 1369-1376.

Wang, Y., Nielsen, T. S., Jensen, O. K., & Larsen, T. (2014, 14-16 May 2014). *X-parameter based GaN device modeling and its application to a high-efficiency PA design.* Paper presented at the 2014 International Conference on Numerical Electromagnetic Modeling and Optimization for RF, Microwave, and Terahertz Applications (NEMO).

Wang, Y., Nielsen, T. S., Jensen, O. K., & Larsen, T. (2015, 9-10 July 2015). *GaN HEMT device modeling using X-parameters with emphasis on complexity reduction of harmonic load-pull measurement.* Paper presented at the 2015 International Symposium on Signals, Circuits and Systems (ISSCS).

Wang, Y., Nielsen, T. S., Sira, D., Jensen, O. K., & Larsen, T. (2013). X-parameter-based modelling of polar modulated power amplifiers. *IET Microwaves, Antennas & Propagation, 7*(14), 1161-1167.

Weiguo, Y., Chengguo, L., Shuai, Z., Zhipeng, W., & Jingwei, Z. (2016, 5-8 June 2016). *Design and measurement analysis of Class AB power amplifier.* Paper presented at the 2016 IEEE International Conference on Microwave and Millimeter Wave Technology (ICMMT).

Woodington, S. (2011). *Behavioral model analysis of active harmonic load-pull measurements.* (Doctoral Thesis), Cardiff University,

Yang, M., Xia, J., Guo, Y., & Zhu, A. (2016). Highly Efficient Broadband Continuous Inverse Class-F Power Amplifier Design Using Modified Elliptic Low-Pass Filtering Matching Network. *IEEE Transactions on Microwave Theory and Techniques, 64*(5), 1515-1525.

Yarman, B. S. (2008). Design of Ultra Wideband Antenna Matching Networks Via Simplified Real Frequency Technique.

Yarman, B. S. (2010). *Design of Ultra Wideband Power Transfer Networks*. New York, NY, USA: Wiley.

Yarman, B. S., & Ejaz, M. E. (2015, 30 Nov.-2 Dec. 2015). *Practical consideration to design broadband X-Band power amplifiers: Comparative results.* Paper presented at the 2015 IEEE 15th Mediterranean Microwave Symposium (MMS).

Zhou, X. Y., Zheng, S. Y., Chan, W. S., Chen, S., & Ho, D. (2017). Broadband Efficiency-Enhanced Mutually Coupled Harmonic Postmatching Doherty Power Amplifier. *IEEE Transactions on Circuits and Systems I: Regular Papers, 64*(7), 1758-1771.

Zisheng, L., Wenhua, C., & Ghannouchi, F. M. (2013, 7-9 April 2013). *High-efficient harmonic-tuned power amplifier with more than an octave bandwidth.* Paper presented at the WAMICON 2013.

LIST OF PUBLICATIONS

Krishnamoorthy, R., Kumar, N., Grebennikov, A., & Ramiah, H. (2018). A High-Efficiency Ultra-Broadband Mixed-Mode GaN HEMT Power Amplifier. *IEEE Transactions on Circuits and Systems II: Express Briefs, 65*(12), 1929-1933.

Krishnamoorthy, R., Kumar, N., Grebennikov, A., Yarman, B. S., & Ramiah, H. (2020). Broadband RF Power Amplifier with Combination of Large Signal X-Parameter and Real Frequency Techniques. *IEICE Transactions on Electronics,* E103.C(5), 225-230.